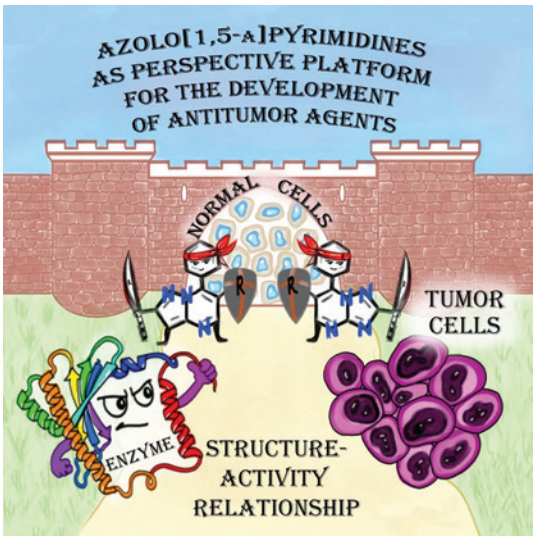
https://doi.org/10.59761/RCR5245

Azolo[1,5-*a*]pyrimidines as a promising platform for the development of antitumour agents. Structure–activity relationship

Evgeny M. Mukhin, Konstantin V. Savateev, Eva V. Bersneva, Sergey V. Androv, Vladimir L. Rusinov

Ural Federal University named after the First President of Russia B.N.Yeltsin, 620002 Ekaterinburg, Russian Federation

Malignant tumours are the second leading cause of death among working-age population; meanwhile, prevention and treatment of these diseases is hampered by the wide diversity of cell types that can become malignant or develop resistance to chemotherapy. Recent years have witnessed a considerable growth of the fascination with azolo[1,5-*a*]pyrimidines as a promising platform for developing antitumour agents; several drugs based on this platform are already in clinical trials or are used in practice. The present review, devoted to this platform, considers the diversity of oncogenic targets that are affected by azolo[1,5-*a*]pyrimidines and demonstrates their cytotoxic action against various types of cancer cells. The main focus is on the antitumour potential of azole[1,5-*a*]pyrimidines. Analysis of modern literature including 132 studies reveals the key structure–activity relationships and provides conclusions about the most promising substitution patterns in the heterocyclic system depending on the macromolecular target. The structures of the lead compounds are presented, and the cell lines most sensitive to azolopyrimidines are listed.
The bibliography includes 196 references.
Keywords: azolopyrimidines, azoles, pyrimidines, kinase inhibitors, structure–activity relationship, malignant tumours, cancer, cytotoxicity.



Contents

1. Introduction 1
2. Azolo[1,5-*a*]pyrimidines as a basis for the design of targeted anticancer drugs 3
2.1. Kinases and kinase inhibitors 3
2.1.1. Serine/threonine kinase inhibitors 3
2.1.2. Tyrosine kinase inhibitors 10
2.1.3. Inhibitors of other kinases 13
2.2. Non-kinase enzymes and epigenetic regulators 16
2.2.1. Hydrolase and transferase inhibitors 16
2.2.2. Inhibitors of epigenetic enzymes 19
2.2.3. Inhibitors of helicases and repair proteins 19
2.3. Receptors, signalling proteins, and cellular models 21
2.3.1. Compounds that affect membrane and intracellular receptors 21
2.3.2. Compounds that affect signalling proteins and regulatory proteins 23
2.3.3. Pyroptosis inducers 24
2.4. Summary of Section 2 25
3. Cytotoxic action of azolo[1,5-*a*]pyrimidines 25
3.1. Compounds with cytotoxic activity in the low and submicromolar ranges 25
3.2. Compounds with cytotoxic activity in the mid-micromolar range 32
3.3. Compounds showing cytotoxicity in the high micromolar range or showing no cytotoxicity 37
3.4. Summary of Section 3 38
4. Conclusion 39
5. List of abbreviations and symbols 40
6. References 41

1. Introduction

Malignant tumours pose a serious challenge to global public health, as they are the second leading cause of death, being only behind cardiovascular diseases.[1] The challenge of combating cancer diseases largely stems from the fact that this group of diseases covers a wide range of pathophysiological conditions of various origins that have in common uncontrolled division of cells capable of invading other organs and tissues of the body. Since any dividing cell in the body can actually be susceptible to malignancy, while malignization may involve mutations in a number of oncogenes, anti-oncogenes, and mRNA genes,[2] a separate therapeutic approach is needed for each particular disease in this group. Despite the most recent advances in the treatment of malignant tumours such as development of antitumour vaccines,[3] oncolytic viruses,[4] and antigen-specific antibodies,[5] the use of small molecules is still a key and highly relevant approach to the treatment of cancer. In 2025, the U.S. Food and Drug Administration (FDA) approved 46 medications out of which 31 were based on small

Received 3 June 2026
© 2026 Uspekhi Khimii, ZIOC RAS, Russian Academy of Sciences

molecules. Among anticancer drugs, these numbers were 16 and 10, respectively.[6]

An important structural motif in biologically active compounds is represented by nitrogen-containing heterocycles, which are present in more than 75% of drugs approved for clinical use.[7] Bi- and polycyclic aza-heterocycles, azoloazines, hold a special place in this class, as they are bioisostere analogues of natural purines, which play a key role in the storage of genetic information and signal transduction between cells. The azoloazine subclass includes azolo[*a*]pyrimidines (azaindolizines), which are nitrogen-containing fused systems with a bridging nitrogen atom. A number of research teams, including ours, have shown[8–15] that these compounds are a privileged class of heterocycles in medicinal chemistry, owing to diverse biological activities they possess. The studies[16–23] carried out by our research team between 2022 to 2025 were related to the search for azolo[*a*]pyrimidines with a potential anticancer effect. This area of research has become especially relevant over the past few years, since FDA approved a number of anticancer drugs based on heterocycles of this class; some of these derivatives are currently in Phase II and III clinical trials. These compounds exhibit activity against a number of kinases: zanubrutinib is a Bruton's tyrosine kinase inhibitor,[24] larotrectinib inhibits ROS1 receptor tysosine kinase and pan-TRK and ALK (anaplastic lymphoma kinases),[25] repotrectinib is a tropomyosin-receptor kinase (TRK) inhibitor,[26] dinaciclib inhibits cyclin-dependent kinases,[27] and samuraciclib is a selective inhibitor of cyclin-dependent kinase 7 (CDK7)[28] (Fig. 1).

In view of the above, it is evident that the first step in identification of the most promising avenues for the development of anticancer agents based on azole[*a*]pyrimidines is to systematize the data available from the literature. The existing reviews on this topic often describe the broad spectrum of biological activity of heterocycles in this series,[29–33] without focusing on anticancer activity as a key property; as a result, they lack an analysis of the important structure–activity relationship. The specifically focused papers that discuss the antitumour potential of azolopyrimidines are devoted either exclusively to the effects of such compounds on oncogenic macromolecular targets,[34,35] or to the quantitative determination of cytotoxic activity,[36] or include other fused systems.[37] The most comprehensive relevant review[38] published in 2025 is limited to pyrazolo[1,5-*a*]pyrimidines, with emphasis being placed on their synthesis, while paying little attention to structure–activity relationships.

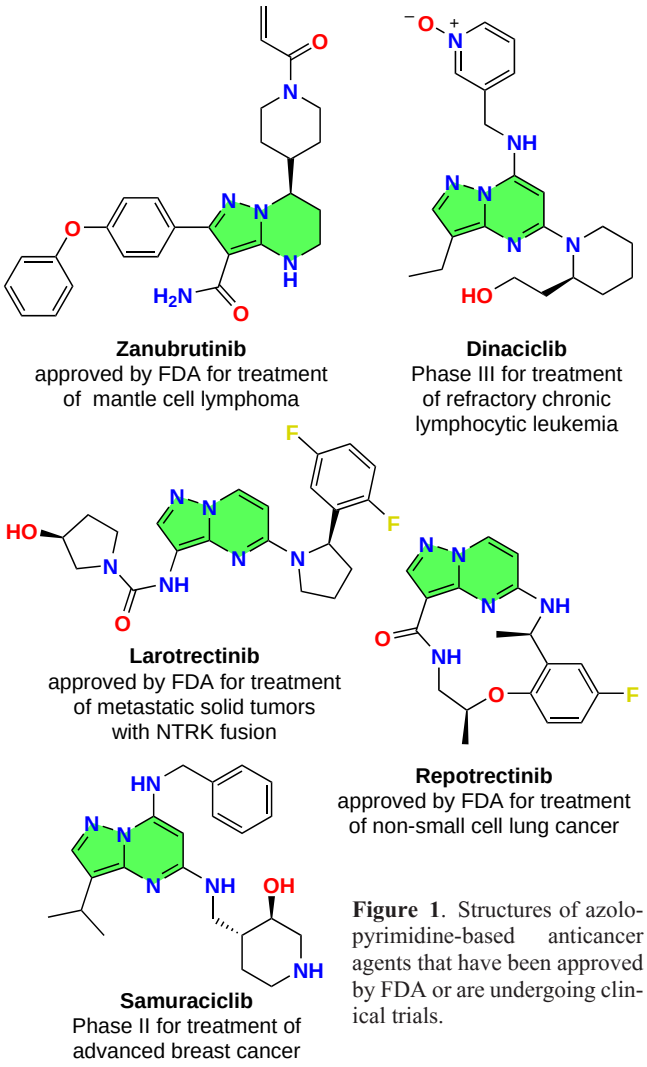


Figure 1. Structures of azolopyrimidine-based anticancer agents that have been approved by FDA or are undergoing clinical trials.

This review analyzes recent publications on pyrazolo- and 1,2,4-triazolo[1,5-*a*]pyrimidines (Fig. 2), which have a cytotoxic effect against tumour cells and/or influence molecular targets involved in oncogenic pathways. Particular attention is paid to ways for structure optimization of these aza-heterocycles in order to increase their affinity for a specific target and/or enhance their cytotoxic activity. The main structure–activity relationships (SARs) have been identified, and the most

E.**M**.**Mukhin**. PhD, Junior Researcher at the ChemPharm Centre of UrFU.
E-mail: mukhin.evg.m@gmail.com
Current research interests: abnormal nucleosides, chemical modification of antibiotics and antiviral drugs, synthesis of azaheterocyclic compounds, study of the structure–activity relationship.
K.**V**.**Savateev**. Doctor habilitatus, Associate Professor, Research at the Problem Laboratory of Physiologically Active Compounds of the Institute of Chemical Engineering, UrFU.
E-mail: i-krafttt@yandex.ru
Current research interests: azoloazines, azolopyrimidines, azolopurines, abnormal nucleosides, nitriles, chlorodeoxygenation, structure–activity relationship, medicinal chemistry, anticancer agents, antiviral agents.
E.**V**.**Bersneva**. Research Engineer at the ChemPharm Centre.
E-mail: miass10bersneva@mail.ru
Current research interests: azolo[1,2,4]triazines, chemical modification of antibiotics and antiviral drugs, synthesis of azaheterocyclic compounds, ANRORC reactions, study of structure–activity relationship.
S.**V**.**Androv**. Research Assistant at the ChemPharm Centre.
E-mail: sergioandrov@gmail.com
Current research interests: fluoroquinolones, hybrid molecules, abnormal nucleosides, chemical modification of antibiotics and antiviral drugs, synthesis of azaheterocyclic compounds, azoloazines, nitriles, study of structure–activity relationship.
V.**L**.**Rusinov**. Corresponding Member of RAS, Doctor habilitatus, Head of the Department of Organic and Biomolecular Chemistry of UrFU. E-mail: v.l.rusinov@urfu.ru
Current research interests: abnormal nucleosides, chemical modification of antibiotics and antiviral drugs, synthesis of azaheterocyclic compounds, study of structure–activity relationship.

Translation: Z.P.Svitanko

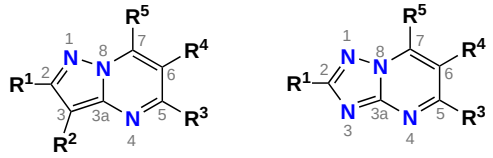


Figure 2. General structural formulas of pyrazolo- (*on the left*) and 1,2,4-triazolo[1,5-*a*]pyrimidines (*on the right*) with atom numbering in the heterocyclic core.

promising substitution patterns on the central heterocyclic ring were emphasized.

For standardization and clear presentation of the literature data (as well as for correct comparison of the data), this review uses the following principle: the half-maximal inhibitory concentration (IC_{50}) for macromolecular targets is expressed in nmol L^{-1} (nM), while the half-maximal growth inhibitory concentration against cell lines is denoted by GI_{50} and is expressed in μmol L^{-1} (μM).

2. Azolo[1,5-*a*]pyrimidines as a basis for the design of targeted anticancer drugs

2.1. Kinases and kinase inhibitors

2.1.1. Serine/threonine kinase inhibitors

Cyclin-dependent kinases play a central role in mammalian cell division[39] and are considered as promising targets for cancer therapy.[40] The drug dinaciclib inhibiting CDK2 (see Fig. 1) was taken as a parent compound to vary substituents in the pyrazolopyrimidine core[41] (Fig. 3). It was found that the colorectal carcinoma cell line (HCT-116) is generally quite sensitive to heterocycles **1**–**4**. Ten of the twenty compounds tested at a concentration of 10 μM reduced proliferative activity of HCT-116 cells by more than 50% compared to that for triple-negative breast cancer cells (MDA-MB-231). Compound **2a** (see Fig. 3) proved to be most promising, as it reduced the proliferative activity of HCT-116 and MDA-MB-231 cancer cells and WI-38 cells (human lung fibroblasts) in the submicromolar range and inhibited CDK2 more effectively than roscovitine [IC_{50} (CDK2) = 140 nM].

For other dinaciclib analogues reported by Almehmadi *et al.*,[42] it was found that all nine compounds **5** they studied inhibit CDK2 in a low or sub-micromolar range; however, high cytotoxicity against T-lymphoblastic leukaemia cells (MOLT-4) and promyelocytic leukaemia cells (HL-60) was found for compounds containing a halogen atom in the *para*-position of the benzene ring at the C(7) atom. Compound **5a** was most promising in this series: it showed a higher cytotoxicity than dinaciclib and inhibited CDK2 to the same extent (Fig. 4).

Evaluation of pyrazolo[1,5-*a*]pyrimidine derivatives **6** (see Fig. 4) as CDK2 inhibitors indicated that these heterocycles are not sufficiently active (the maximum inhibition at a concentration of 10 μM was 28%).[43] The subsequent assessment of the cytotoxic activity on cell lines of breast ductal adenocarcinoma (MCF-7), hepatocellular carcinoma (HepG2), lung adenocarcinoma (A549), and human colorectal adenocarcinoma (Caco-2) also confirmed that all compounds **6** are markedly inferior to doxorubicin (IC_{50} for the indicated cell lines ranges from 10.05 to 111.22 μM, while that for doxorubicin is 0.44–8.51 μM).

Phillipson *et al.*[44] investigated the inhibitory properties of pyrazolopyrimidines **7**–**10** against CDK9. A consistent study of SARs has revealed that the substitution pattern in the (hetero)-aryl moiety of sulfonamide is exceptionally important for the

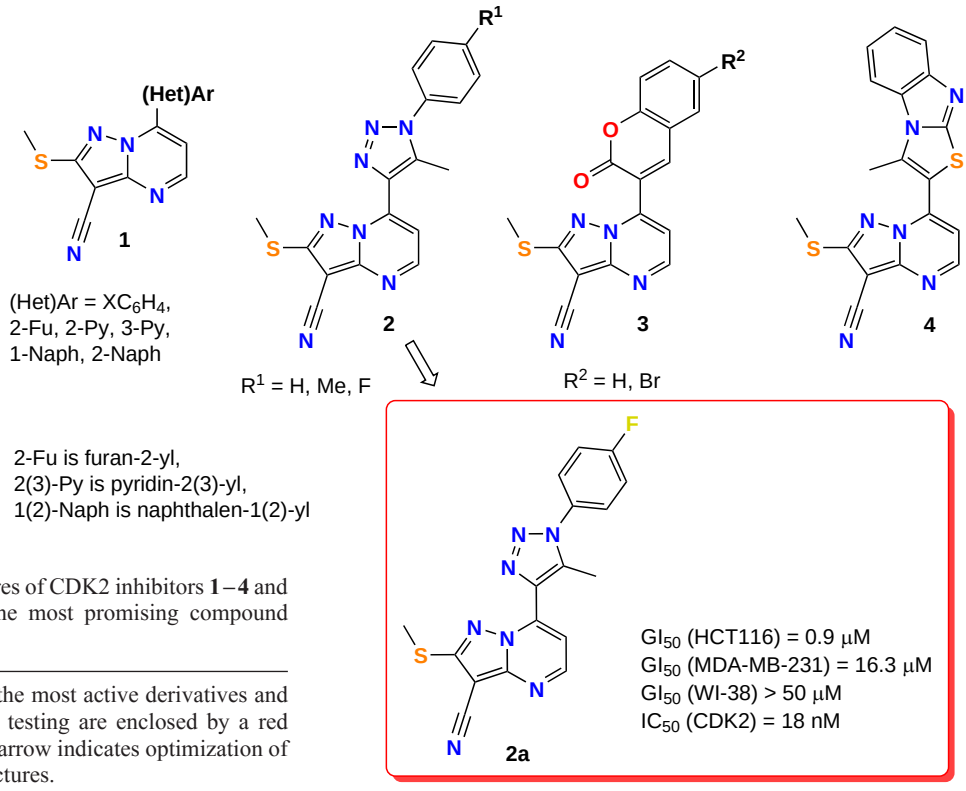


Figure 3. Structures of CDK2 inhibitors **1**–**4** and activity data for the most promising compound **2a**.†

† Here and below, the most active derivatives and the results of their testing are enclosed by a red line, and the blank arrow indicates optimization of the compound structures.

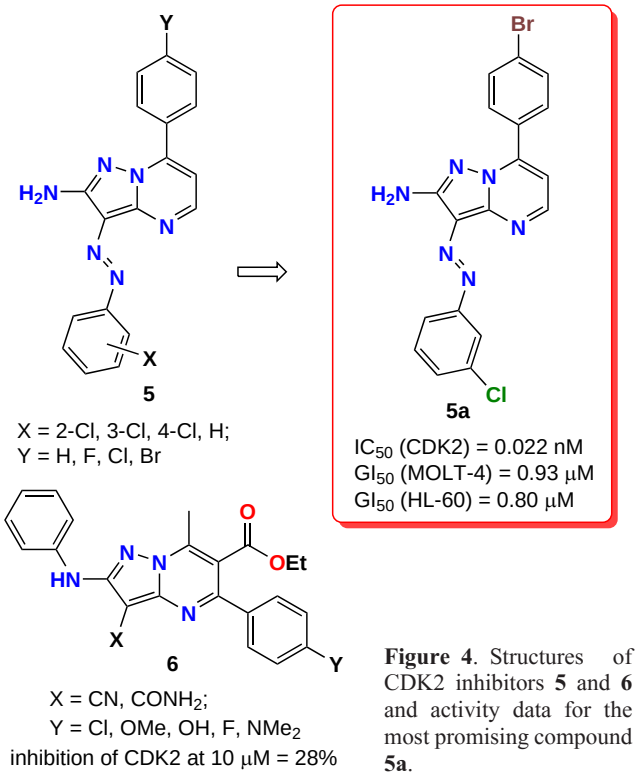


Figure 4. Structures of CDK2 inhibitors **5** and **6** and activity data for the most promising compound **5a**.

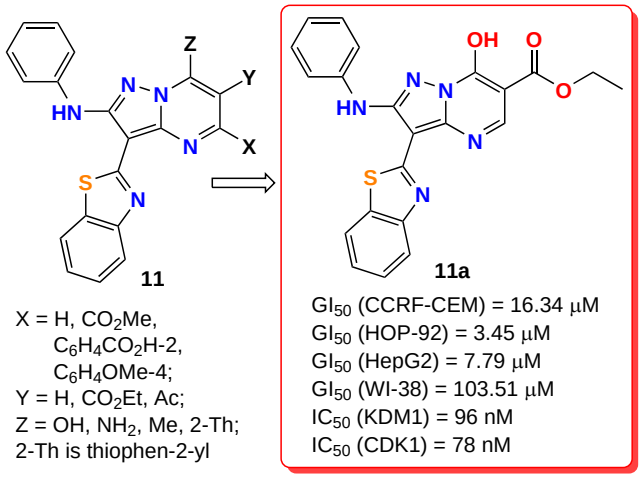


Figure 6. Structures of compounds **11** and activity data for the most promising derivative **11a**.

presence of activity. Furthermore, the optimal substituent at the C(5) position is a chlorine atom, while the hydrazone bridge between the azolopyrimidine and the sulfonamide, although most preferable in terms of inhibitory activity, is metabolically labile; therefore, it was replaced by an ethylamine moiety (structure **10a**) (Fig. 5). In addition, compound **10a** exhibited the highest selectivity to CDK7 and PI3Kα (phosphatidylinositol 3-kinase alpha), despite its reduced inhibitory activity against the target CDK9 kinase.

Husseiny[45] incorporated a benzothiazole moiety into azolopyrimidine molecules and studied the cytotoxic properties of six representatives of this family: compounds **11**. Derivative **11a** proved to be most promising; the half-maximal inhibitory concentrations were determined for this compound in extended tests. It was found that the mechanism of action of this compound may be attributable to the inhibition of the CDK1 and KDM1 proteins, as it causes cell cycle arrest in the G2/M phase and induces apoptosis (Fig. 6).

Elgiushy *et al.*[46] continued optimization of the pyrazolopyrimidine skeleton **12** for the development of dual inhibitors, inhibiting both the CDK2 enzyme and tubulin

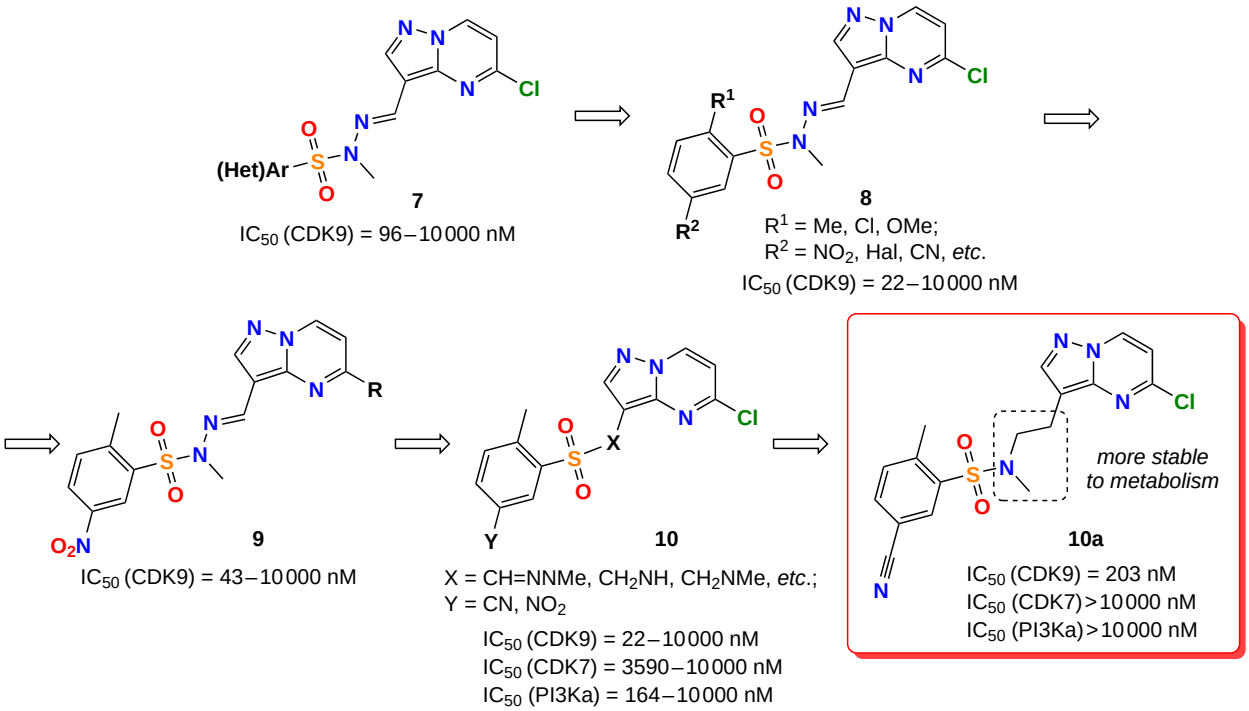


Figure 5. Structure optimization and inhibition characteristics of compounds **7**–**10**, including the most promising derivative **10a**.

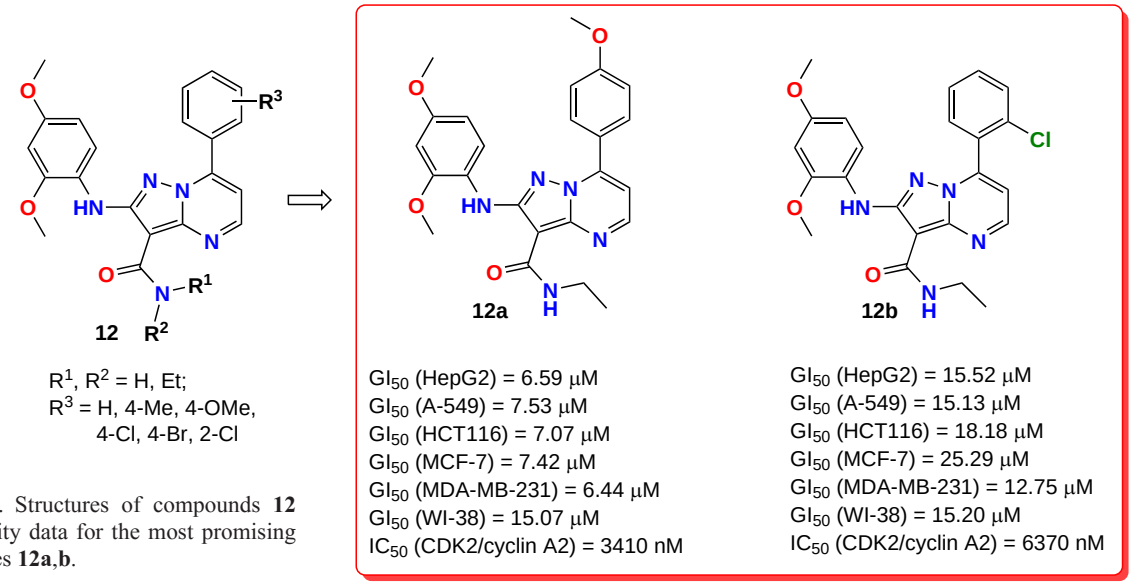


Figure 7. Structures of compounds **12** and activity data for the most promising derivatives **12a**,**b**.

polymerization. The initial assessment of the activity of compounds **12** in the MTT assay[‡] showed that the unsubstituted amide or diethylamide moiety is less preferable than the monoethylamide group. The introduction of a halogen atom into the *para*-position of the benzene ring at C(7) resulted in the disappearance of the cytotoxic effect. When a methyl group was present at this position, the corresponding derivative exhibited some activity, while the 4-methoxy group and an *ortho*-chlorine atom proved to be the optimal choice. It was found that the cytotoxic activity of compounds **12a**,**b** is due to the inhibition of tubulin polymerization (which is more pronounced than that by colchicine) and the CDK2 enzyme. However, these compounds caused a decrease in the viability of not only tumour cells but also normal cells such as the WI-38 diploid human fibroblasts (Fig. 7).

Casein kinase 2 (CK2) is a key regulator of numerous oncogenic pathways, which is overexpressed in cells of breast carcinoma, lung adenocarcinoma, prostate carcinoma, and lymphoma.[47] Krämer *et al*.[48] paid particular attention to optimization of the structure of pyrazolopyrimidines and their macrocyclic analogues **13** to enhance their inhibitory activity against CK2 and reduce their affinity for other targets. The most promising molecules **13a**,**b** were less active than CK2 inhibititor silmitasertib (IC_{50} = 100–500 nM), with the IC_{50} values *in vitro* for these compounds being in a low micromolar range (Fig. 8).

Study of a series of macrocyclic pyrazolo[1,5-*a*]pyrimidines **14** showed that C(3)-carbonitrile derivatives are the most potent CK2 inhibitors; however, due to their low selectivity in a panel assay involving 126 different kinases, the nitrile group was replaced by a chlorine atom (Fig. 9).[49] Quantitative structure–activity relationships were also established for other variable moieties R^1 and R^2; the most promising compound **14** characterized by IC_{50} (CK2) = 160 nM contained a 3,3-difluorocyclobutyl substituent and a carboxyl group in the pyrrolidine ring.

A search for selective CK2 inhibitors performed by sequential variation of the substituents at the C(5) and C(7) positions in pyrazolo[1,5-*a*]pyrimidinecarbonitriles was described by

[‡] MTT is 3-(4,5-dimethylthiazol-2-yl)-2,5-diphenyltetrazolium bromide.

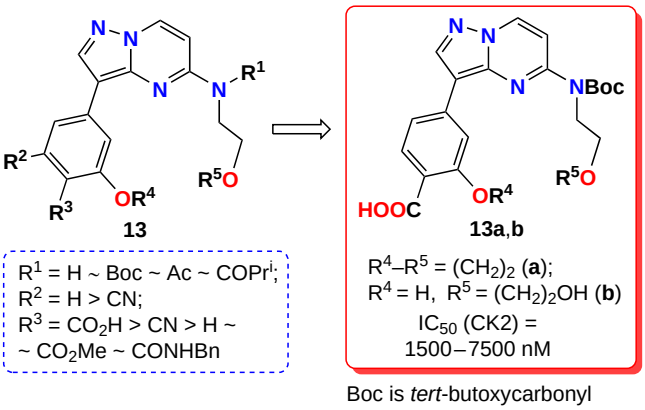


Figure 8. Structures and SARs for compounds **13** and ranges of IC_{50} values for the most promising derivatives **13a**,**b**.[§]

Dowling *et al*.[50,51] (Fig. 10). According to initial screening, the most promising compounds for this purpose are pyrazolo[1,5-*a*]-pyrimidine-3-carbonitriles **15**–**18**, which contain aryl and heteroaryl moieties at the C(5) atom and a secondary amino group at the C(7) atom, with a small carbocyclic or heterocyclic moiety as a substituent at the nitrogen atom. Most of the compounds considered in this study inhibited the growth of HCT-116 colorectal carcinoma cells in the submicromolar range, and one compound of the series **17** demonstrated a moderate anticancer activity in a DLD-1 xenograft model in immunodeficient mice.

A promising class of CK2 inhibitors was found among a series of 6-(tetrazol-5-yl)azolopyrimidines **19** and **20**.[52] The performed screening revealed several compounds with IC_{50} values in the submicromolar range and also made it possible to establish some structure–activity relationships (Fig. 11). It was noted that 1,2,4-triazolo[1,5-*a*]pyrimidines **20** were generally less active than pyrazolo[1,5-*a*]pyrimidines **19**. The inhibitory

[§] Here and below, the blue dashed box shows SARs: qualitative relationships between the activity of compounds in a single series and the nature of the substituent, as indicated by the symbols < (less than), > (greater than), a comma, or the symbol ~ (approximately equal).

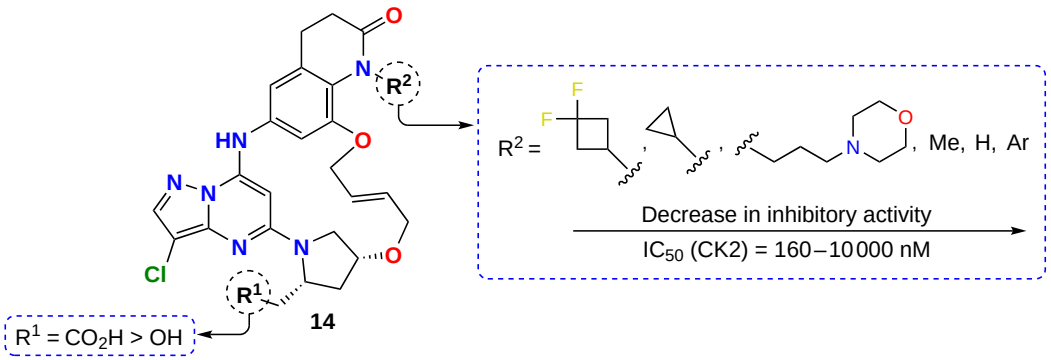


Figure 9. Structures and SARs of compounds **14**.

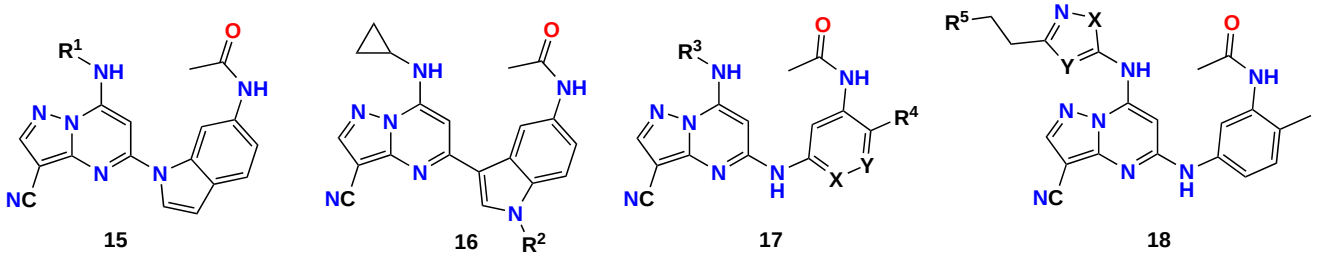


Figure 10. Structures of CK2 inhibitors **15**–**18** and activity data for these compounds.

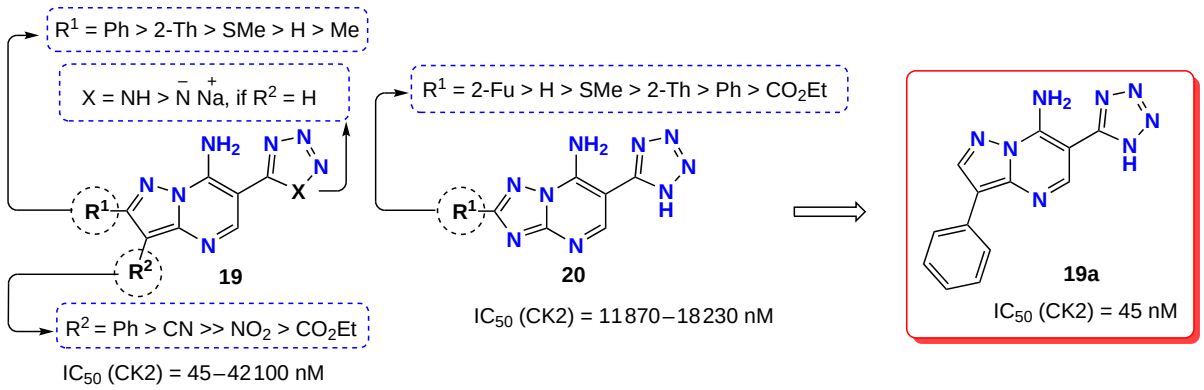


Figure 11. Structures, SARs, and data on the activity of compounds **19** and **20**, including the most promising compound **19a**.

effect of the latter may be enhanced by introducing a lipophilic moiety into the azole ring (see, for example, compound **19a**).

Wang *et al.*[53] identified SARs for pyrazolo[1,5-*a*]pyrimidines **21** as inhibitors of Pim-2 kinase, which is an important protein providing growth and survival in multiple myeloma.[54] Molecular design of inhibitors **21** was carried out using X-ray diffraction data for the complex formed by compound **21a** with the active site of this enzyme. It was found that the presence of a hydrogen atom at the C(7) position is preferred over the hydroxyl group, even though in the latter case, hydrogen bond formation with Lys-67 is possible in the active site of Pim-2 (Fig. 12). The replacement of the aryl amide group by a heteroaryl amide group and introduction of a linker between the azoloazine system and the piperidine moiety were effective strategies, which led to the optimized structure for the new lead compound **21b**.

Dwyer *et al.*[55] performed a search for Pim-1 and Pim-2 kinase inhibitors, because both proteins were shown[56] to be overexpressed in various types of malignant tumours in humans. The initial high-throughput screening identified several hits in the pyrazolo[1,5-*a*]pyrimidine series, and structural optimization was carried out based on this core structure (Fig. 13). First, for a compound with a naphthalene moiety fixed at the C(3) position, derivative **22** containing an ethylenediamine group [R = $(CH_2)_2NH_2$] was found to have the strongest inhibitory properties. The (hetero)aryl moiety at the C(3) position of ethylenediamine derivative **23** was optimized considering these data. It was found that replacement of the fused naphthalene rings by a combination of aryl and heteroaryl moieties leads to an increase in the inhibitory properties, with *meta*-substituted derivatives (compound **23a**) being more active than the *ortho*- and *para*-isomers.

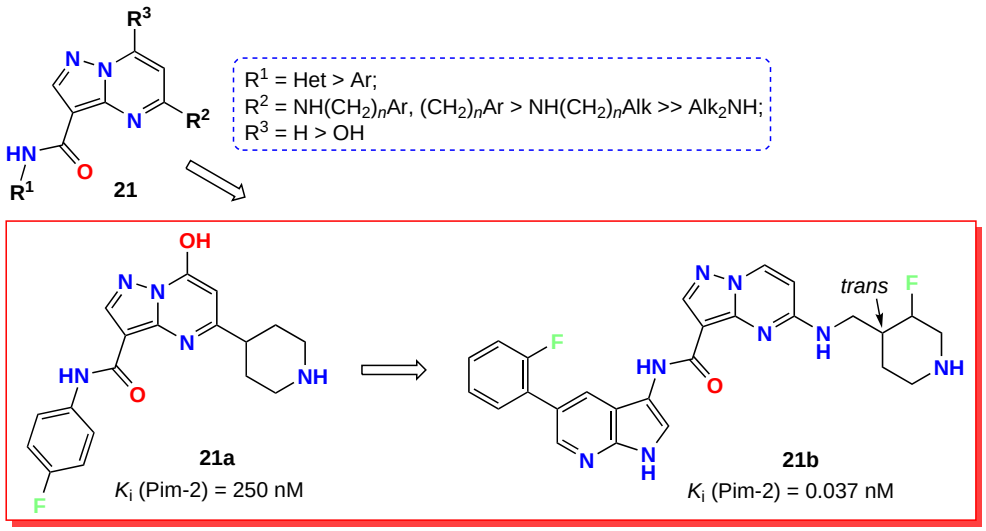


Figure 12. Structure optimization and SARs of compounds **21** and the inhibition constant (K_i) for derivatives **21a**,**b**.

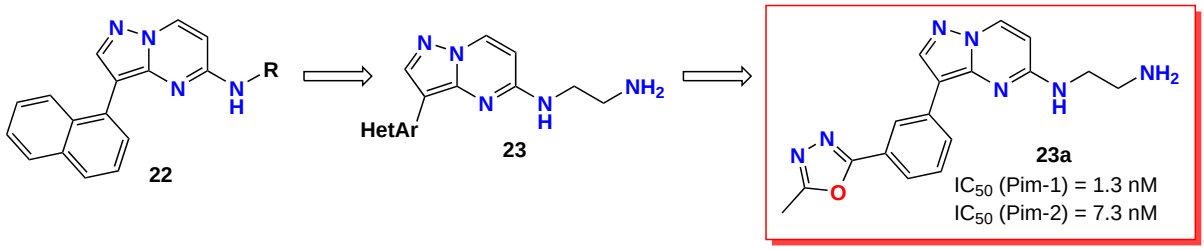


Figure 13. Structure optimization for compounds **22** and data on the activity of the most promising compound **23a**.

A similar optimization of the structure of the original hit was also carried out in a later study.[57] The authors noted that for Pim-1 inhibition by heterocycles **24**, an electron-withdrawing group (EWG), trifluoromethyl group or a chlorine atom, must be present at the *meta*-position of the benzene ring at the C(3) atom. In turn, the C(5) position must contain a group capable of acting as a hydrogen bond acceptor (HBA) for the Asp-128 and Asp-131 residues in the kinase active site. It turned out, however, that amino group is preferred for this position over a hydroxyl group, ester group, or sulfonic group. Compound **24a**, which inhibited Pim-1 in the mid-nanomolar range, was most active in this series (Fig. 14).

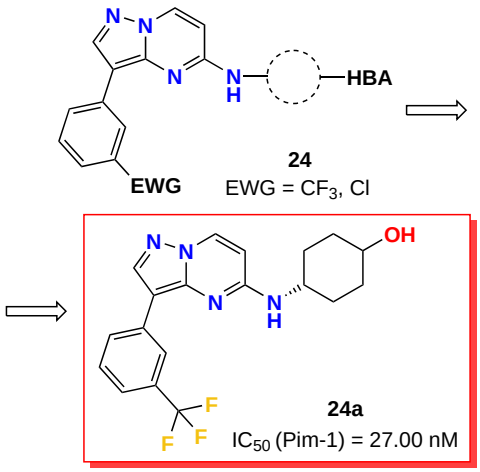


Figure 14. Structures of Pim-1 inhibitors **24** and the inhibitory concentration for the most promising compound **24a**. The dashed ring stands for an aliphatic ring or a saturated heterocycle.

A series of Pim serine/threonine kinase inhibitors was described by Abdulrahman *et al.*[58] (Fig. 15). The primary evaluation of the cytotoxic activity of compounds **25** using three

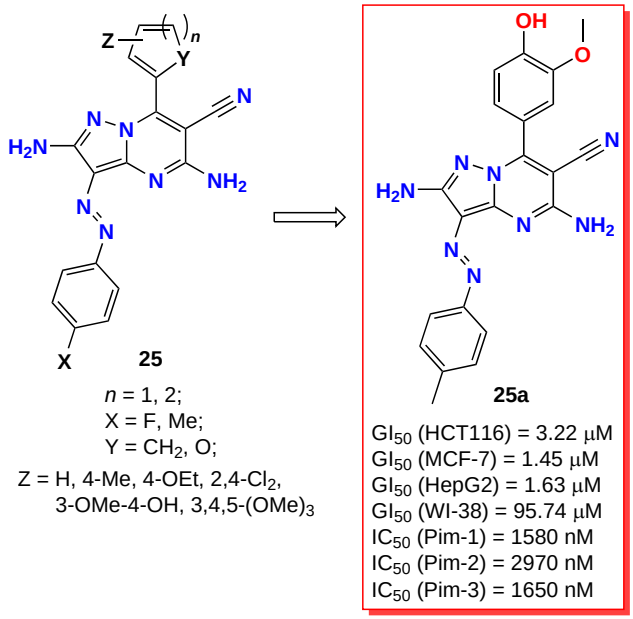


Figure 15. Structures of Pim-1 inhibitors **25** and data on the activity of the most promising compound **25a**.

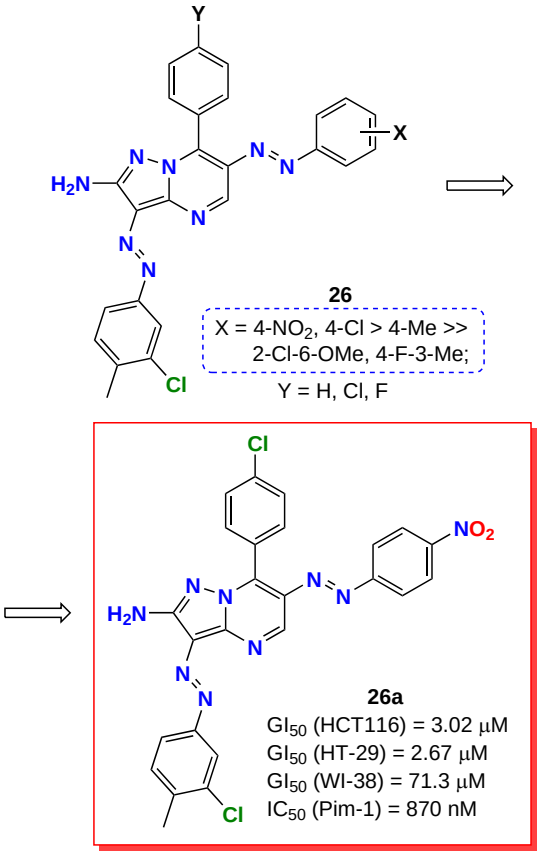


Figure 16. Structures and SARs for compounds **26** and data on the activity of the most promising derivative **26a**.

cell lines showed that substituent X has little effect on cytotoxicity. On the one hand, replacement of the aryl group at C(7) by a furan-2-yl group increased the cytotoxic activity of the corresponding derivatives; on the other hand, compound **25a**, which contained a 4-hydroxy-5-methoxyphenyl group, proved to be the most active. This compound inhibited Pim kinases in the submicromolar range at the level of the staurosporine drug [IC_{50} (Pim) = 77–477 nM].

While expanding the series of derivatives **25**, Farghaly *et al.*[59] obtained azolopyrimidines **26** containing two azo groups at the C(3) and C(6) positions (Fig. 16). All compounds **26** exhibited cytotoxic activity in the low micromolar range, and

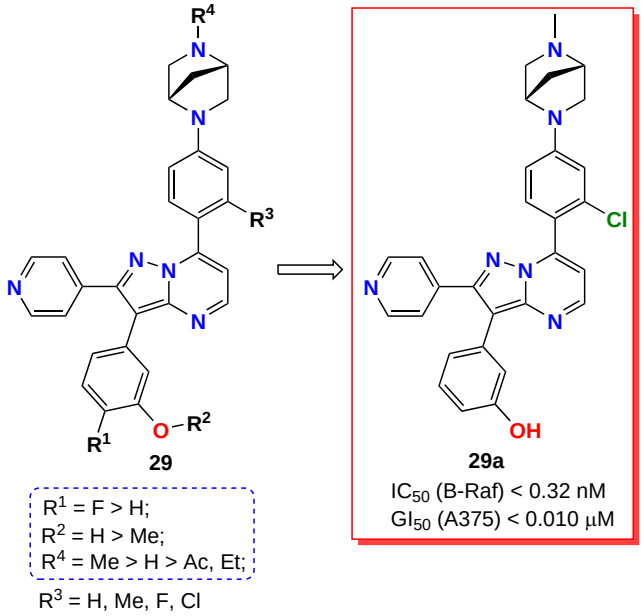


Figure 18. Structures and SARs for compounds **29** and activity data for the most promising derivative **29a**.

the most active derivative **26a** surpassed doxorubicin in selectivity by inhibiting Pim-1 kinase with IC_{50} of 870 nM.

The initial screening of eleven structural analogues of known Pim-1 inhibitors (**27** and **28**), which exhibited cytotoxic activity against colorectal carcinoma (HCT-116) and breast ductal adenocarcinoma (MCF-7) cell lines was performed by Philoppes *et al.*[60] (Fig. 17). The authors did not conduct a systematic study of SAR. However, the reported data indicate that compounds **28** are, on average, more active against HCT-116 cells, whereas heterocycles **27** are more effective at reducing the proliferative capacity of MCF-7 cells. For several derivatives characterized by the greatest cytotoxic effect, in particular for compound **28a**, IC_{50} values for Pim-1 were determined; all values were in the low micromolar range.

In 66% of cases of malignant melanoma, there is increased activity of the B-Raf kinase, making it a promising target for treating this type of tumour.[61] Wang *et al.*[62] reported a search for B-Raf inhibitors among pyrazolo[1,5-*a*]pyrimidines **29** (Fig. 18). It was shown that the presence of a diazabicyclo[2.2.1]-heptanyl moiety linked to a benzene ring is the most favourable

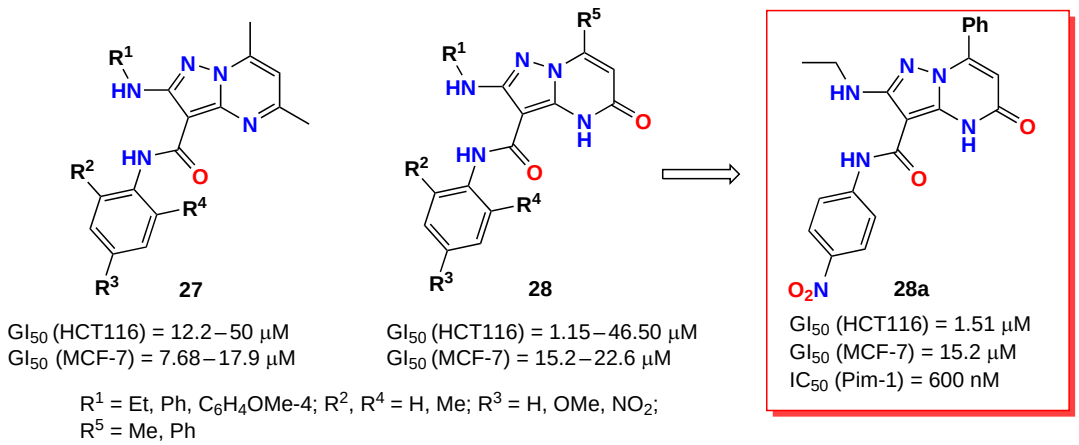


Figure 17. Structures and data on the activity of Pim-1 inhibitors **27**, **28**, including the most promising compound **28a**.

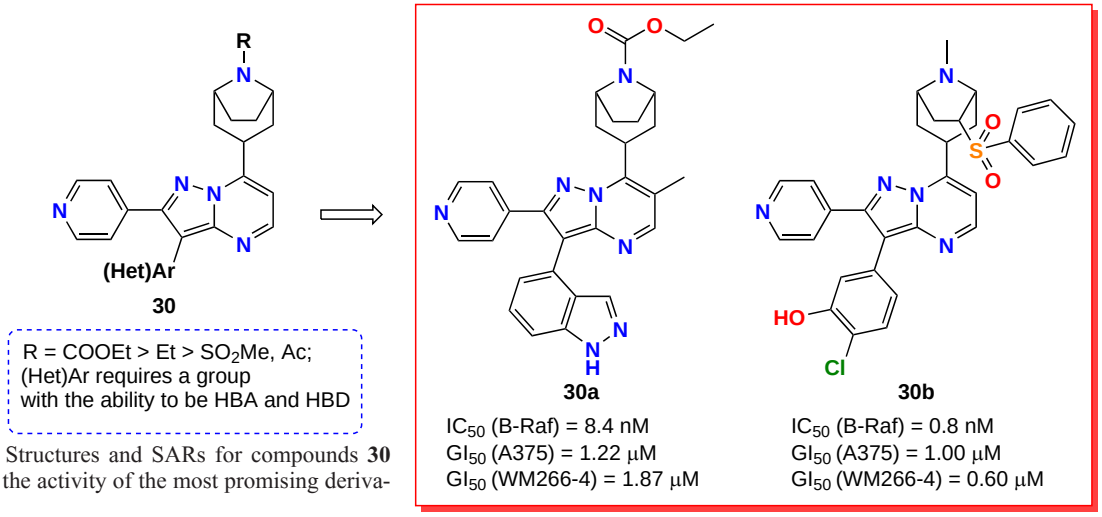


Figure 19. Structures and SARs for compounds **30** and data on the activity of the most promising derivatives **30a**,**b**.

factor influencing both B-Raf inhibition and activity against the A375 cell line. A hydroxy group present in the C(3) phenyl substituent also appears to be an important condition for the manifestation of inhibitory activity. In addition, compounds containing a tertiary amino group in the diazabicyclo[2.2.1]-heptanyl moiety are more active than derivatives with secondary or acylated amino groups. The structural optimization resulted in compound **29a**, which effectively inhibited B-Raf and decreased the proliferative capacity of A375 melanoma cells.

B-Raf inhibitors of a similar series of pyrazolo[1,5-*a*]-pyrimidines **30** were studied by Di Grandi *et al.*[63] The structural optimization involved the variation of the (hetero)aryl moiety at the C(3) position of the azoloazine skeleton and the N-substituent in the tropane ring (Fig. 19). Considering the SAR and molecular docking data, it was found that for a noticeable inhibitory effect, groups that can act as hydrogen bond donors (HBD) and acceptors (HBA) are required in the (hetero)aryl moiety; the 4-indazole (**30a**) and *o*-chlorophenol (**30b**) moieties are optimal for this purpose. The effect of substituent in the tropane ring on the inhibitory activity is less pronounced: various groups may be present, but the activity against malignant melanoma cells (A375 and WM266-4 cell lines) is best preserved in the presence of an ethyl or ethoxycarbonyl group.

Berger *et al.*[64] synthesized 3-(hetero)aryl-7-arylpyrazolo-[1,5-*a*]pyrimidines **31** as potential B-Raf inhibitors. In the optimization of the structures of these compounds, the main focus was on the substituent at the C(3) position of the heterocyclic system (Fig. 20). It was shown that the presence of a (hetero)aryl moiety containing a tertiary alkylamino group (**31a**) is most favourable for the inhibitory activity. The inhibitory activity somewhat decreases upon removal of the tertiary amino group and decreases even further when the (hetero)aryl ring is replaced by an ester or alkyne group.

A somewhat lower inhibitory activity against B-Raf was inherent in pyrazolo[1,5-*a*]pyrimidines **32** reported by Gopalsamy *et al.*[65] It was found that for the activity of these compounds, it is preferable that an amide moiety linked to a tertiary amino group by an alkyl chain be present at the C(3) position. In addition, an urea moiety is more advantageous as a linker between the two phenyl groups than an amide group (Fig. 21). This combination of structural features led to the synthesis of the most potent inhibitor in this series, compound **32a**.

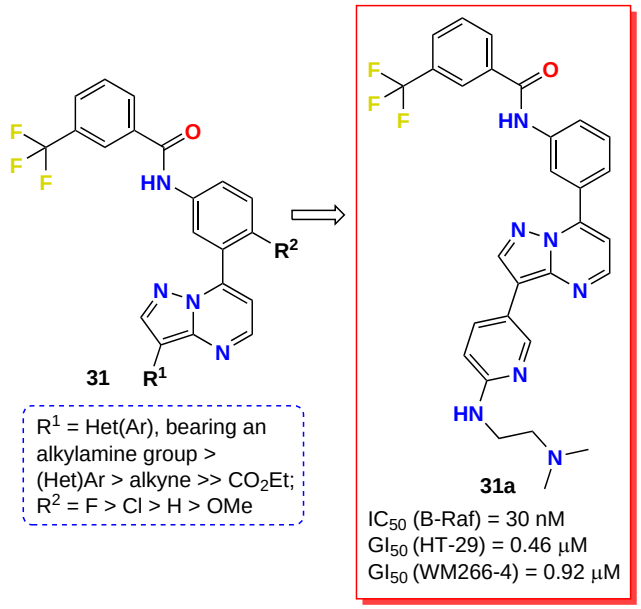


Figure 20. Structures and SARs for compounds **31** and data on the activity of the most promising derivative **31a**.

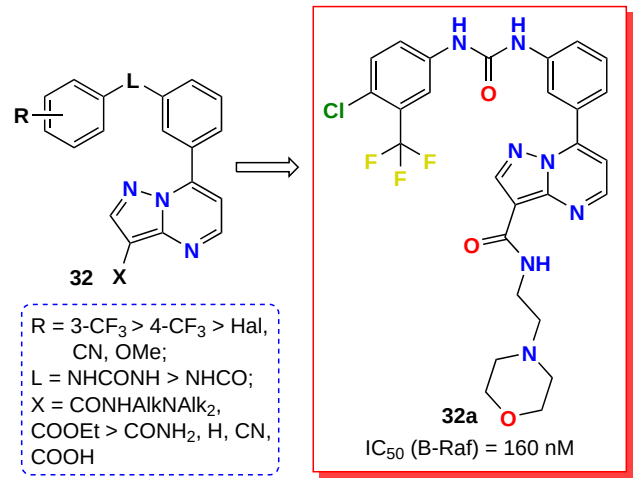


Figure 21. Structures and SARs for compounds **32** and data on B-Raf inhibition for the most promising derivative **32a**.

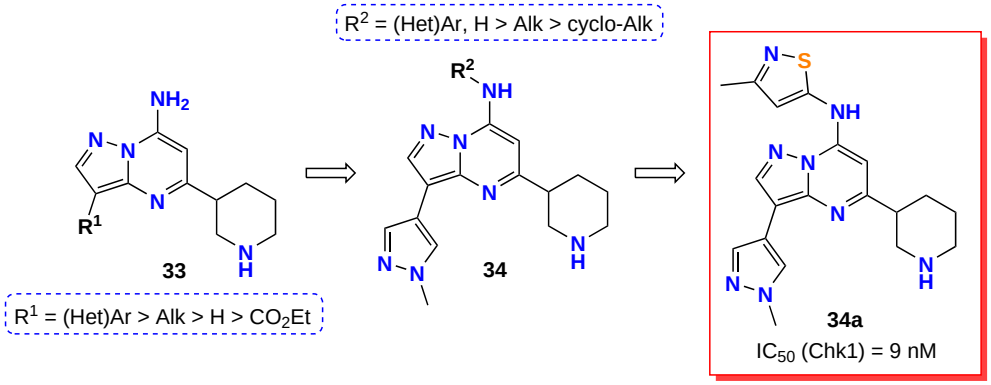


Figure 22. Structure optimization and SARs of Chk1 inhibitors **33** and data on the activity of the most promising compound **34a**.

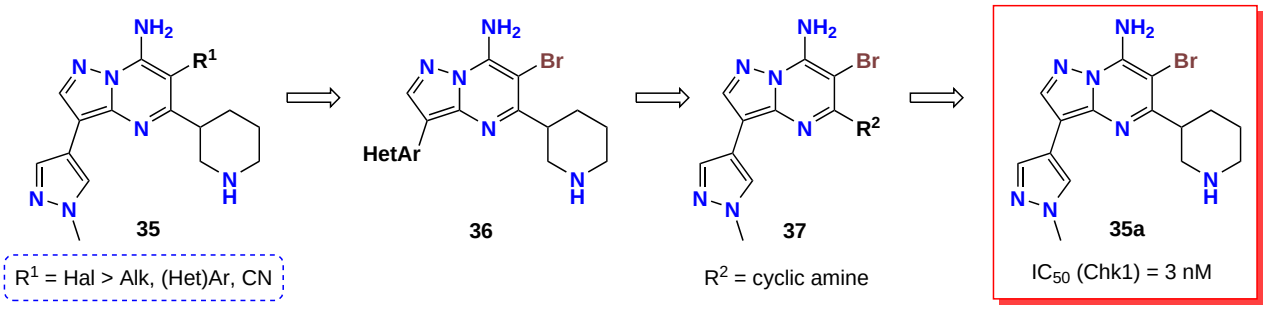


Figure 23. Structure optimization and SARs of Chk1 inhibitors **35** and data on the activity of the most promising compound **35a**.

The serine/threonine kinase Chk1 regulates the cellular response to DNA damage and is, therefore, considered to be a promising target for the development of anticancer agents.[66] A SAR study of Chk1 inhibitors[67] in the pyrazolo[1,5-*a*]pyrimidine series revealed certain correlations, which are shown in Fig. 22. Thus, by sequential variation of the corresponding substituents in molecules **33** and **34**, the optimized structure **34a** was obtained.

Further studies[68] indicated that for amino derivatives **35**, a halogen atom is the preferred substituent at the C(6) position of the heterocyclic system, since alkyl, (hetero)aryl, and nitrile derivatives were less active than halogen-containing molecules (IC_{50} values were in the mid- to high nanomolar range) (Fig. 23). The replacement of the *N*-methylpyrazole ring by an alternative heterocyclic substituent (pyridin-3-yl, furan-2-yl, or thiophen-2-yl) did not produce more active derivatives **36**. A similar trend was also observed for the C(5) position of molecule **37**: all alternative cyclic amine residues were inferior to the initially selected piperidin-3-yl ring. As a result, the only modification was the introduction of a bromine atom at the C(6) position, yielding compound **35a**.

2.1.2. Tyrosine kinase inhibitors

Bruton's tyrosine kinase (BTK) is an important protein for the development and functioning of B-lymphocytes.[69] A few FDA-approved BTK inhibitors are used in clinical practice to treat certain types of malignant tumours.[70] Guo *et al.*[71] reported data on the discovery of zanubrutinib (see Fig. 1) as an effective and selective covalent BTK inhibitor (Fig. 24). Regarding the relationship between the inhibitory activity and structure, it was found that the biphenyl ether moiety at the C(2) position is the optimal choice, since replacement of the terminal benzene ring by an alkyl group or replacement of the whole hydroxyphenyl moiety by OMe, OCF_3, CF_3, Me, Cl, or F resulted in lower activity. The inhibitory activity increased by two orders of magnitude upon transition from the pyrimidine-based compound **38** to tetrahydropyrimidine derivatives **39**, and further variation of the C(7)-substituent made it possible to decrease the IC_{50} value for structures **40** and **41** by yet another order of magnitude. The *S*-isomer of zanubrutinib **41** was 3.5 times more active than the corresponding *R*-isomer (a similar difference in activity depending on the stereochemistry was also observed for other derivatives in this series; however, the absolute configuration of the stereocentre was not determined in such cases).

Myeloproliferative disorders involve a mutation in Janus kinase 2 (JAK2), which leads to its permanent activation.[72] Hanan *et al.*[73] reported the design of pyrazolo[1,5-*a*]pyrimidine-based JAK2 inhibitors (Fig. 25). The variation of the heteroaryl moiety (pyridine, pyrazole, oxazole, and thiazole rings) in compounds **42** showed that the two last-mentioned options produce compounds possessing the highest inhibitory activity against JAK2. However, they caused undesirable inhibition of cytochrome P450 family enzymes, which was not observed for pyrazole derivatives **43**. Later, it was found that replacement of the N(1)-methyl group in pyrazole by a larger substituent R^2 leads to decreasing inhibitory effect. Finally, variation of the substituents on the benzene ring and introduction of C(5)-amino group afforded a series of heterocycles **44**, among which lead compound **44a** exhibited activity in the subnanomolar range.

Tropomyosin receptor kinases are involved in signalling pathways that trigger cell proliferation, differentiation, and survival; in the case of mutation of the corresponding gene, this leads to oncogenesis.[74] Among the TRK inhibitors approved for clinical use, larotrectinib and repotrectinib contain azolo-pyrimidine as a heterocyclic ring. Gong *et al.*[75] tested

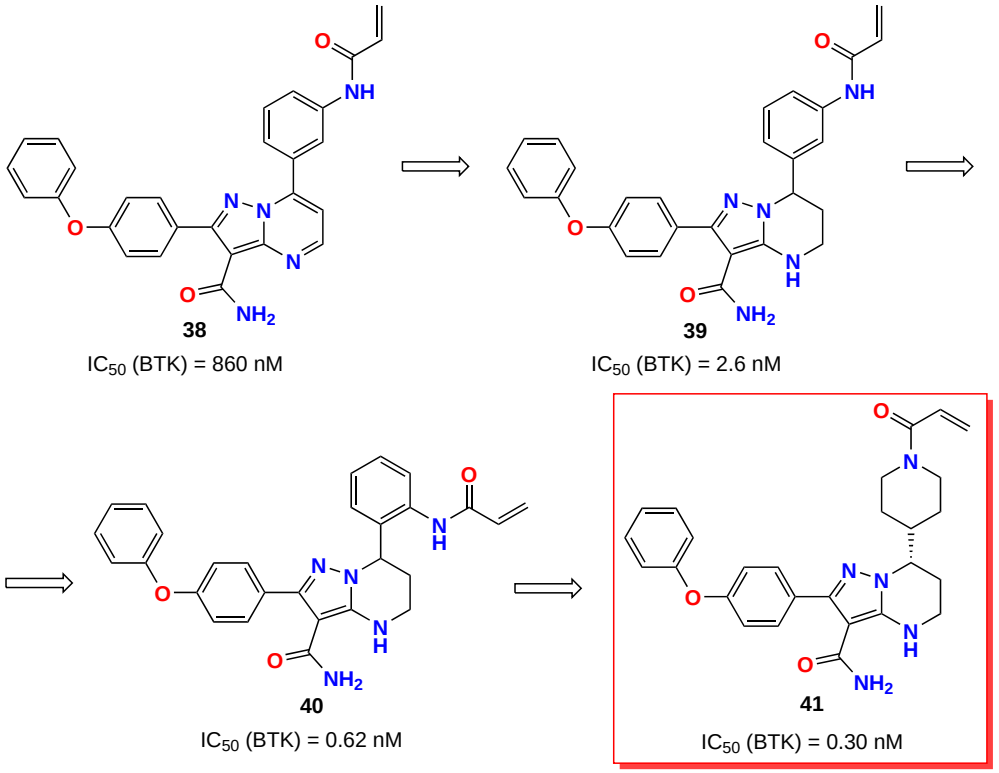


Figure 24. Structure optimization for compounds **38** and activity data for the most promising compound **41** (zanubrutinib).

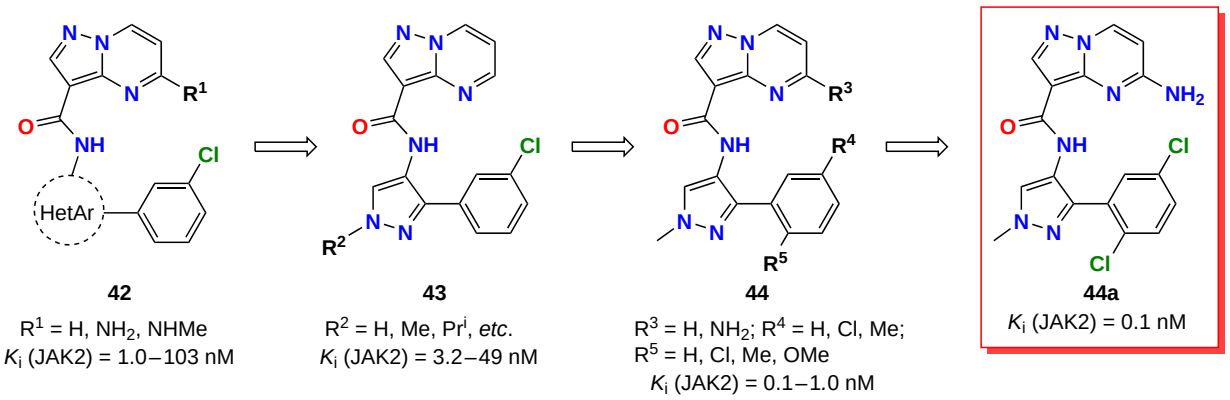


Figure 25. Structure optimization for compounds **42** and characteristics of JAK2 inhibition for compounds **42**–**44**, including the most promising compound **44a**.

modifications of various substituents in the azoloazine skeleton taking account of the X-ray diffraction data for complexes of known TRK inhibitors. It was found that replacement of the hydrogen atom in the NH group of the pyrazole ring in molecule **45** leads to increasing inhibitory activity, with the exception of bulky substituents [R = $(CH_2)_2OMe$, CH_2CMe_2OH]. Cycloalkyl groups and their analogues containing an oxygen atom in the saturated ring (for example, compound **45a**) also show promise in terms of activity (Fig. 26).

Further studies of this chemotype **45** provided the following conclusions. On the one hand, the pyrazole ring at the C(3) position of the heterocyclic system can be replaced by an urea moiety without any loss of activity (Fig. 27).[76] On the other hand, derivatives **46** containing thiourea or cyclobut-3-ene-1,2-dione moieties were much less active against all three TRK isoforms, unlike their analogues containing an aromatic ring at the urea nitrogen atom or a cyclic amino group (*e.g.*, compound **46a**). The methylation of the C(5)-amino group resulted in a further increase in activity (compound **46b**).

Jiang *et al.*[77] optimized the pharmacokinetic characteristics (low oral bioavailability, short half-life) of the initial threonine tyrosine kinase (TTK) inhibitor found as a result of virtual screening by replacing the central pyrazolo[3,4-*d*]pyrimidine scaffold with pyrazolo[1,5-*a*]pyrimidine (Fig. 28). Structure–activity relationship studies demonstrated that the most favourable substitution pattern in the C(5)-benzene ring of heterocycle **47** is the presence of two fluorine atoms at positions 2 and 3 and a methoxy group at position 4. The replacement of the cyclopropylamide substituent by other alkylamide groups resulted in a decrease in activity, so did the variation of the group at the C(7) atom. The most promising compound **47a** exhibited cytotoxic activity against several tumour cell lines,

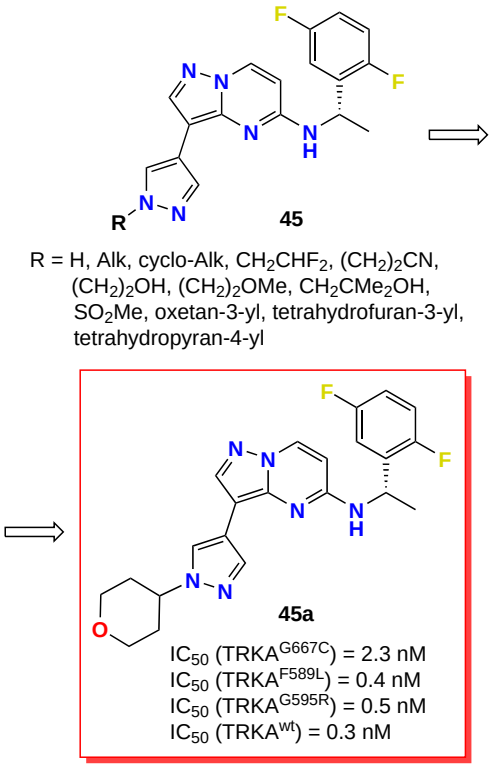


Figure 26. Structures of TRK inhibitors **45** and activity data for the most promising compound **45a**. IC_{50} values are presented for secondary mutant forms of the TRKA protein as well as wild type.

MDA-MB-468, HCT116, and A2780 (endometrioid ovarian carcinoma), in the submicromolar range.

Anaplastic lymphoma kinase (ALK) is a promising target for the treatment of non-small-cell lung cancer.[78] Liu *et al.*[79] combined a pyrazolopyrimidine scaffold and a steroid moiety to give compounds **48** and **49**, among which the search for ALK inhibitors has been performed. A primary evaluation of cytotoxicity against A875 melanoma and Huh-7 hepatocellular carcinoma cell lines identified the most promising compound **49a**; however, investigation of the inhibitory activity of this compound against ALK revealed only a moderate effect at a concentration of 10 μM (Fig. 29).

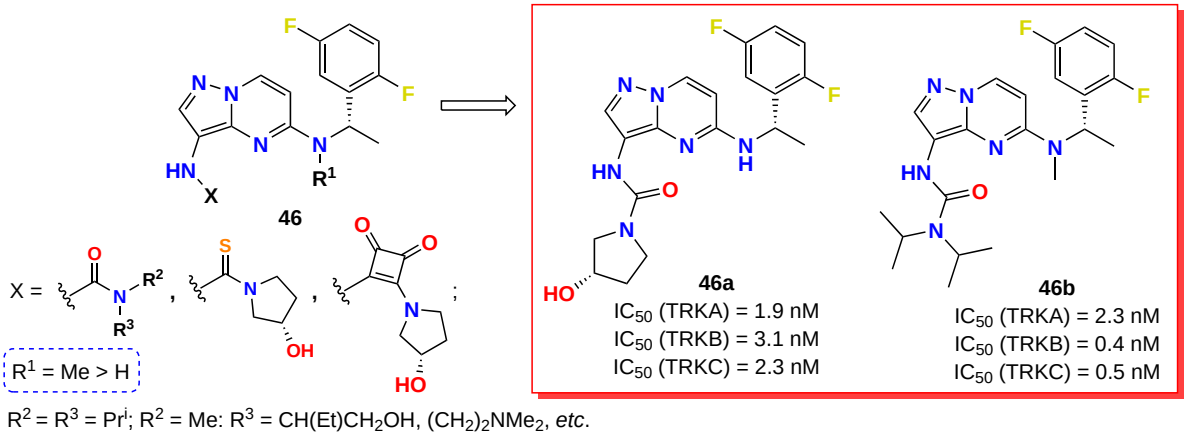


Figure 27. Structures and SARs for TRK inhibitors **46** and data on inhibition of three isoforms (A, B, C) of this enzyme by the most active compounds **46a**,**b**.

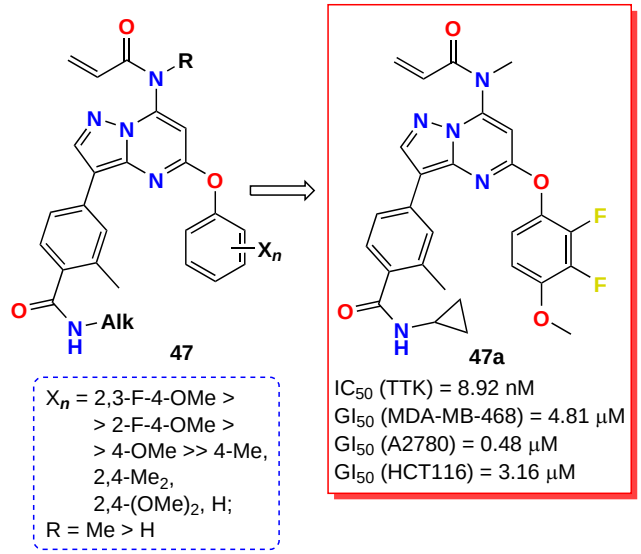


Figure 28. Structures and SARs for compounds **47** and data on the activity of most promising derivative **47a**.

The c-Met kinase is a key component of signalling pathways that trigger cell division, differentiation, migration, apoptosis, and morphogenesis. In some malignant neoplasms, this kinase is dysregulated, leading to tumour metastasis and angiogenesis.[80] Considering the structure of known c-Met II inhibitors, Luo *et al.*[81] designed a series of azoloazines **50**. A study of cytotoxic activity showed that compounds containing a heteroaryl or benzyl moiety at the amide bond (*e.g.*, derivative **50a**) show cytotoxic activity in the mid-micromolar range. Meanwhile, aryl-substituted analogues were inactive, except those containing *meta*- and *para*-fluorine atoms and *para*-methoxy groups (in particular, derivative **50b)**. The authors selected eight most active heterocycles **50** to evaluate their inhibitory activity against c-Met: they found that heteroaryl derivatives and compounds containing the electron-withdrawing group R^2 in the benzene ring exhibit fairly pronounced inhibitory properties (Fig. 30).

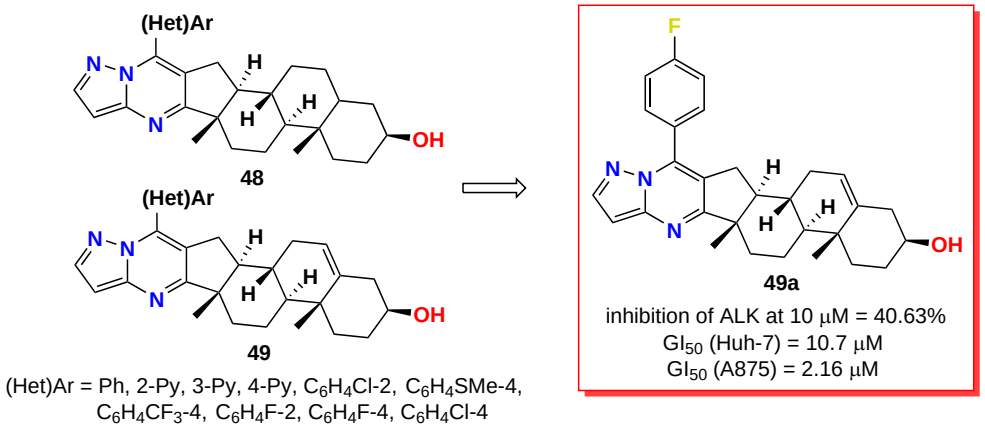


Figure 29. Structures of ALK inhibitors **48** and **49** and data on the activity of the most promising derivative **49a**.

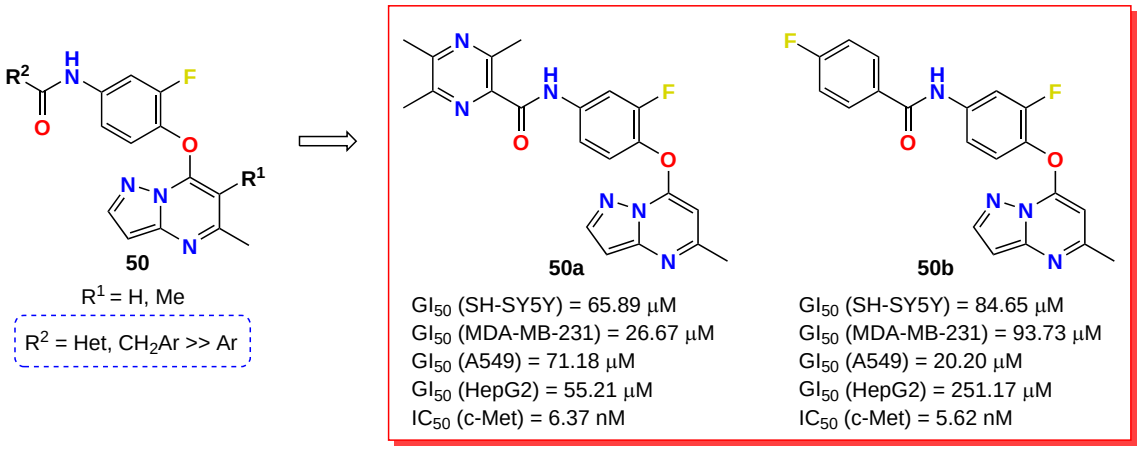


Figure 30. Structures and SARs of c-Met inhibitors **50** and activity data for the most promising compounds **50a**,**b**.

2.1.3. Inhibitors of other kinases

Phosphatidylinositol 3-kinase γ and δ inhibitors are used in the immunotherapy of malignant tumours,[82] but to reduce adverse effects, selective action of an agent on a specific isoform is important.[83] Screening of an author's in-house library revealed a hit among pyrazolo[1,5-*a*]pyrimidines **51**, the structure of which was subsequently optimized (Fig. 31).[84] It was shown that

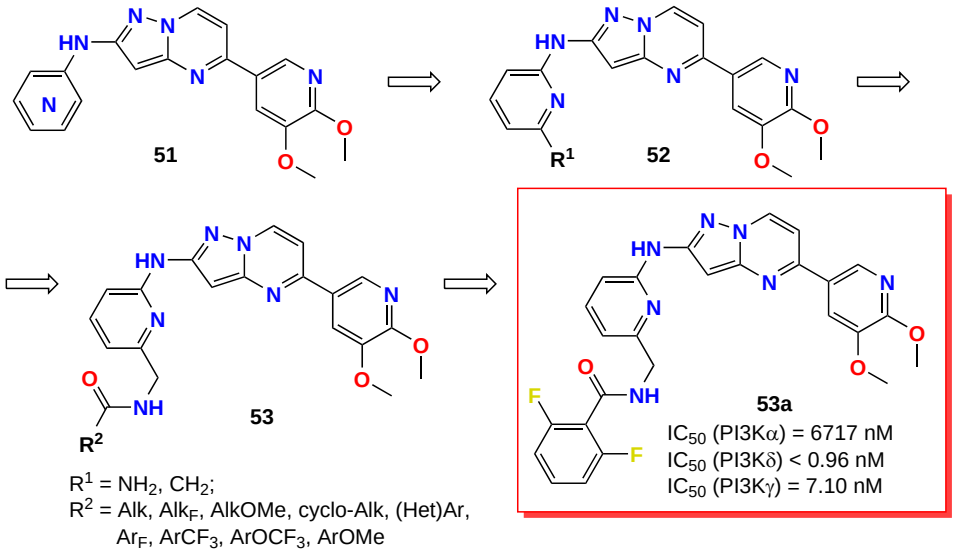


Figure 31. Structure optimization for PI3K inhibitors **51** and activity data for the most promising compound **53a**.

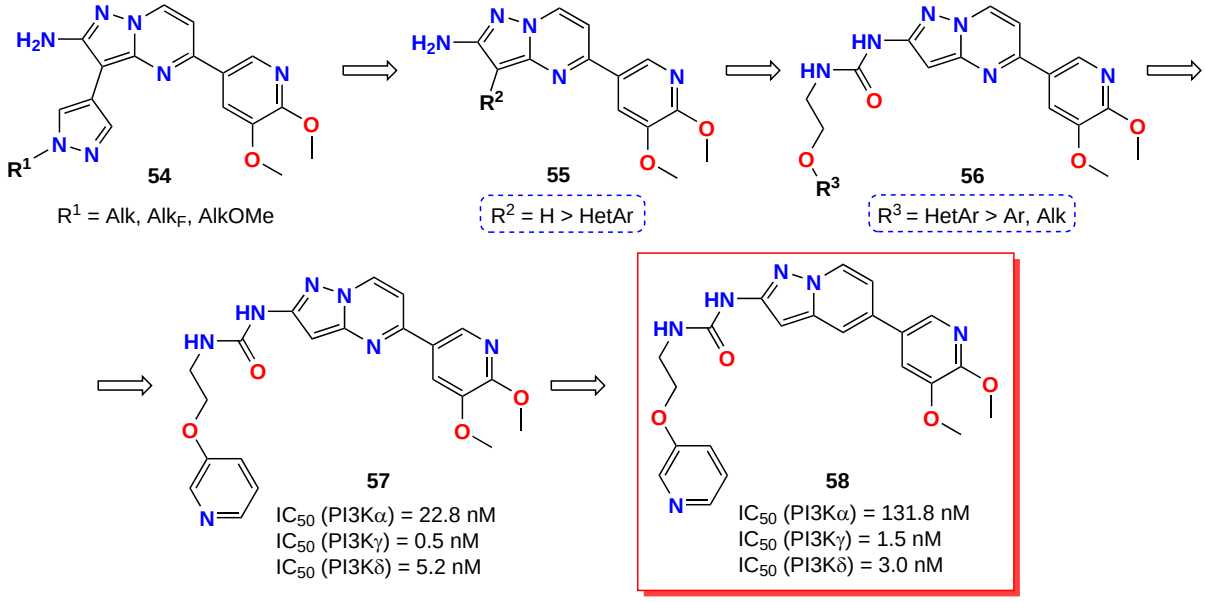


Figure 32. Structure optimization for PI3K inhibitors **54**, SARs for compounds **55** and **56** and characteristics of compound **57** and the most active and selective inhibitor **58**.

replacement of the pyridine-2-yl moiety in compounds **52** by a 3- or 4-substituted isomer decreases the activity. The introduction of a CH_2NHR^1 group (R^1 varies over a broad range and has little effect on activity) in the C(6) position of the pyridine ring further enhances the inhibitory properties, and acylated amines **53** were found to be most effective. Irrespective of the nature of R^2, which also varies over a wide range and has little effect on activity, amines **53** exhibited high inhibitory properties against PI3Kδ(γ), though with varying degrees of selectivity for the α-isoform. This parameter was high for compounds containing a fluorinated benzoyl moiety [for example, for heterocycle **53a**, which inhibited the tumour growth *in vivo* in the MC-38 syngeneic mouse xenograft model (mouse colon adenocarcinoma) *in vivo*].

Further expansion of this series of pyrazolopyrimidines (Fig. 32) showed that replacement of the pyrazole ring at the C(3) atom in derivatives **54** by a hydrogen atom or a heteroaryl moiety (compounds **55**) is preferred.[85] Modification of the C(2)-amino group by conversion to a urea moiety resulted in increasing selectivity of pyrazolo[1,5-*a*]pyrimidines **56** and **57** to PI3Kα; however, replacement of the pyrazolopyrimidine central core by a pyrazolopyridine one (compound **58**) proved to be even more effective in this regard.

Using the sunitinib parent structure, Anwer *et al.*[86] designed 3-arylazopyrazolopyrimidin-5-ones **59** as potential inhibitors of VEGFR (vascular endothelial growth factor receptors) and Aurora kinase. The latter is a serine/threonine kinase that regulates mitosis and cell division; for this reason, overexpression of this protein is observed in a number of malignant tumours.[87] Of the nine studied heterocycles **59**, three compounds (including derivative **59a**) decreased the proliferative capacity of HepG2 hepatocellular carcinoma cells and the hormone-sensitive MCF-7 ductal adenocarcinoma cells with GI_{50} values of 3–6 μM; similar cytotoxicity was also observed against normal peripheral blood mononuclear cells (PBMCs). Nevertheless, according to *in vivo* assays on mice, heterocycle **59b** (X = 2,6-Cl_2, Y = Me) had median lethal dose (LD_{50}) > 1500 mg kg^{-1} and no acute hepato- and nephrotoxicity; however, the authors did not evaluate the antitumour effect of this compound **59b** (Fig. 33).

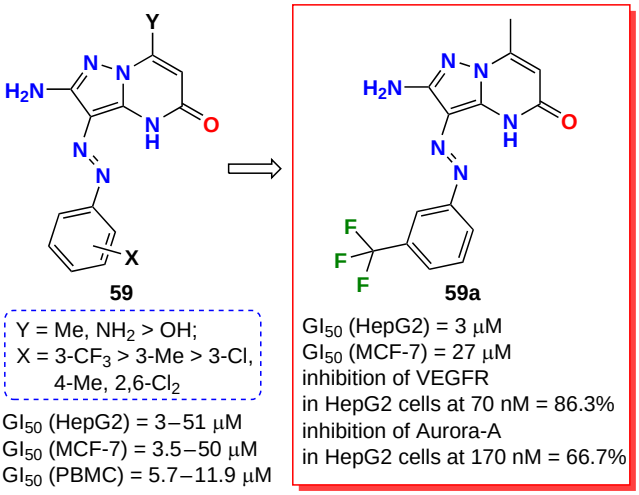


Figure 33. Structures, SARs and activity data of compounds **59** and most promising derivative **59a**.

Alsulaimany *et al.*[88] designed a series of pyrazolo[1,5-*a*] pyrimidines **60** based on the pharmacophore groups of the anticancer drugs sorafenib and pasopanib.[88] On the basis of the molecular docking data, it was assumed that compounds **60** have high affinity for the active sites of both VEGFR-2 and the mutant epidermal growth factor receptor ($EGFR^{T7980M}$). In the subsequent *in vitro* experiments, heterocycles **60** showed half-maximal inhibitory concentrations in the low micromolar range (IC_{50} = 260–5340 nM). The accompanying determination of cytotoxic properties also revealed the ability of heterocycles **60**, including the most promising structure **60a**, to inhibit the proliferative capacity of a number of tumour cells in the low- or mid-micromolar range with a selectivity index of 4–10 over normal VERO cells (Fig. 34).

Epidermal growth factor receptors, EGFR and HER2 proteins, are often overexpressed in malignant breast tumours.[89] Sivaiah *et al.*[90] investigated the cytotoxicity of a small series of 2-trifluoromethyl pyrazolopyrimidine derivatives **61** (Fig. 35).

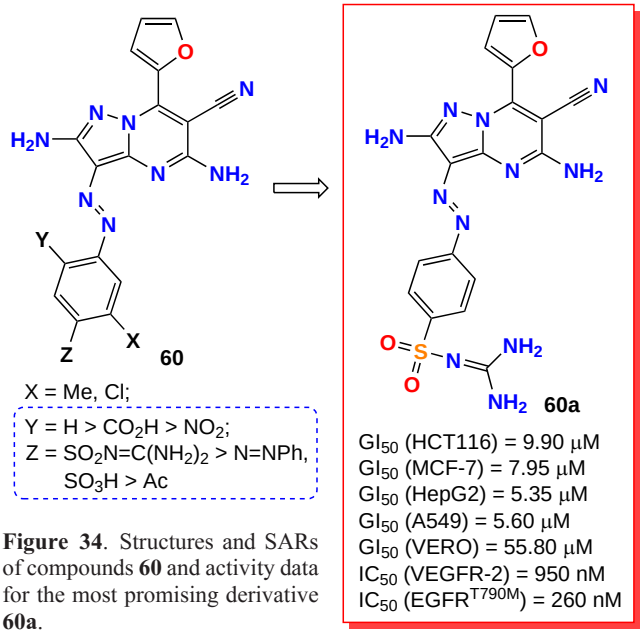


Figure 34. Structures and SARs of compounds **60** and activity data for the most promising derivative **60a**.

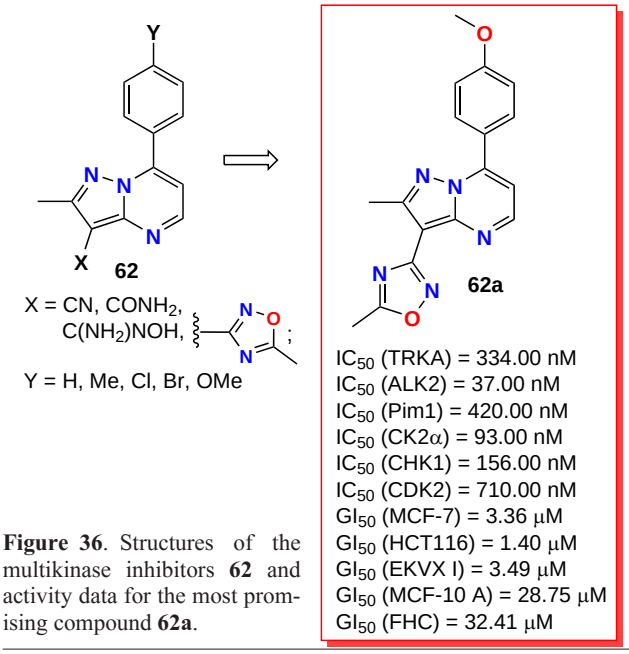


Figure 36. Structures of the multikinase inhibitors **62** and activity data for the most promising compound **62a**.

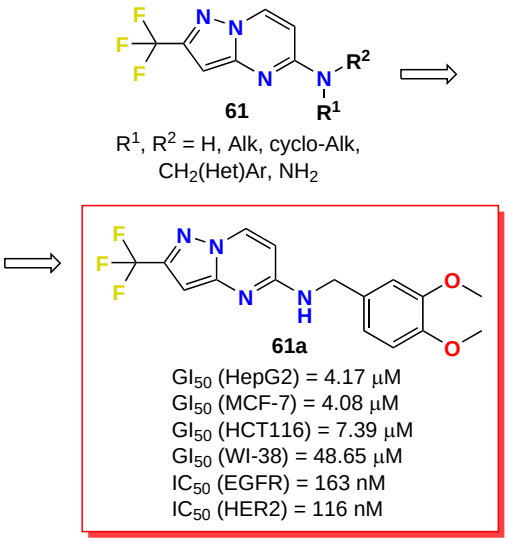


Figure 35. Structures of EGFR and HER2 inhibitors **61** and activity data for the most promising derivative **61a**.

It was shown that the cytotoxic effect is enhanced in the presence of a (hetero)aryl group linked to the C(5)-amino group *via* a methylene bridge. Several most promising compounds such as heterocycle **61a** were evaluated for their inhibitory activity against EGFR and HER2: they were slightly inferior in activity to the reference agents sorafenib [IC_{50} (EGFR) = 112 nM] and staurosporine [IC_{50} (HER2) = 53 nM].

The design of ATP-competing multikinase inhibitors **62** was reported by Al-Qadhi *et al.*[91] The *in vitro* studies confirmed the initial hypothesis of the authors: all 20 investigated compounds **62** inhibited various kinases with half-maximal inhibition characteristics in the submicromolar and low micromolar ranges (Fig. 36). The most promising compound **62a** showed cytotoxicity against a number of tumour cell lines [HCT-116, MCF-7, and EKVX (human non-small-cell lung cancer)] at a level comparable to that of doxorubicin (GI_{50} = 3.42–5.73 μM), while the corresponding value for non-tumorigenic breast epithelial cells (MCF-10A) and normal human colon epithelial cells (FHC) proved to be 10–15 times lower.

Further expansion of this family of azole[1,5-*a*]pyrimidines revealed that the introduction of C(6)-nitrile and C(7)-amino groups into the pyrimidine ring to form triazolo[1,5-*a*] pyrimidines **63** generally increases the cytostatic activity of the

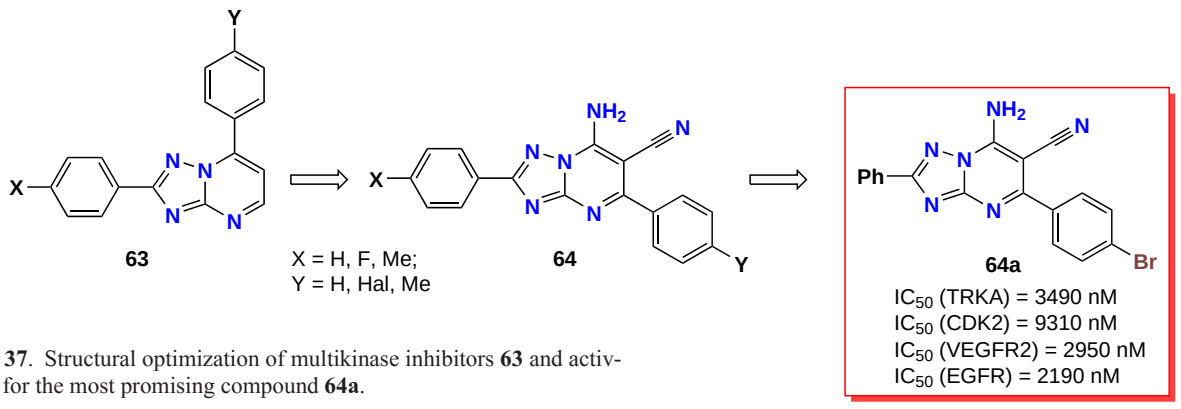


Figure 37. Structural optimization of multikinase inhibitors **63** and activity data for the most promising compound **64a**.

compounds. Out of a panel comprising 60 different tumour cell lines, 58 or 59 cell lines were sensitive to heterocycles **64**, while the starting compounds **63** exhibited a cytostatic effect only against a small portion of the cells (12 to 21 cell lines).[92] Derivatives **64** also showed more pronounced inhibition of various kinases; however, they were inferior in inhibitory activity to pyrazolopyrimidines **62** described in the previous study (Fig. 37).

2.2. Non-kinase enzymes and epigenetic regulators

2.2.1. Hydrolase and transferase inhibitors

Carbonic anhydrases IX (hCA IX) and XII (hCA XII) are expressed in normal cells by a limited amounts; however, these enzymes are often overexpressed in tumours, leading to a lower pH in the extracellular matrix and the invasion of tumour cells into adjacent tissues.[93] Said *et al.*[94] investigated 1,2,4-triazole derivatives, including triazolopyrimidines **65**, as inhibitors of these carbonic anhydrases (Fig. 38).

Another strategy for the development of hCA IX and XII inhibitors involved combining pyrazolopyrimidine and coumarin fragments in compounds **66** (Fig. 39).[95] It was found that hCA inhibition requires the introduction of zinc-binding groups, such as sulfonamide, thiol, or carboxyl groups (see, *e.g.*, compound **66a**). Conversely, an inverse correlation was observed for manifestation of noticeable cytotoxic properties: compounds with zinc-binding groups were inactive, whereas derivatives with substituents X = 4-H, 4-Me, and 4-OMe reduced the proliferative capacity of tumour cells (from a panel of >50 cell lines). The highest efficiency was found for derivative **66b** for which median growth inhibitory concentrations (GI_{50}-MID) were in a low micromolar range, although the selectivity index was also moderate (2–4). A probable mechanism of the cytotoxic action of this compound **66b** was the inhibition of tubulin polymerization, since the IC_{50} value in the relevant assay was 5.28 μM.

The identified patterns were confirmed for an additional series of derivatives **67** of this family: only heterocycles containing a sulfonamide group effectively inhibited hCA. However, only compound **67a** had a pronounced cytostatic effect: the GI_{50}-MID value for a panel of several dozen tumour cell lines was 13.18 μM (Fig. 40).[96]

The replacement of the coumarin moiety at the C(7) position by a benzene ring resulted in the formation of structures **68**, which effectively inhibited hCA and reduced the proliferative capacity of tumour cells (Fig. 41).[97] The authors noted that more effective hCA inhibitors are compounds that contain a halogen atom in the *para*-position of the benzene ring (*e.g.*, **68a**,**b**) and a methyl group at the C(2) position of the heterocycle (**68b**).

Methionine aminopeptidase 2 (MetAP-2) plays a key role in the regulation of angiogenesis;[98] inhibitors of this enzyme were shown to have an antiproliferative effect.[99] Heinrich *et al.*[100] mentioned three nitrogen-bridged azolopyrimidines **69**–**71**, which inhibited MetAP-2 in the submicromolar range (Fig. 42).

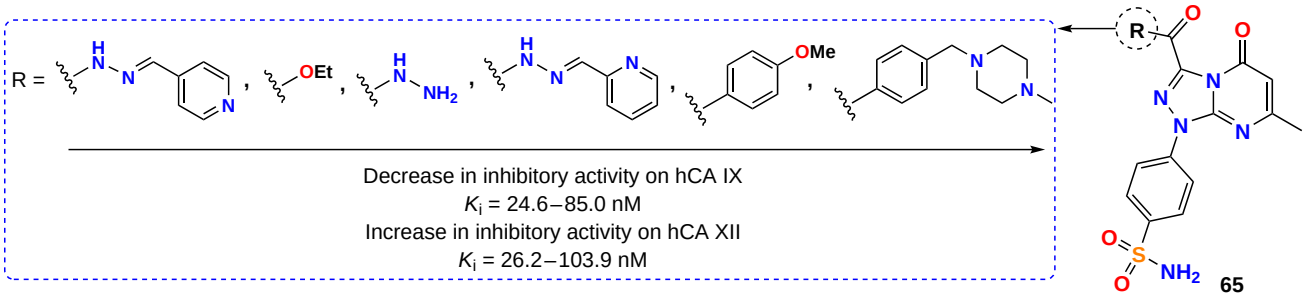


Figure 38. Structures and SARs of compounds **65** and ranges of inhibition constants toward two hCA isoforms.

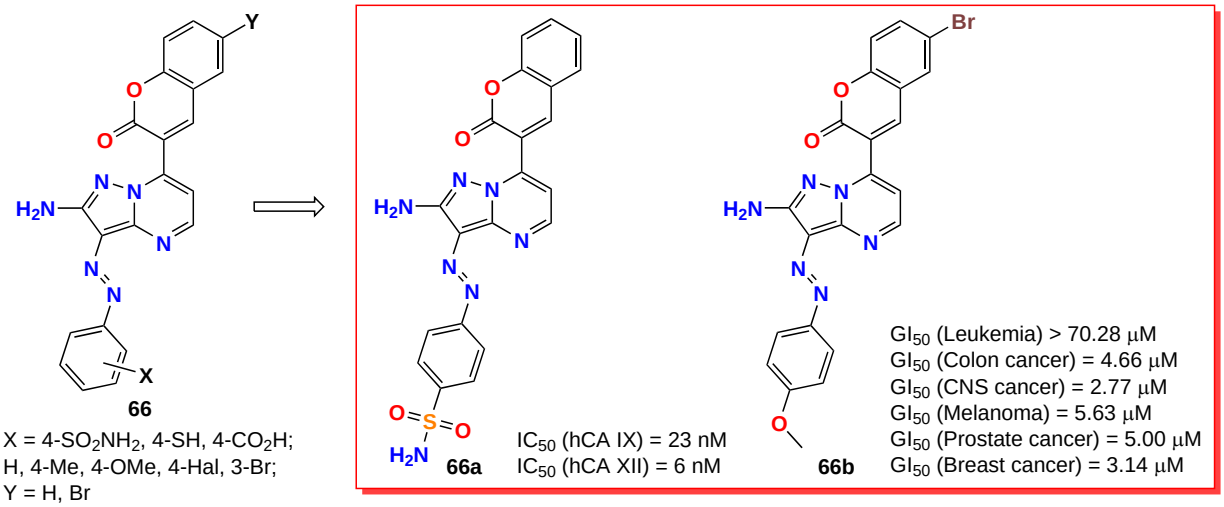


Figure 39. Structures of hCA inhibitors **66** and activity data for the most promising compounds **66a**,**b**.

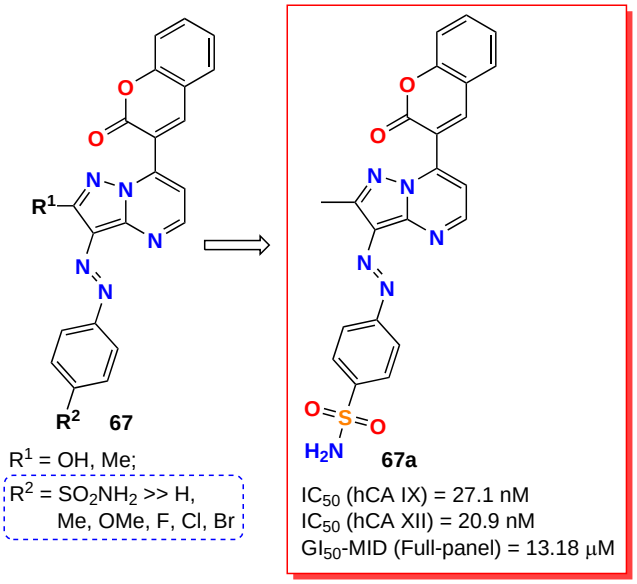


Figure 40. Structures and SARs of compounds **67** and activity data for the most promising derivative **67a**.

Spermine oxidase (SMOX) is a flavin-containing enzyme involved in the synthesis of polyamines, which determine numerous cellular functions, including cell division, differentiation, and migration; disruption of SMOX activity leads to carcinogenesis.[101] Llaveria *et al.*[102] performed a high-throughput screening and identified several pyrazolopyrimidine structures **72** that are SMOX inhibitors. According to SAR data, an increase in the size of the alkyl moiety at the C(7) atom leads to increasing activity, whereas the replacement of the alkyl group by nitrogen-containing saturated heterocycles causes the opposite effect. The introduction of a benzene ring at the C(7) position yields compound **72a**, which has the highest inhibitory activity, while further variation of the amide moiety and the C(7) substituent does not result in more active compounds **73** (Fig. 43).

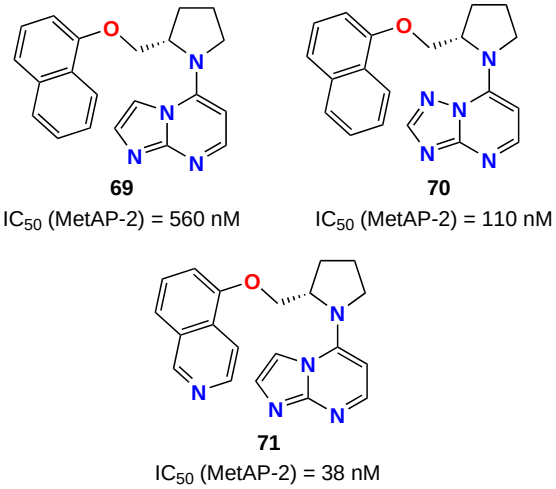


Figure 42. Structures and IC_{50} values of MetAP-2 inhibitors **69**–**71**.

Methionine adenosyltransferase 2A (MAT2A) is an attractive target for the therapy of tumours with a deletion of the methylthioadenosine phosphorylase (MTAP) gene.[103] Konteatis *et al.*[104] performed screening of a library of compounds, which resulted in identification of pyrazolo-pyrimidin-7-ones as promising scaffolds. Using X-ray diffraction data for the MAT2A–*S*-adenosylmethionine–**74** (one of the compounds) ternary complex, further structural modification was predicted. It was found that increasing the polarity of the C(2)-substituent reduces the inhibitory properties of compounds **74**, whereas the C(3) position should better bear a cycloalkane or piperidine moiety in place of the phenyl group, to afford compounds **75**. The variation of the substituent at the C(6) atom for the series of compounds **76** provided the conclusion that the introduction of a (hetero)aryl moiety capable of forming hydrogen bonds with the MAT2A active site increases the activity of the derivatives. Further modifications, which led to compounds **77**, were aimed, first of all, at

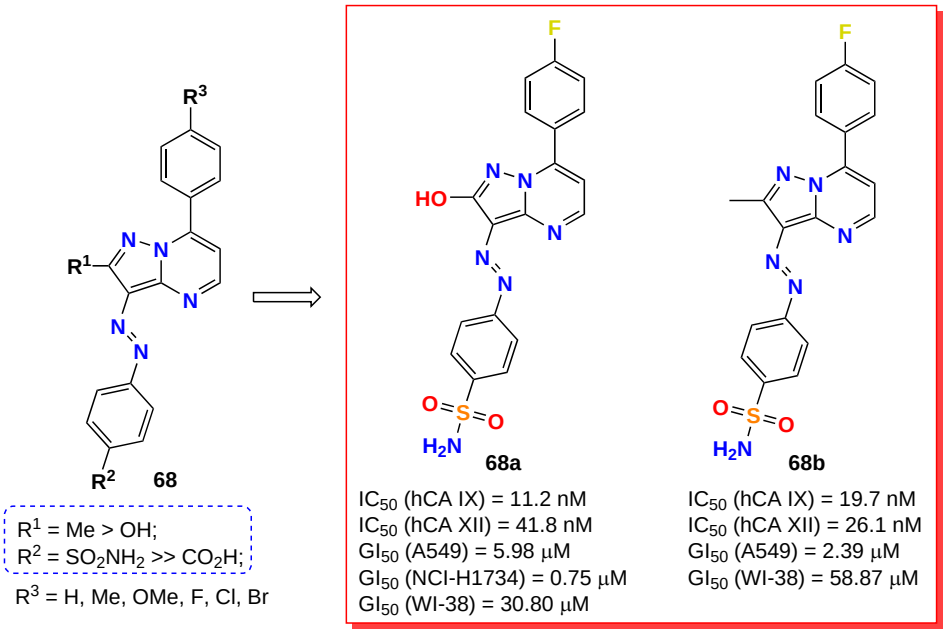


Figure 41. Structures and SARs of compounds **68** and activity data for the most promising compounds **68a**,**b**. NCI-H1734 is lung adenocarcinoma cell line.

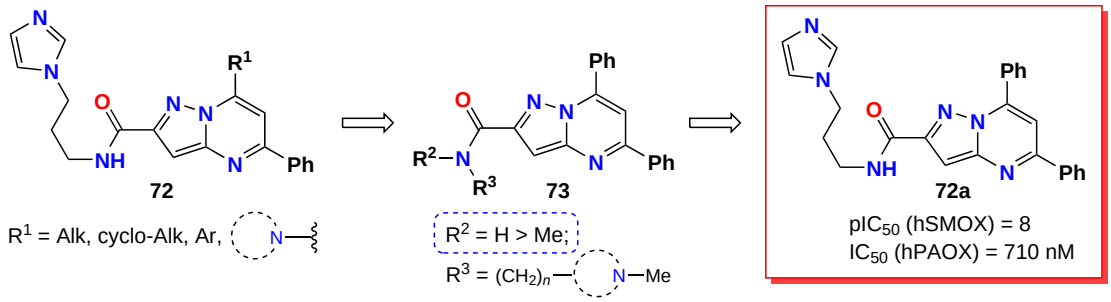


Figure 43. Structures of SMOX inhibitors **72** and **73** and activity data for the most promising compound **72a**.

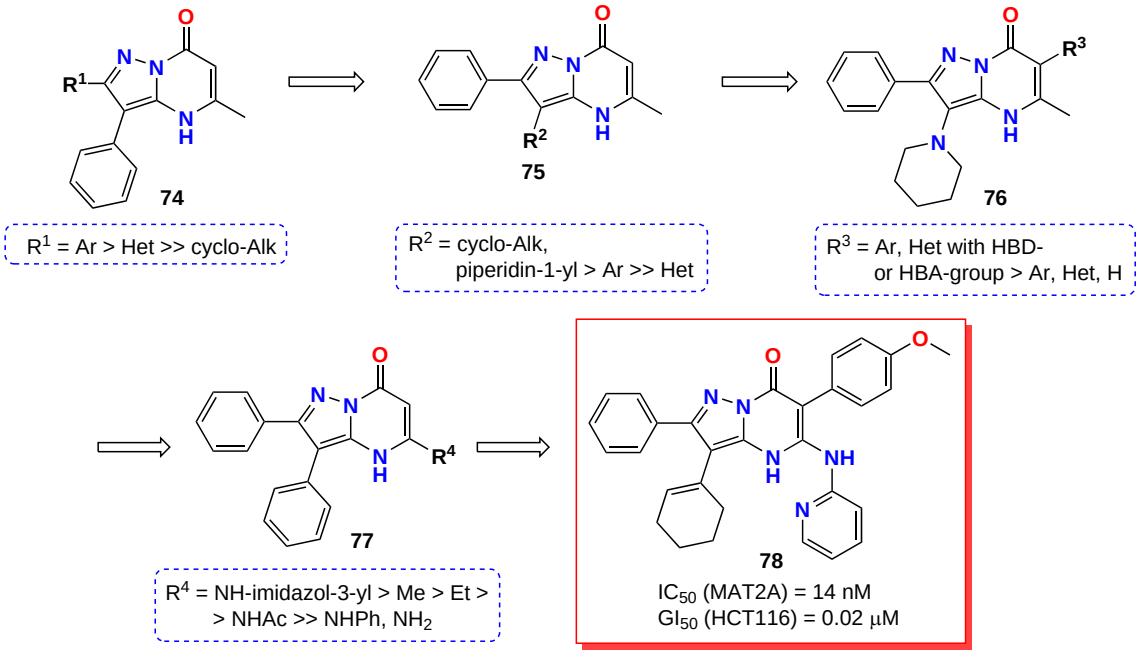


Figure 44. Structures and SARs of MAT2A inhibitors **74**–**77** and activity data for the most promising compound **78**.

improving the pharmacokinetic characteristics. This resulted in the development of compound **78**, which has entered Phase I clinical trials as an antitumour agent (Fig. 44).

Tyrosyl DNA phosphodiesterase 2 (TDP2) in atypical cells is responsible for the mechanisms of resistance to anticancer agents that act as topoisomerase II inhibitors.[105] Screening of a series of 1,2,4-triazolo[1,5-*a*]pyrimidines **79** for the inhibitory activity against TDP2 showed that most of these compounds are inactive.[106] Only 5-phenyl derivatives **80** containing a *meta*-electron-withdrawing group on the benzene ring of the C(2)-arylamide substituent (*e.g.*, compound **80a**) were active in the mid-micromolar range (Fig. 45).

The enzyme Alk homologue 5 (ALKBH5) is a Fe^{II}/2-oxoglutarate-dependent dioxygenase able to demethylate *N*6-methyladenosine and involved in the oncogenesis of certain tumours.[107] In a pharmacophore-based screening conducted by Wang *et al.*,[108] azolopyrimidine structure was identified as a potential ALKBH5 inhibitor (Fig. 46). SAR measurements showed that 2-hydroxy group as R^1 and 5-nitro group as R^2 are irreplaceable for compounds **81** to exhibit high inhibitory activity. The nature of the *para*-substituent on the benzene ring at the C(2) atom had a noticeable effect on the activity of compounds **82**: the presence of a chlorine atom led to decreasing activity, while ester groups, conversely, resulted in an increase

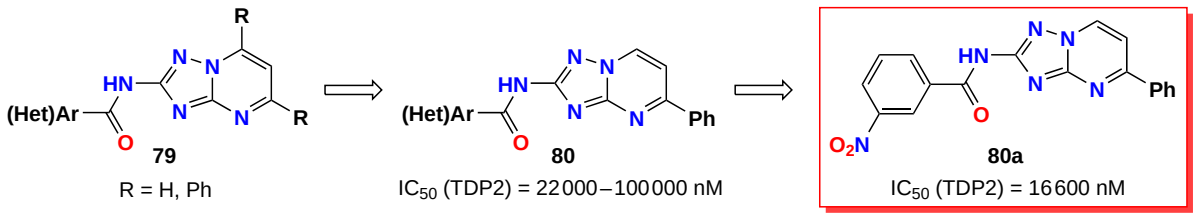


Figure 45. Structures of TDP2 inhibitors **79** and **80** and data on the activity of compounds **80**, including the most promising compound **80a**.

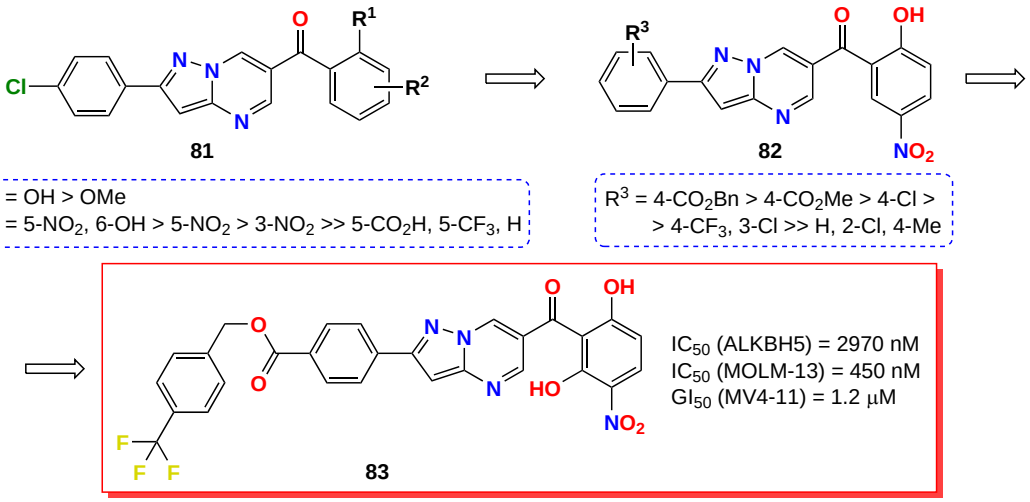


Figure 46. Structures and SARs for ALKBH5 inhibitors **81** and **82** and activity data for the most promising compound **83**. MOLM-13 is acute monocytic leukaemia cell line.

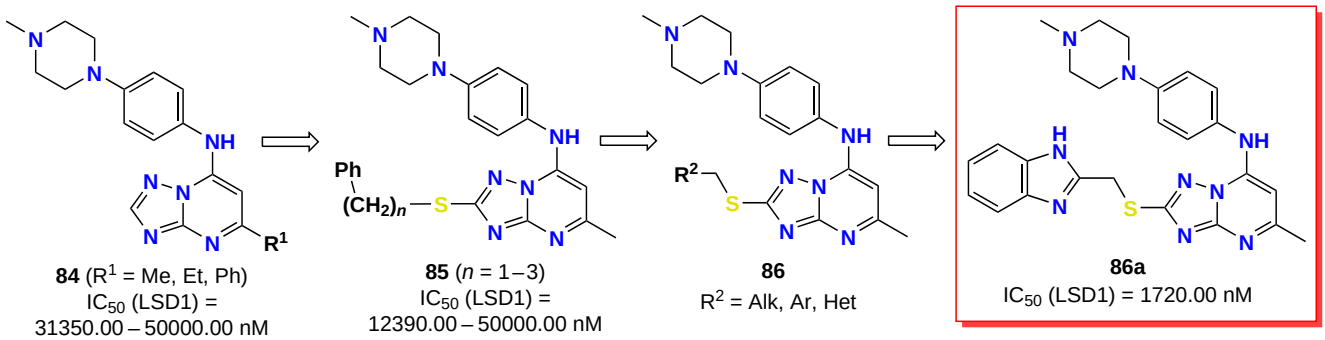


Figure 47. Structural optimization of LSD1 inhibitors **84** and data on the inhibition of this enzyme by derivatives **84** and **85** and by the most promising compound **86a**.

in the activity, with benzyl esters being most effective. The most active compound **83** exhibited cytotoxic properties in the low micromolar range and demonstrated antitumour activity in MV4-11 acute myeloid leukaemia xenografts in mice (the tumour weight halved at a dose of 10 mg kg^{-1} of compound **83** compared to the negative control).

2.2.2. Inhibitors of epigenetic enzymes

Lysine-specific histone demethylase 1 (LSD1) is overexpressed in various tumour cells and is capable of promoting oncogenesis.[109] A study of inhibitors of this enzyme, 1,2,4-triazolo[1,5-*a*]pyrimidines **84**, showed that the optimal substituent at the C(5) position is a methyl group (compounds **85**). At the same time, the presence of a thiomethylene bridge linking the triazole ring to (hetero)aryl moiety is desirable at the C(2) position (compounds **86**); among (hetero)aryls, the 2-benzimidazole ring is the best choice in terms of inhibitory activity (compound **86a**) (Fig. 47).[110]

Yan *et al.*[111] considered the design of dual-action molecules that combine the properties of A_{2A} receptor antagonists and histone deacetylase (HDAC) inhibitors for the immunotherapy of cancer. This mainly concerned triazolo[1,5-*c*]pyrimidines, but one [1,5-*a*]-type annulated derivative **87** was also mentioned; the activity of this compound was comparable to that of the heterocycles selected for the extended assays (Fig. 48).

2.2.3. Inhibitors of helicases and repair proteins

The overexpression of Rho-associated coiled-coil kinase (ROCK) is related to increased tumour cell invasiveness.[112] Cao *et al.*,[113] who used the central scaffold replacement approach, investigated pyrazolopyrimidine derivatives as ROCK2 inhibitors (Fig. 49). It was found that replacement of the C(5) substituent in the starting heterocycle **88** by piperidine slightly enhances the inhibitory properties of compound **89**, while acylation of the N(4) atom leads to even more active structures. It was noted that the expansion of the piperidine ring in compounds **90** to a diazepine ring is undesirable and that

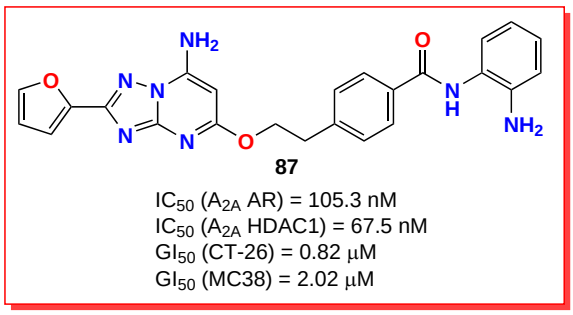


Figure 48. Structure and activity data of A_{2A} receptor antagonist **87**. CT26 is murine colorectal carcinoma cell line.

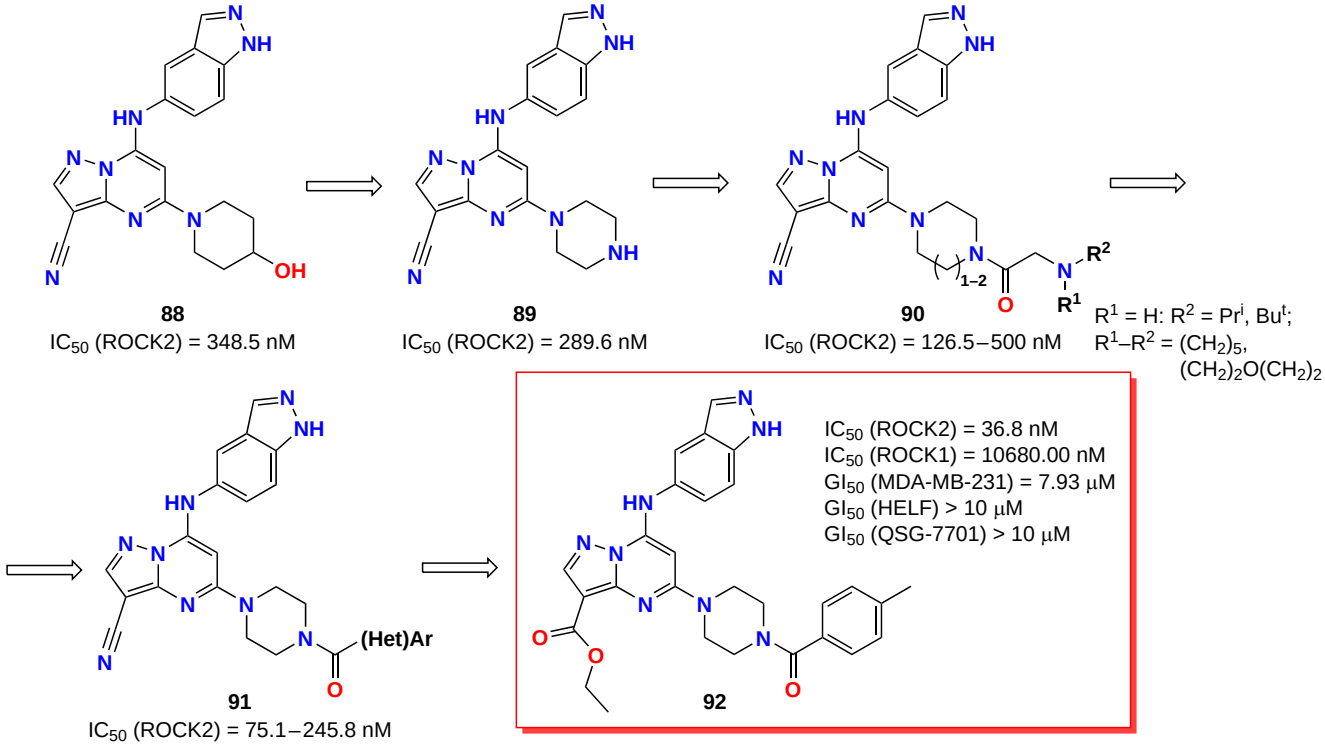


Figure 49. Structural optimization of ROCK2 inhibitors **88**–**92** with IC_{50} values and activity data for the most promising compound **92**. HELF is the human embryonic lung fibroblast line, QSG-7701 is normal (non-tumour) human liver cell line.

(hetero)arylated derivatives **91** are markedly more active than their methyleneamine analogues **90**. Finally, the replacement of the nitrile group at the C(3) position of azoloazine by an ester group yielded the most promising structure **92**, which effectively and selectively inhibited ROCK2 and exhibited cytotoxicity against triple-negative breast cancer cells (MDA-MB-231).

Topoisomerase II (Topo II) inhibitors are well known in medicinal chemistry, in particular as potential anticancer agents.[114] Farghaly *et al.*[115] reported nine tetracyclic pyrazolo[1,5-*a*]pyrimidine derivatives **93** and **94**, which were investigated as Topo IIα inhibitors. Because of the small number of compounds, it is difficult to establish structure–activity relationships. It can be noted that both scaffolds **93** and **94** were comparable in activity [IC_{50} (Topo IIα) = 2350–22400 nM], and only compound **94a** exhibited an affect comparable to that of doxorubicin [IC_{50} (Topo IIα) = 2710 nM] regarding both topoisomerase inhibition and cytotoxicity (Fig. 50).

Werner syndrome helicase (WRN) is responsible for DNA uncoiling during replication; there is a relationship between WRN and malignant tumours with microsatellite instability (colorectal cancer, gastric cancer).[116] A molecule with a triazolo[1,5-*a*]pyrimidine skeleton has entered clinical trials is a WRN inhibitor.[117] Sui *et al.*[118] investigated the relationship between the structure and the inhibitory and cytotoxic activity against microsatellite instability cells for molecules **95**–**97** (Fig. 51). It was found that replacement of the carbonyl group (denoted by the symbol X) by a methylene bridge in compounds **95** results in a complete loss of inhibitory and cytotoxic activity. A similar effect occurs upon the introduction of halogen atoms or a methyl group into the heteroaryl moiety, while the replacement of the pyridine ring by an indole ring slightly reduces the inhibitory properties of the corresponding derivatives. Having introduced a 3-hydroxypyridyl residue into the molecule of **96**, the authors varied the C(2) substituent using

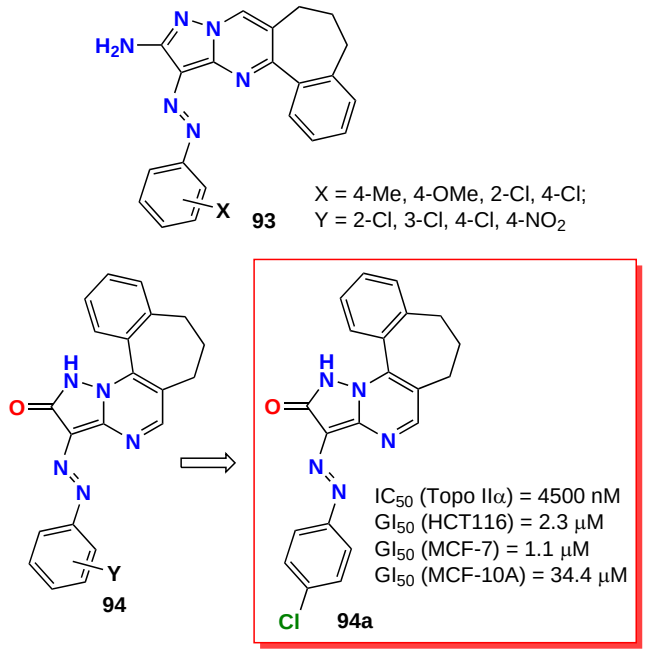


Figure 50. Structure of Topo II inhibitors **93** and **94** and activity data for the most promising compound **94a**.

a series of cyclic amines. Thus, azetidine and pyrrolidine derivatives were markedly weaker inhibitors than spirocyclic piperidines **97**. The presence of six-membered saturated rings in the molecule proved to be preferable. The subsequent variation of two amide moieties confirmed that the introduction of substituents in the α-position of the pyridine ring decreases the activity of the compounds, whereas replacement of the pyridine

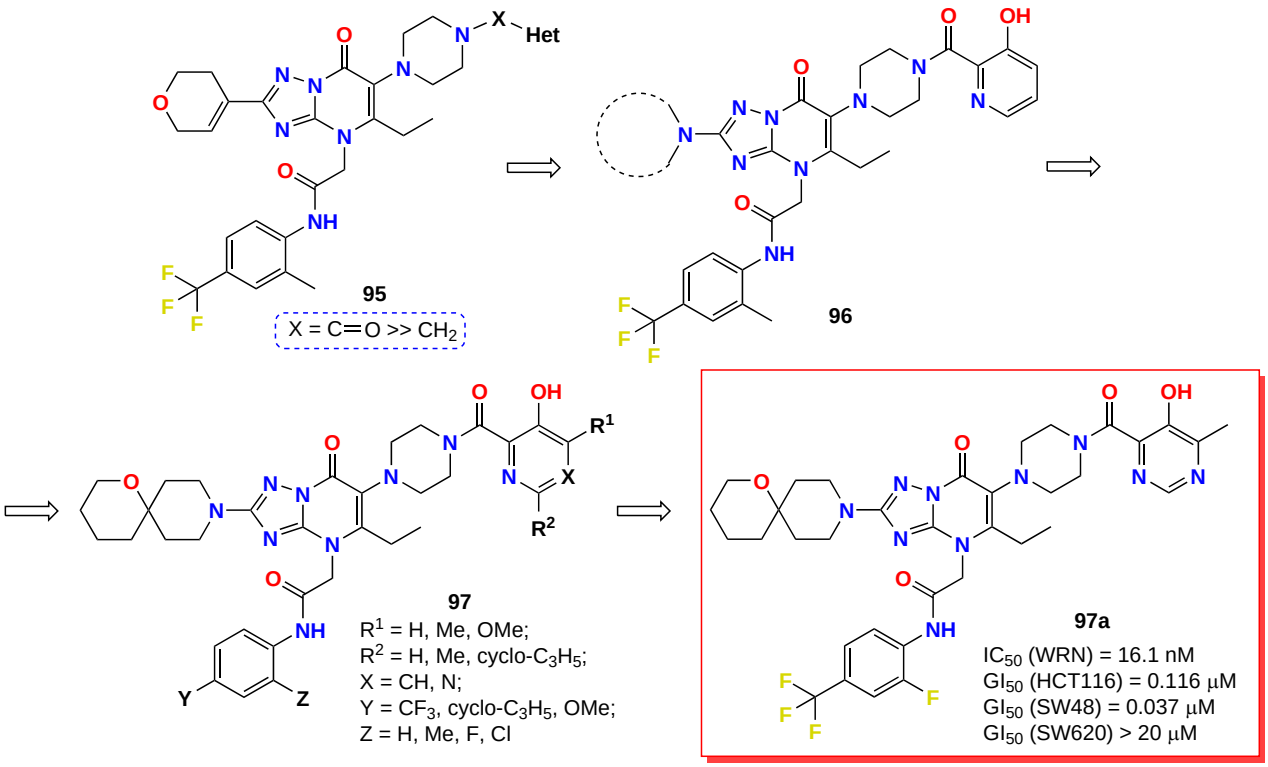


Figure 51. Structural optimization and SARs of WRN inhibitors **95** and activity data for the most promising compound **97a**.

ring by a 4-hydroxy-5-methylpyrimidine moiety, and the replacement of the methyl group in the benzene ring by a fluorine atom lead to increasing inhibitory effect and cytotoxicity. The most promising compound **97a** had an inhibitory effect on WRN in the mid-nanomolar range and reduced tumour cell proliferation with GI_{50} values in the 0.037–0.306 μM range and showed an excellent selectivity index when tested on SW620 metastatic colorectal adenocarcinoma cells without microsatellite instability.

The ataxia telangiectasia mutated Rad3-related protein (ATR) plays a key role in DNA repair, which makes some types of tumours dependent on the ATR-Chk1 signalling pathway and sensitive to the inhibition of this serine/threonine protein kinase.[119] Nitrogen-containing heterocycles represent the central core of several ATR inhibitors that have entered clinical trials; this was taken into account in the structural optimization of compounds **98** and **99**.[120] First, variation of substituents at the C(3) atom was carried out using pyrazoles with different substituent configurations. It was shown that methylation of the pyrazole NH moiety leads to a decrease in the inhibitory and cytotoxic activities, so does the replacement of the pyrazole ring by a phenyl moiety. In addition, the substituents at the C(5) and C(7) positions are interchangeable and do not have a critical effect on the activity. Further optimization focused on the search for substituents in the pyridine ring of compounds **100**: the derivative with unsubstituted pyridine ring was most promising in terms of inhibition of the target and cytotoxic activity, whereas the introduction of certain groups preserved the ability to inhibit ATR but reduced cytotoxicity (Fig. 52).

The most active compound **100a** exhibited cytotoxic activity against a panel of ~20 cancer cell lines, with average $GI_{50} \approx 1$ μM. Its anticancer activity was confirmed by *in vivo* experiments using a lung cancer xenograft.

2.3. Receptors, signalling proteins, and cellular models

2.3.1. Compounds that affect membrane and intracellular receptors

ATP-binding transporter proteins are among the main causes of cancer cell resistance resulting from the efflux of drug molecules.[121] One of the best studied targets in this category is the ABCB1 protein. Liu and co-workers[122,123] reported the design of modulating agents **101**–**103** (Fig. 53), which enhanced the cytotoxic action of paclitaxel, while the biological effect was evaluated in terms of the RF coefficient.[¶] It was found that the introduction of a thioether bridge to the C(2) position of the 1,2,4-triazolo[1,5-*a*]pyrimidine system **101** increases the RF coefficient. By varying the R group of the thioether moiety, the authors prepared 29 compounds **102**; the introduction of alkyl and aryl moieties did not induce a significant increase in this parameter. Compounds **103** containing a benzimidazole ring provided an exception; the introduction of this ring into the molecule led to an increase in the RF value, and further replacement of the aryl moiety made it possible to identify the most active compound **103a**.

In a later study,[124] a series of pyrazolopyrimidines **104** was investigated in a similar way: the authors evaluated the enhancement of paclitaxel cytotoxicity against the hormone-sensitive MCF-7/ADR breast cancer cell line, which is resistant to doxorubicin. It was shown that the presence of (hetero)aryl groups at the C(2) position is much more effective than the presence of alkyl groups. An increase in the number of methoxy

[¶] The RF (reversal fold) coefficient characterizes the efficiency of the modulating agent in the reversal of the multiple drug resistance (MDR) of cancer cells to cytostatic agents; the higher this coefficient, the better.

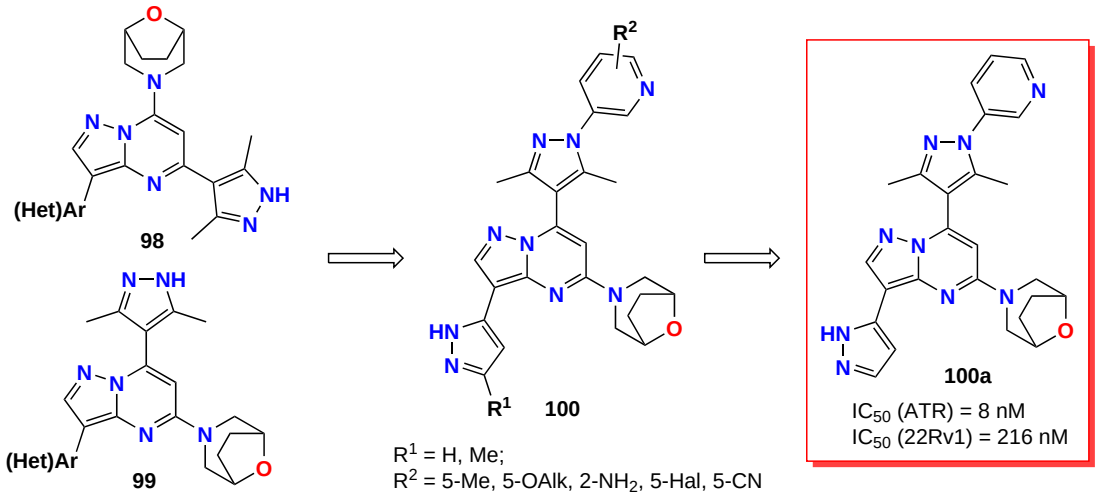


Figure 52. Structural optimization of compounds **98** and **99** and activity data for the most promising derivative **100a**.

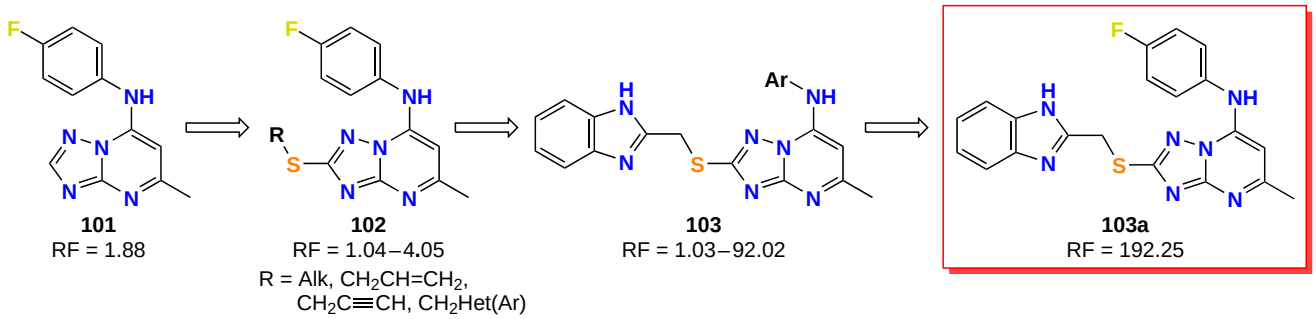


Figure 53. Structural optimization and RF values for compounds **101**–**103** including the most promising compound **103a**.

groups in the benzene ring at the C(6) atom also leads to increasing RF value (compound **104a**), while the replacement of the *para*-methoxy group by a halogen atom causes a pronounced decrease in the activity of the corresponding derivative (Fig. 54).

Translocation protein (TSPO) is overexpressed in a number of tumours, including glioma, breast cancer, and colorectal cancer cells.[125] Elucidation of the potential to inhibit this target among various pyrazolo[1,5-*a*]pyrimidines **105** and **106** revealed that the optimal length of the alkyl groups in the amide is two carbon atoms, and that one of the alkyl groups can be replaced by a benzene ring (Fig. 55).[126] Further development of this chemotype did not increase the affinity for the target and revealed that compounds **105** and **106** reduce the proliferative capacity of T98G human glioblastoma cells in the mid-micromolar range.[127]

A protein from the transient receptor potential channel 6 (TRPC6) subfamily is overexpressed in certain types of prostate and breast tumours, as well as in tumours of the liver, kidneys, and stomach.[128] Ding *et al.*[129] performed structure optimization for the initial hit compound **107a** (Fig. 56). It turned out that replacement of the carbamate group in compounds **107** by any other moiety markedly decreases the antagonistic activity. The Boc moiety is an exception; however, in this case, a fluorine atom is required in the *para*-position of the C(3) benzene ring, while the replacement of fluorine by a chlorine atom or a trifluoromethyl group results in compounds that lack antagonistic activity. A similar effect on the affinity for the target was also observed when the piperidine ring at the C(5) position in compounds **108** was replaced by other groups. Thus, the

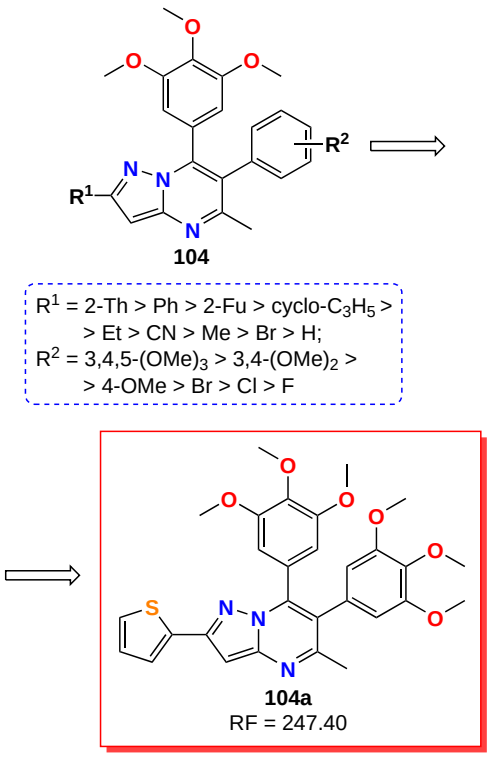


Figure 54. Structures and SARs of compounds **104** and RF for the most promising compound **104a**.

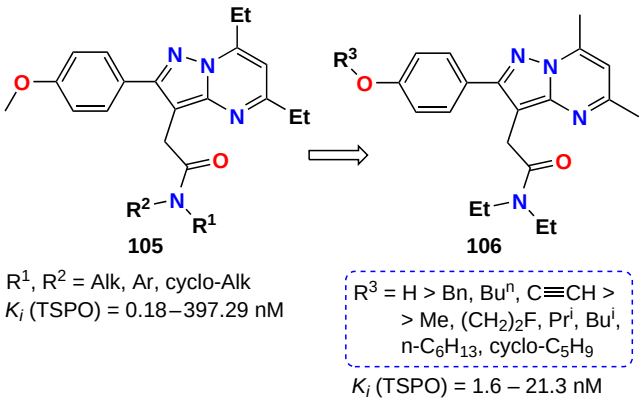


Figure 55. Structures and data on the activity of TSPO inhibitors **105** and **106** and SARs for compounds **106**.

modification of two substituents in compound **107a** furnished a more effective heterocycle **107b**.

2.3.2. Compounds that affect signalling proteins and regulatory proteins

A potential target for anticancer drugs is the DCN1 protein, which is often dysregulated in squamous cell skin carcinoma.[130] Wang *et al.*[131] investigated the inhibition of the interaction of this protein with the UBC12 enzyme by 1,2,4-triazolo[1,5-*a*]-pyrimidines **109–111**. It was established that for manifestation of the effect, groups containing a quaternized nitrogen atom are most preferred in the tetrazole ring of these compounds (Fig. 57). The replacement of the C(5)-phenyl group by a methyl group increased the activity of compound **109** twofold, whereas substitution of other alkyl groups into this position resulted in compounds with lower activity. The variations of the substituent at the sulfur atom at the C(2) position of the heterocyclic system showed that *para*-substituted benzyl derivatives **111** are most effective.

Another way to regulate the immune response is stimulation of interferon genes.[††,132] This pathway is activated *via* cyclic guanosine monophosphate–adenosine monophosphate (2′,3′-cGAMP), which is hydrolyzed by ectonucleotide

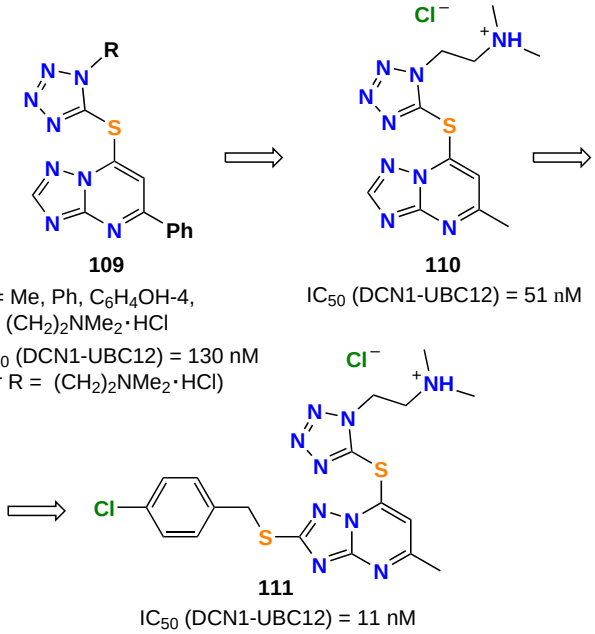


Figure 57. Structural optimization of compounds **109** and characteristics of the DCN1-UBC12 inhibition for derivatives **109–111**.

pyrophosphatase/phosphodiesterase (ENPP).[133] Thus, inhibitors of the ENPP family, along with STING agonists, are of great interest as immunoactivators. The initial virtual screening carried out by Kawaguchi *et al.*[134] identified hit compound **112** (Fig. 58). Optimization of its structure was reduced to the introduction of an amino group into the benzyl moiety at C(6). It was shown that the *meta*-position (compound **113**) is more favourable for the activity than the *para*-position (compound **114**). Replacement of the dimethylamino group by other amine residues made it possible to establish some structure–activity relationships for a series of derivatives **115**.

†† The stimulator of interferon genes (STING) is a key adapter protein of the innate immune system that recognizes foreign or damaged DNA in the cytoplasm of cells and triggers a protective inflammatory response.

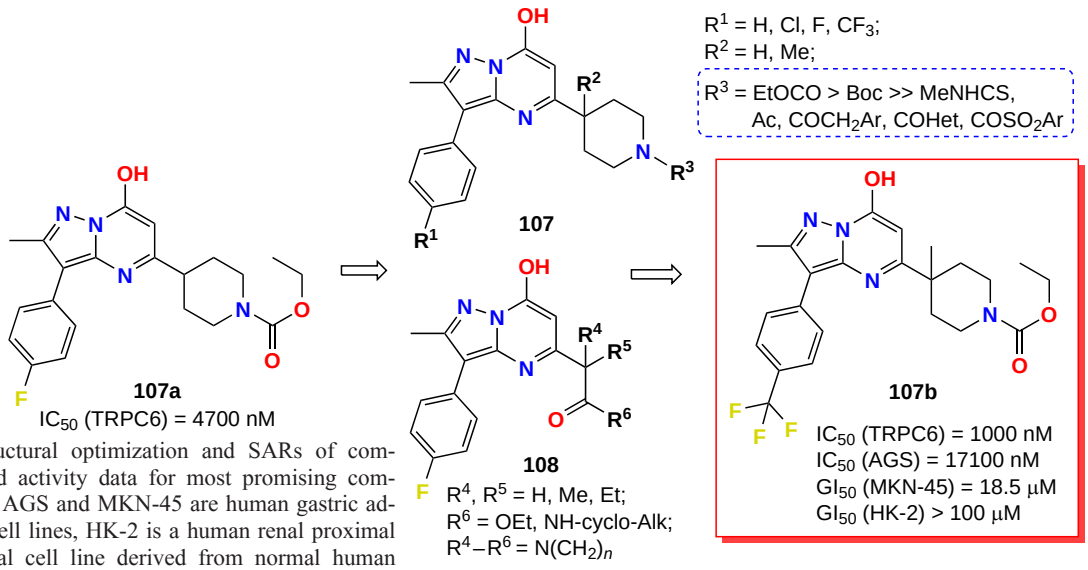


Figure 56. Structural optimization and SARs of compounds **107** and activity data for most promising compounds **107a**,**b**. AGS and MKN-45 are human gastric adenocarcinoma cell lines, HK-2 is a human renal proximal tubular epithelial cell line derived from normal human kidney cortex.

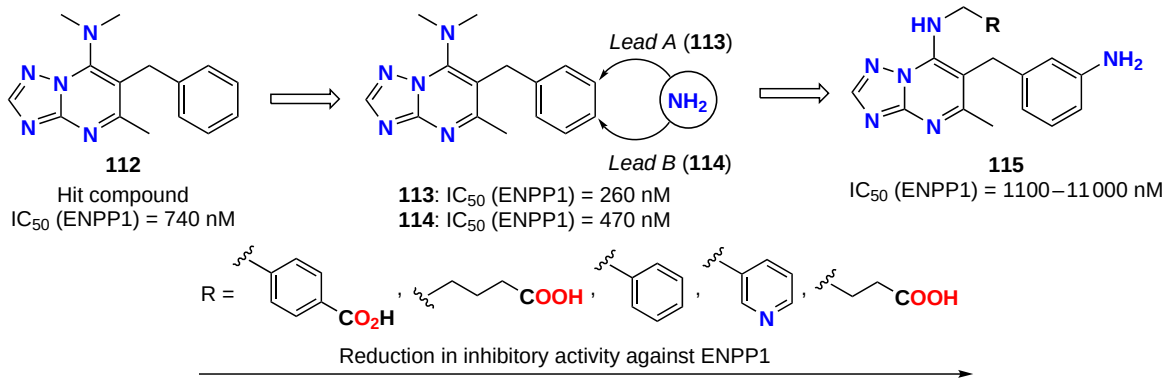


Figure 58. Structural optimization of hit **112**, ENPP1 inhibition indices for compounds **112**–**115**, and SARs for derivatives **115**.

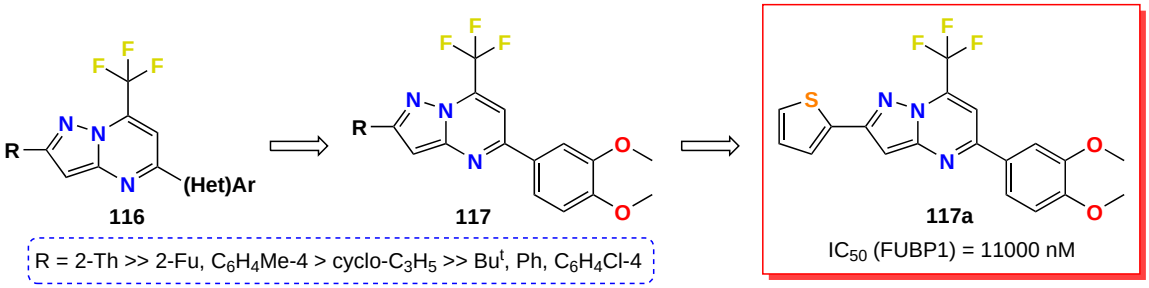


Figure 59. Structures and SARs of compounds **116** and **117** and FUBP1 inhibition index for the most promising compound **117a**.

The transcriptional regulator FUSE-binding protein 1 (FUBP1) is involved in the carcinogenesis of several malignant tumours.[135] Study of the structure–activity relationships for a number of inhibitors of this target revealed that replacing the thiophene moiety in the pyrazole ring of compounds **116** and **117** by other substituents markedly decreases the activity.[136] This finding also proved to hold for the replacement of the dimethoxyphenyl group at the C(5) position: any other (hetero)aryl substituents afforded structures **116** that did not exhibit pronounced inhibitory activity (Fig. 59).

S-Phase kinase-associated protein 2 (Skp2) plays an important role in the recognition of ubiquitin-tagged substrates that are prepared for degradation. Elevated levels of Skp2 are observed in various malignant tumours, making this target attractive for the development of new chemotherapy methods.[137] High-throughput screening of an in-house library identified 2-benzylthio-5-methyl-7-(2,4,6-trimethoxy)-phenyltriazolo[1,5-*a*]pyrimidine **118** (R = Ph) as the first hit.[138] In the subsequent studies, it was found that replacement of the benzene ring in the thiobenzyl moiety by (cyclo)alkyl groups considerably decreases the inhibitory activity in the Skp2-Cks1 protein interaction assay. A similar effect was observed upon introduction of other (hetero)aryl groups, with the exception of a phenyl substituent bearing a *para*-halogen atom (Fig. 60).

Having fixed the substituent at the C(2) position, the authors varied the group at the C(7) atom, thus obtaining a series of compounds **119**. It was found that the replacement of methoxy groups in the benzene ring leads to a decrease in activity, especially if hydrogen-bond donors are introduced. This gave compound **119a** possessing cytotoxic activity against MGC-803 hybrid gastric cancer cells.

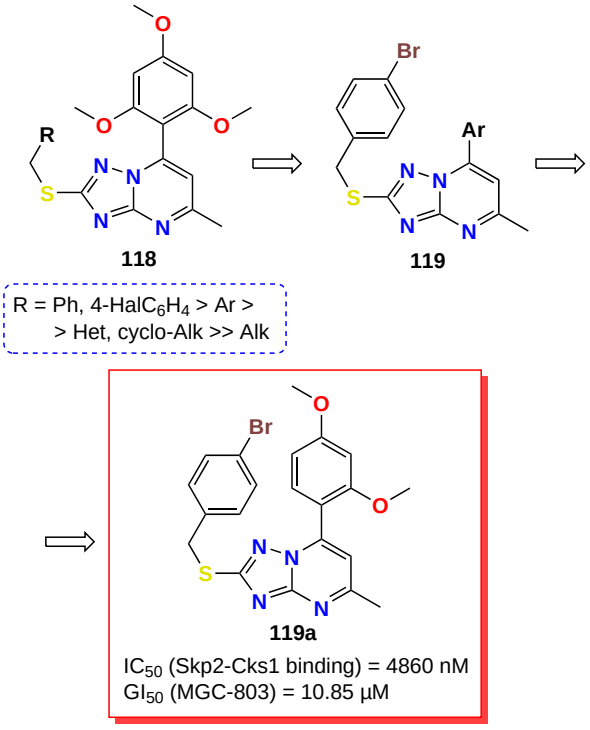
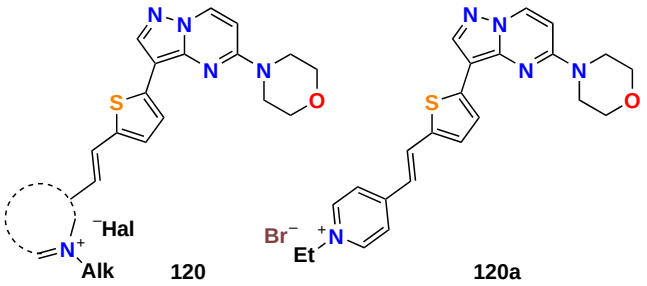


Figure 60. Structural optimization and SARs of compounds **118** and activity data for the most promising derivative **119a**.

2.3.3. Pyroptosis inducers

Zhang *et al.*[139] discovered a group of six photosensitizers, quaternary ammonium salts **120** based on the pyrazolo[1,5-*a*]-pyrimidine scaffold, which trigger pyroptosis in cancer cells.[139] In the absence of light, heterocycles **120** did not exhibit cytotoxic



in the dark:
GI_{50} (MDA-MB-231) > 10 μM
under 400–700 nm irradiation:
GI_{50} (MDA-MB-231) =
0.22–1.01 μM

in the dark:
GI_{50} (MDA-MB-231) > 10 μM
under 400–700 nm irradiation:
GI_{50} (MDA-MB-231) > 10 μM

Figure 61. Structures and data on the activity of photosensitizers **120**, including the most promising compound **120a**.

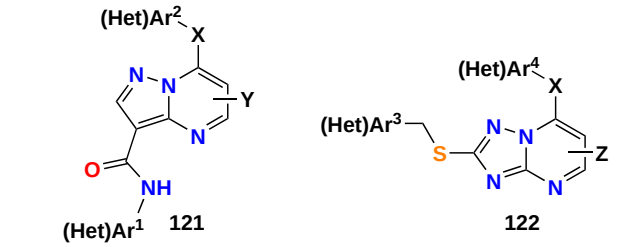
activity against the MDA-MB-231 triple-negative breast cancer cell line. However, on exposure to light with a wavelength of 400–700 nm, most derivatives containing benzoannulated rings exhibited a pronounced cytotoxic effect, with GI_{50} values ranging from 0.22 to 1.01 μM. One heterocycles of this series **120** inhibited tumour growth in *in vivo* experiments using tumour-bearing mice (a highly aggressive 4T1 triple-negative model of breast cancer in mice). At the same time, compound **120a** with a quaternary nitrogen atom in the pyridine ring was an exception and did not possess cytotoxic activity both under light and dark conditions (Fig. 61).

2.4. Summary of Section 2

As noted above, malignant tumours are one of the leading causes of death worldwide; therefore, the search for and discovery of new targets to combat this disease are highly relevant. Since cancer aetiology has not been definitively established, it seems reasonable that azolopyrimidines can target a variety of macromolecules. The targets include various transporter proteins and enzymes involved in the development of chemotherapy resistance; vascular endothelial growth factor receptors, methionine aminopeptidase, and other proteins involved in angiogenesis; a wide variety of kinases, including B-Raf, Pim, CDK, Bruton's tyrosine kinase, Janus kinases, and casein kinase type 2.

In view of the diversity of targets, summarizing the presented data provides the conclusion that kinase inhibitors based on fused azoloazines, including those approved for clinical use, are exclusively pyrazolo[1,5-*a*]pyrimidine derivatives. The most promising substitution pattern is represented by structure **121**, which contains a (hetero)arylamide moiety at the C(3) position of the heterocyclic system and a second (hetero)aryl ring linked to the C(7) atom either directly or *via* a sulfur, oxygen, or nitrogen atom (Fig. 62). Conversely, in the case of non-kinase targets, including enzymes or receptors, 1,2,4-triazolo[1,5-*a*]-pyrimidine-based effectors predominate; the most promising substitution pattern for these compounds is represented by structure **122**.

Although most of the reported data on the pharmacological effects of azoloazines were obtained in *in vitro* experiments, a small number of studies also describe *in vivo* animal studies. In the latter case, the following xenograft mouse models were used: the DLD-1 colorectal cancer (compound **17**, the putative target is CK2), MC-80 breast cancer (compound **53a**, the



Generalized structure of the most promising **kinase inhibitors** of pyrazolo[1,5-*a*]pyrimidine series

Generalized structure of the most promising **non-kinase effectors** of triazolo[1,5-*a*]pyrimidine series

Figure 62. General structures of the most promising effectors **121** and **122** with respect to oncogenic targets.

putative target is PI3Kδ), MV4-11 acute myeloid leukaemia (compound **83**, the putative target is ALKBH5), NCI-H1703 squamous cell lung cancer (compound **100a**, the putative target is ATR), and 4T1 triple-negative breast cancer (compound **120a**, the putative mechanism is the induction of pyroptosis).

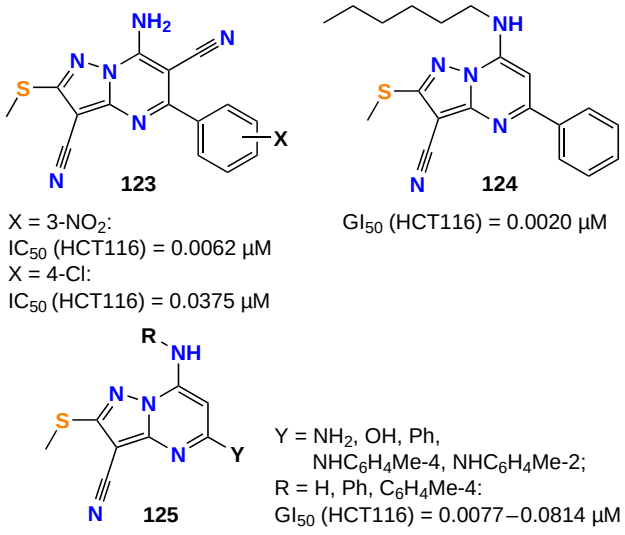
3. Cytotoxic action of azolo[1,5-*a*]pyrimidines

Quite a number of studies addressing the anticancer potential of azoloazines are devoted to their cytotoxic effects on various cell lines rather than to their effect on specific macromolecular targets involved in oncogenesis. The material in this Section is arranged as follows: the structures of the most active compounds are presented in the order of decreasing cytotoxicity index.

3.1. Compounds with cytotoxic activity in the low and submicromolar ranges

The most pronounced cytotoxic action against HCT-116 human colorectal carcinoma cells was found for pyrazolo[1,5-*a*]-pyrimidines **123**–**125**, which were superior to doxorubicin [GI_{50} (HCT116) = 0.007 μM] used in clinical practice (Fig. 63).[140]

One approach to design of compounds with pronounced cytotoxic activity is combining combretastatin and



X = 3-NO_2:
IC_{50} (HCT116) = 0.0062 μM
X = 4-Cl:
IC_{50} (HCT116) = 0.0375 μM

GI_{50} (HCT116) = 0.0020 μM

Y = NH_2, OH, Ph,
NHC_6H_4Me-4, NHC_6H_4Me-2;
R = H, Ph, C_6H_4Me-4:
GI_{50} (HCT116) = 0.0077–0.0814 μM

Figure 63. Structures and cytotoxic activity of compounds **123**–**125**.

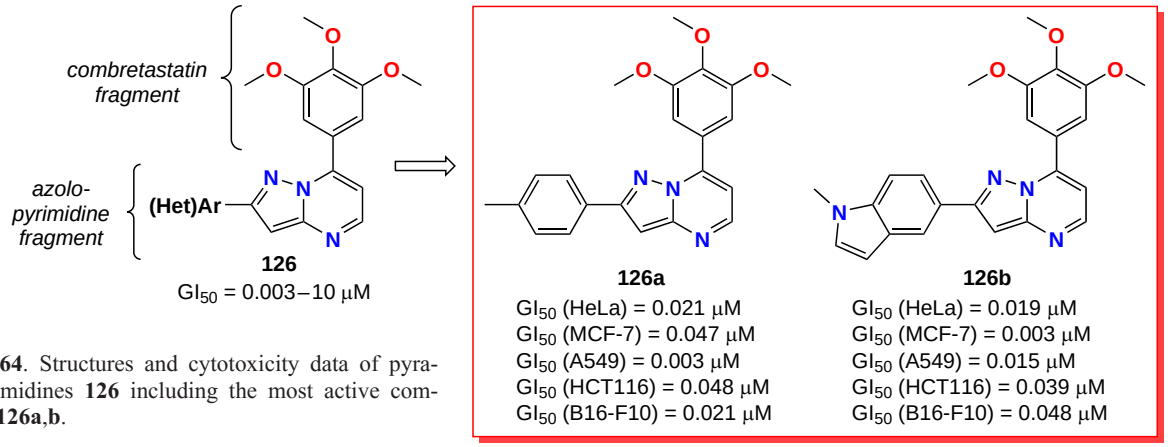


Figure 64. Structures and cytotoxicity data of pyrazolopyrimidines **126** including the most active compounds **126a**,**b**.

azolopyrimidines fragments. Most of 7-(3,4,5-trimethoxyphenyl) pyrazolo[1,5-*a*]pyrimidines **126** showed a cytotoxic activity in a low micromolar and mid-nanomolar ranges (Fig. 64).[141] In general, compounds containing a small electron-donating substituent on the C(2)-benzene ring were more active than those with an electron-withdrawing or bulky substituents. In addition, replacement of the phenyl group by an indol-5-yl ring did not result in a loss of activity, unlike the replacement by the indol-3-yl. The most active compounds **126a**,**b** were slightly superior to the colchicine drug (GI_{50} = 0.018–0.107 μM) against HeLa (cervical adenocarcinoma), MCF-7, A549, HCT116, and B16-F10 (mouse melanoma) cell lines.

One more piece of evidence for increasing cytotoxic action of azolopyrimidines **127** in the presence of a *para*-anisole moiety was reported by Bhogireddy *et al*.[142] The authors showed that an increase in the number of methoxy groups leads to enhancement of the cytotoxic effect and that the most active derivatives, including compound **127a**, show cytotoxicity in the submicromolar range (Fig. 65).

The development of the concept of combining combretastatin and azolopyrimidine fragments within a single molecule was also described by Huo *et al*.[143] Testing of compounds **128** and **129** for cytotoxicity against HeLa cells revealed that heterocycles **129**, containing a 3,4,5-trimethoxyphenyl moiety on the pyrimidine ring rather than on the triazole ring, are more promising in terms of activity. Experiments using an expanded panel of cell lines confirmed this conclusion; furthermore, the compounds **128** and **129** were found to exhibit selectivity, as they did not reduce the viability of human embryonic kidney cells (HEK-293) at a concentration of 100 μM (Fig. 66).

Kim *et al*.[144] carried out pharmacophore analysis of β-tubulin complexes with inhibitors that interact with the colchicine binding site. A key structural unit was the 3,4,5-trimethoxyphenyl group the presence of which in the molecule made it possible to make a selection of compounds, including hydrogenated triazolopyrimidines **130**, from a library of 15 925 structures. Generally, it was shown that compounds **130** inhibit tubulin polymerization (ITP) in a mid-micromolar range and exhibit pronounced cytotoxicity against HL-60 promyelocytic leukaemia cells (Fig. 67).

Zhang *et al*.[145] proved pronounced cytotoxic activity of [1,2,4]triazolo[1,5-*a*]pyrimidines **131** against COLO 205 human colorectal adenocarcinoma cell line and identified some structure–activity relationships (Fig. 68). The mechanism of action of the most effective compounds **131** was investigated, and it was shown that they promote tubulin polymerization and also exhibit anticancer activity in *in vivo* experiments against

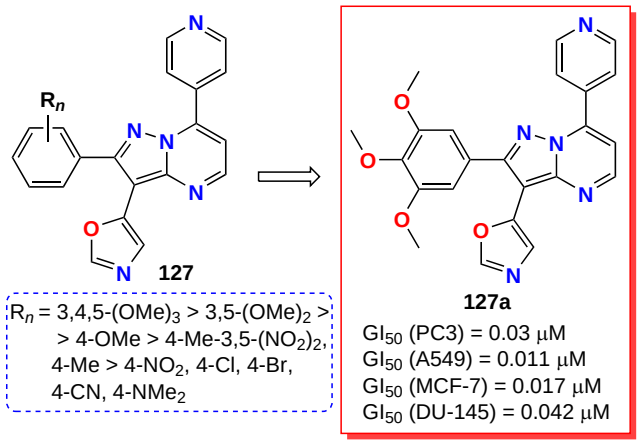


Figure 65. Structures and SARs for compounds **127** and cytotoxicity data for most promising compound **127a**. PC3 and DU-145 are prostate adenocarcinoma cell lines.

U87-MG glioblastoma following intravenous and oral administration.

The subsequent extended studies of the most promising compound[146] demonstrated that [1,2,4]triazolo[1,5-*a*]pyrimidine **131a** inhibits the binding of vinblastine to the αβ-tubulin heterodimer; hence, this ligand may represent a new class of compounds that are active against microtubules.[147] Preclinical trials of this compound have shown[148] that it exhibits antiproliferative activity against tumours resistant to paclitaxel and vincristine. However, Phase I clinical trials of compound **131a** identified a noticeable side effect as neutropenia.[149]

It was shown that pyrazolopyrimidines **132** (Fig. 69) at concentrations in the submicromolar range effectively reduce the proliferative capacity of both A2780 ovarian carcinoma cells and the corresponding resistant mutant A2780AD.[150]

Singleton *et al*.[151] prepared analogues of dorsomorphin, an inhibitor of various kinases with antiproliferative activity, belonging to the class of pyrazolo[1,5-*a*]pyrimidines. The initial screening using A2780 ovarian carcinoma cells indicated that compounds **133** and **134** at a concentration of 10 μM do not exhibit significant cytotoxicity. The introduction of a dorsomorphin-resembling moiety into the C(6)-position of the system resulted in structures **135** with a pronounced cytotoxic effect. As a result, the authors identified several compounds that were more active than dorsomorphine [half-maximal effective concentration, EC_{50} (A2780) = 1.1 μM], *e.g*., heterocycle **135a** (Fig. 70).

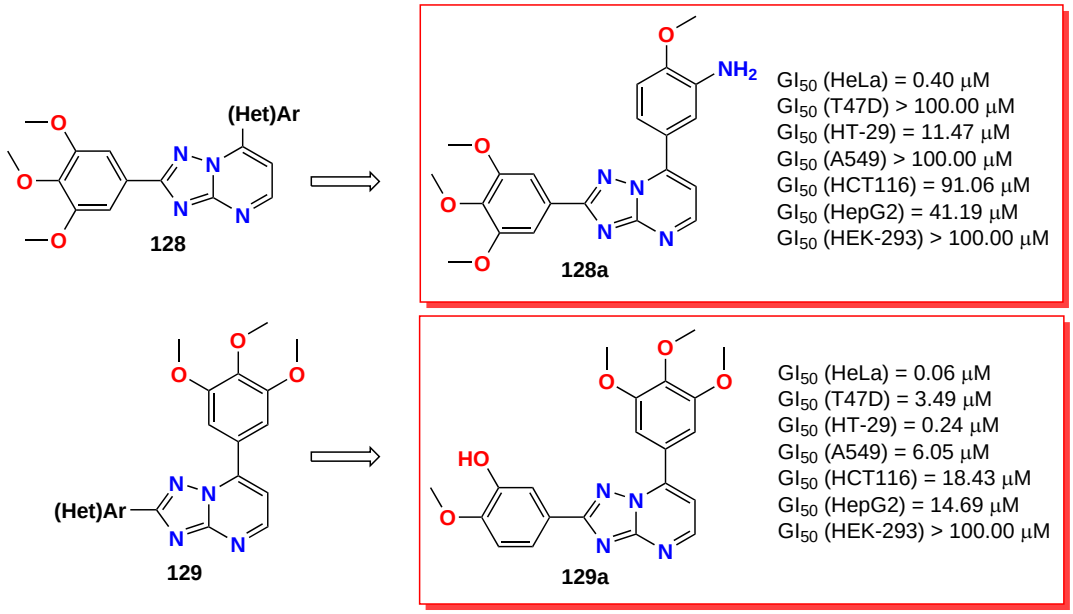
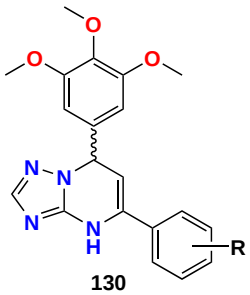


Figure 66. Structures of 1,2,4-triazolopyrimidines **128** and **129** and comparison of the GI_{50} values for the most active representatives **128a** and **129a**. T47D is the breast ductal carcinoma cell line, HT-29 is the colorectal adenocarcinoma cell line.



R	IC_{50} (ITP), μM	GI_{50} (HL-60), μM
H	13.7	0.17
4-Me	12.8	0.13
4-OMe	10.4	0.19
3,4-$(OMe)_2$	>24	0.34
4-Cl	>25	0.39
3-NHAc	>25	0.33
4-Et	>25	0.37

Figure 67. Structures and data on cytotoxicity and inhibitory effect on β-tubulin polymerization for compounds **130**.

Some members of series **136** and **137** also had cytotoxic properties against four cancer cell lines (MGC-803 human gastric cancer, EC109 human esophageal squamous cell carcinoma, A549 lung adenocarcinoma, and PC-9 non-small cell lung cancer) in the low- and mid-micromolar ranges (Fig. 71).[152] The most active compound **136a** comprised a benzimidazole moiety and a combretastatin residue.

Fouda *et al.*[153] performed screening of the cytotoxic activity of 3,6-(hetero)arylazopyrazolopyrimidines **138**; the authors identified a few compounds exhibiting cytotoxicity against HepG2, MCF-7, and HCT116 cells in the low and submicromolar ranges (Fig. 72). Compound **138a** was most effective.

Series of [1,2,4]triazolo[1,5-*a*]pyrimidines **139** and **140**, containing a 3,4,5-trimethoxyphenyl moiety, were reported by Yang *et al.*[154] (Fig. 73). These heterocycles were found to reduce the viability of lung adenocarcinoma (A549) and cervical adenocarcinoma (HeLa) cells in a low micromolar range, while HCT116 colorectal carcinoma cells and HEK-293 human embryonic kidney cells were affected to a lesser extent. Bicyclic derivatives **140** were found to be superior to tricyclic derivatives **139**. However, the most active compound **140a** was inferior to combretastatin CA-4 [GI_{50} (HeLa) = 0.043 μM, GI_{50} (A549) = 0.055 μM] against the two cell lines.

A brief report on assessment of the cytotoxicity of pyrazolopyrimidine **141** against four cell lines was presented by Ahmed *et al.*[155] Compound **141** effectively reduced the

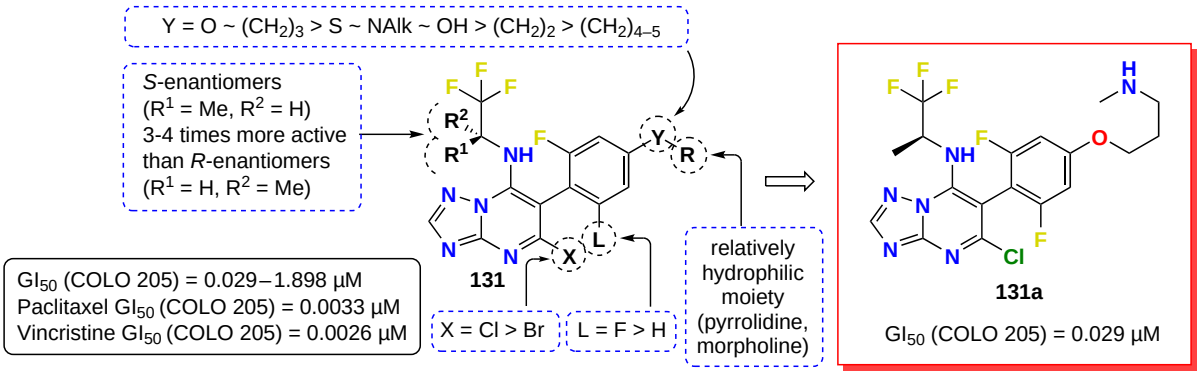
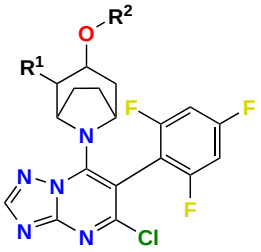


Figure 68. Structures, SARs, and activity data for compounds **131**, including the most promising compound **131a** and comparison with the action of clinically used drugs.



132

R^1	R^2	GI_{50} (A2780), μM	GI_{50} (A2780AD), μM
Me	Me	0.051	0.081
F	Me	0.430	0.620
H	Pr^n	0.600	0.630
H	$CH_2C{\equiv}CH$	0.200	0.250
H	Ac	0.250	0.330

Figure 69. Structures and cytotoxicity data of compounds **132**.

proliferative capacity of tumour cells in the low micromolar range (see Fig. 73).

A study of the cytotoxic effects of hybrid compounds **142** and **143** comprising pyrazolopyrimidine and thiazolobenzimidazole moieties demonstrated that all of them inhibit the proliferation of Caco-2 human colorectal adenocarcinoma cells to a greater extent than doxorubicin; however, they also inhibited the viability of normal BHK cells from the kidneys of baby Syrian hamsters [for doxorubicin, GI_{50} (Caco-2) = 11.2 μM and GI_{50} (BHK) = 0.74 μM] (Fig. 74).[156]

A promising strategy for the treatment of Ewing's sarcoma is to inhibit the Hsp90 protein.[157] Zajec *et al.*[158] reported optimization of the structure of hit compound **144**, which was identified *via* virtual screening (Fig. 75). It was shown that replacing the benzyl moiety at the N(7) atom by a methyl group (compound **145**) or a similar modification in the side-chain piperidine ring (compound **146**) leads to a loss of cytotoxic activity against Ewing's sarcoma cells (SK-N-MC). A similar decrease in the activity was also noticed in the absence of a halogen atom in the benzyl moiety. Furthermore, the benzyl moiety (compound **147**) proved to be more beneficial for the activity than the benzoyl moiety: this modification induced a two- to three-fold increase in the cytotoxicity.

Kamal *et al.*[159] combined a [1,2,4]triazolo[1,5-*a*]pyrimidine scaffold and the AAL993/CI-1040 antitumour anthranilamide moiety within a single molecule (Fig. 76).[160] The resulting derivatives **148** had a marked cytotoxicity against SiHa squamous cell cervical carcinoma and HeLa cervical adenocarcinoma cells. The most active compounds **148** were tested against an expanded panel of cell lines (>50 variants) and also showed GI_{50} values in the low micromolar range.

A similar strategy for conjugate design based on [1,2,4]triazolo[1,5-*a*]pyrimidines was employed by Kamal *et al.*[161] Covalent coupling to various benzothiazoles furnished

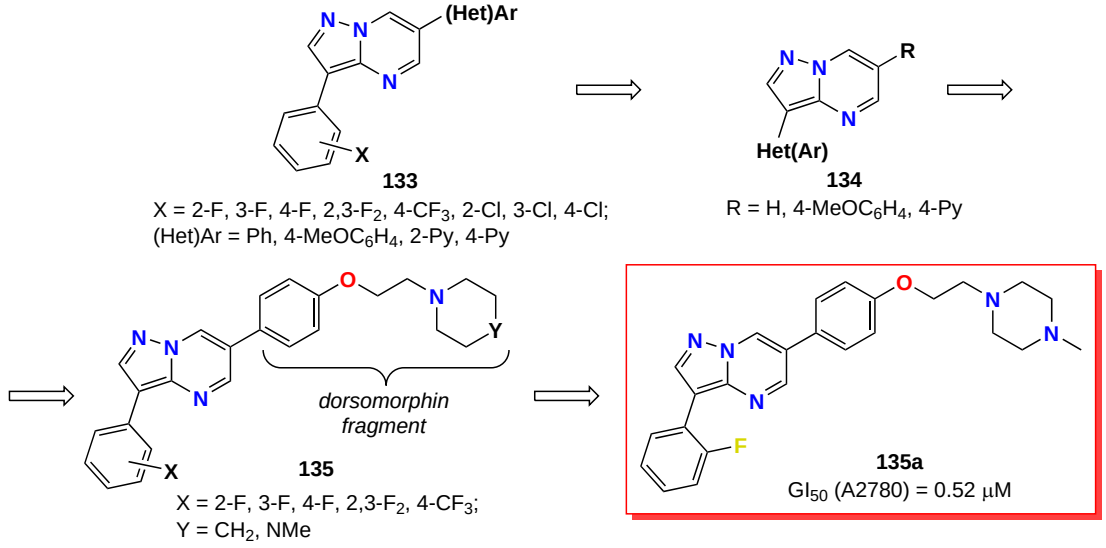


Figure 70. Structural optimization of heterocycle **133** and activity data for the most promising compound **135a**.

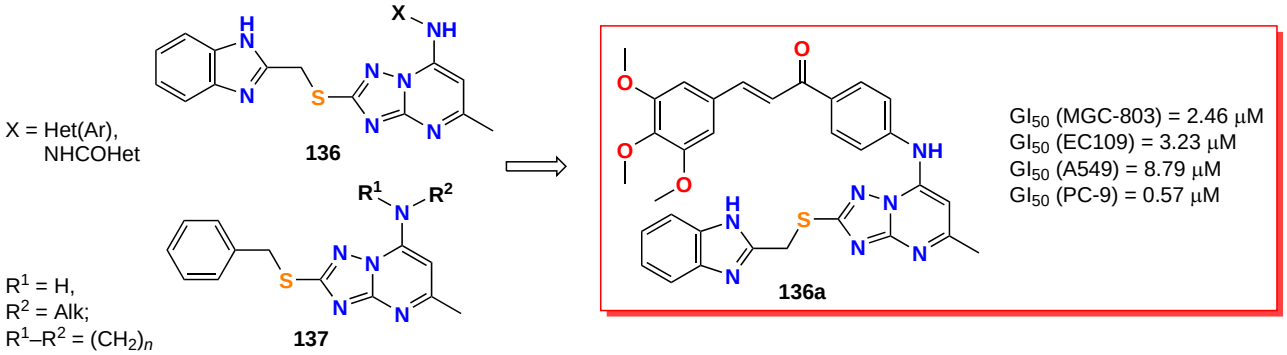


Figure 71. Structures of compounds **136** and **137** and activity data for the most promising compound **136a**.

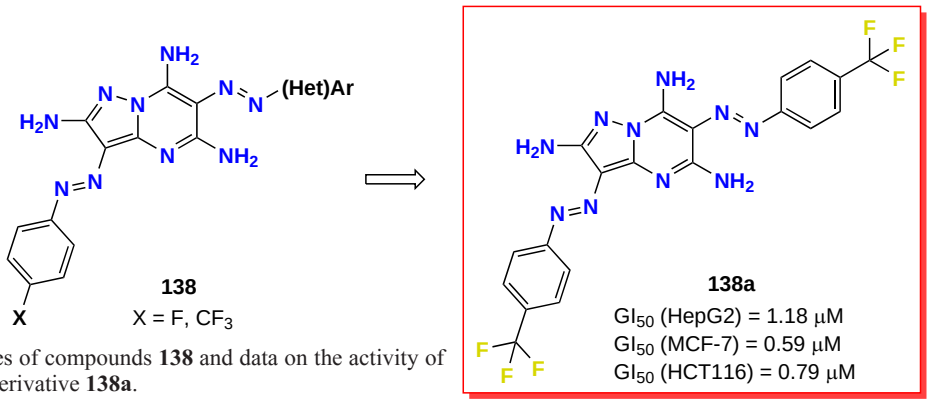


Figure 72. Structures of compounds **138** and data on the activity of the most promising derivative **138a**.

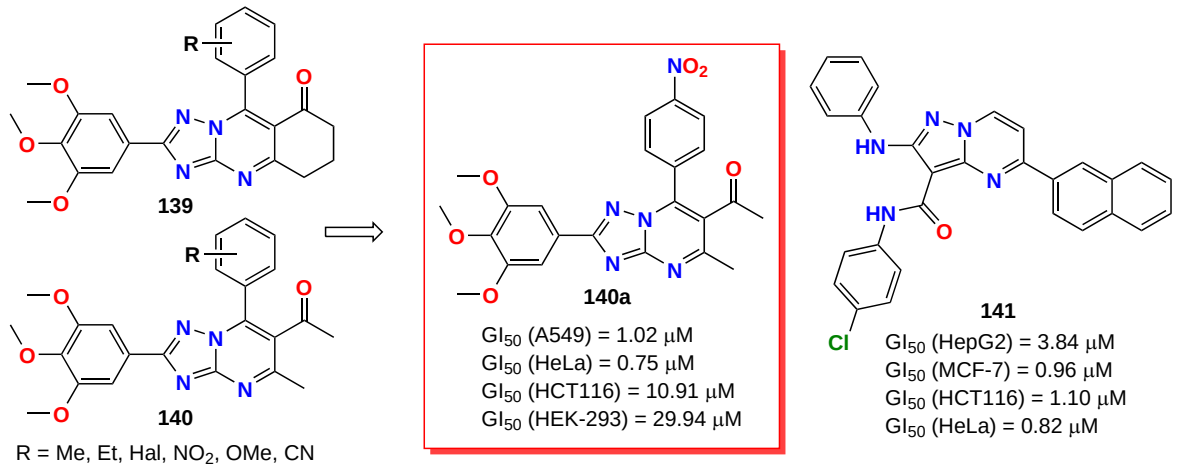


Figure 73. Structures of azolopyrimidines **139**–**141** and activity data for the most promising derivative **140a** and compound **141**.

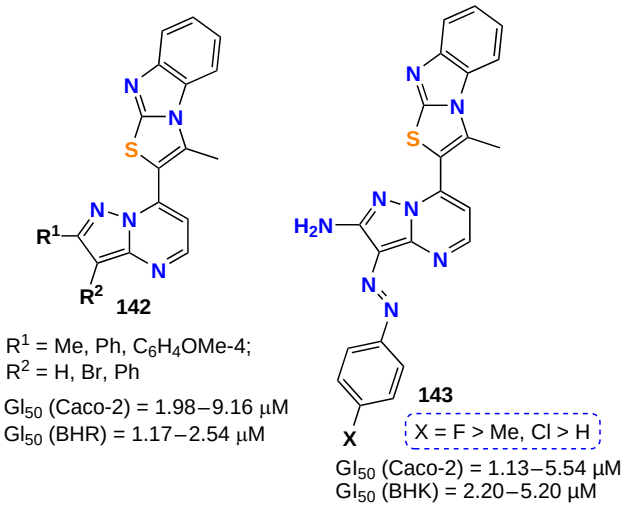


Figure 74. Structures and activity data for compounds **142** and **143** and SARs for the latter.

heterocycles **149**, which exhibited pronounced cytotoxicity against a number of cell lines in the low- and mid-micromolar range (see Fig. 76).

Further development of the approach consisting in the conjugation of azolopyrimidines and anthranilamide derivatives resulted in yet another series of compounds **150**. It was found that substituents on the C(7)-phenyl moiety of compounds **150** exert a more pronounced influence on cytotoxicity than the substitution pattern in the amide portion of the molecule (Fig. 77).[162]

Two heterocycles, **151a** and **151b**, comparable in cytotoxicity to Taxol (GI_{50} = 0.40–5.50 μM) against the HepG2 hepatocellular carcinoma cell line, the HCT116 colorectal carcinoma cell line, and the MCF-7 breast ductal carcinoma cell line, were identified in study [163] among the series of derivatives **151** (Fig. 78).

Unusual spiro[benzo[*h*]tetrazolo[5,1-*b*]quinazoline-7,3′-indoline]triones **152** were described by Wu *et al.*[164] It was established that these heterocycles substantially affect the viability of HepG2 hepatocellular carcinoma cells, with GI_{50} in the range of 2.86–36.34 μM (Fig. 79). The most active compounds contained a substituent at the C(5) or C(7) position of the indole ring. 5-Fluoro derivative **152a** proved to be more cytotoxic against HepG2 cells and more selective in the action on LO2 hepatocytes than tanshinone IIA [GI_{50} (HepG2) = 24.85 μM, GI_{50} (LO2) = 65.29 μM].

A study of two series of compounds **153** and **154** in which a pyrazolo[1,5-*a*]pyrimidine ring was combined with a chalcone moiety revealed differences in their cytotoxic activity against four cell lines.[165] Thus, heterocycles **154** in which the keto group is directly linked to the heterocyclic skeleton has greater cytotoxicity against DU-145 prostate adenocarcinoma cells, while their isomers **153** were more effective at reducing the viability of A549 lung adenocarcinoma and MDA-MB-231 triple-negative breast cancer cells. Certain structure–activity relationships for these compounds were elucidated by screening (Fig. 80).

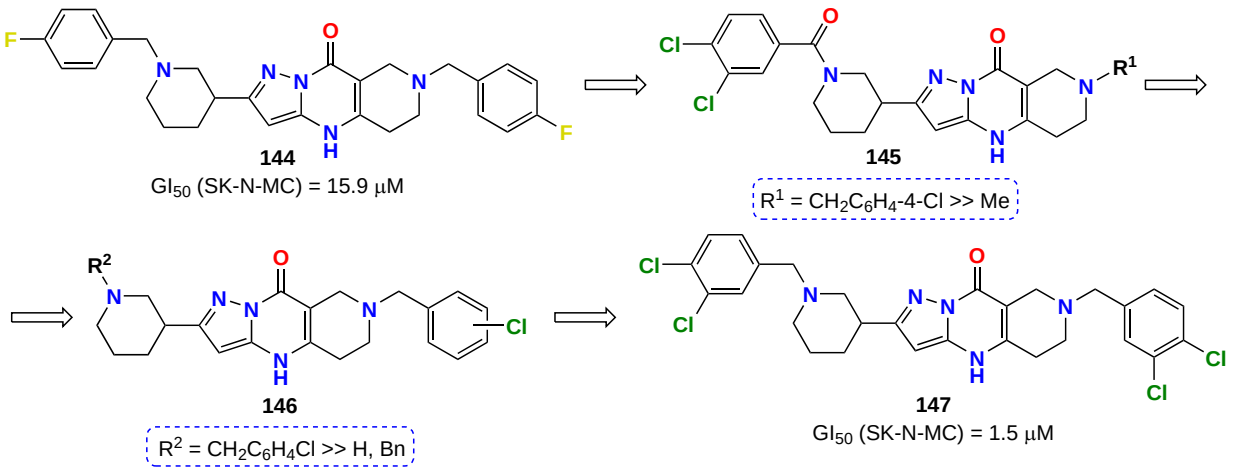


Figure 75. Structural optimization of compound **144**; SARs for derivatives **145** and **146**, and activity data for compound **147**.

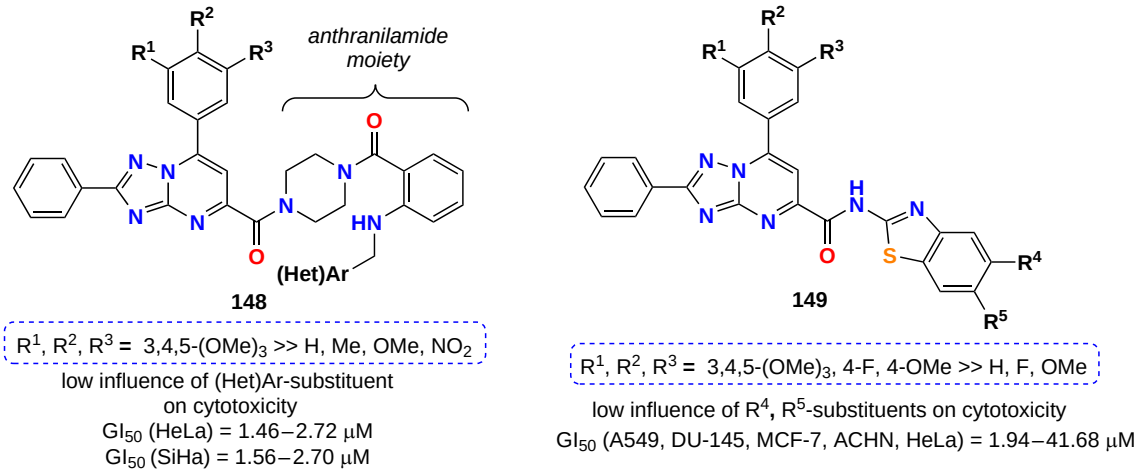


Figure 76. Structures, SARs, and activity data for conjugates **148** and **149**. ACHN is renal adenocarcinoma cell line.

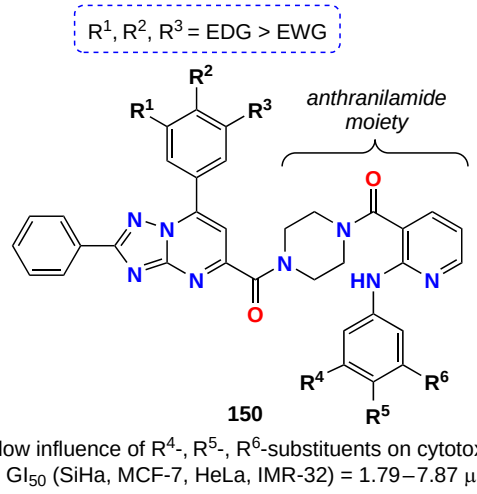


Figure 77. Structures, SARs, and activity data for conjugates **150**. EDG is an electron-donating group, IMR-32 is a neuroblastoma cell line.

Among a small series of 5,7-diaminoazolopyrimidine-6-carbonitriles, Urakov *et al.*[22] identified three promising compounds that exhibited selective cytotoxic activity against A549 lung carcinoma cells (compound **155**), HepG2 hepatocellular carcinoma cells (**156**), and Rd embryonic rhabdomyosarcoma (**157**) cells (Fig. 81).

Of the few 5-(hetero)aryl-[1,2,4]triazolo[1,5-*a*]pyrimidines **158**, only compound **158a** showed a marked cytotoxicity against MCF-7 breast cancer cells, while the GI_{50} values for the other derivatives exceeded 100 μM (Fig. 82).[166]

Attia *et al.*[167] investigated larotrectinib analogues (see Fig. 1), compounds **159**–**161**, for their antiproliferative activity against Huh-7 hepatocellular carcinoma cells, HeLa cervical adenocarcinoma cells, and MCF-7 breast ductal adenocarcinoma cells (Fig. 83). Most of these derivatives exhibited a cytotoxicity index in the mid- and high micromolar range, with the exception of three structures, **159a**,**b** and **160a**. These compounds were additionally tested on the MDA-MB-231 triple-negative breast cancer cell line where they showed cytotoxicity exceeding that of doxorubicin [GI_{50} (MDA-MB-231) = 6.0 μM].

Modification of the pyrazolopyrimidines **162** containing two nitrile groups as peripheral substituents yielded a series of compounds that demonstrated cytotoxic activity in the mid-micromolar range (Fig. 84). The most promising structure **162a** was an order of magnitude more active than the others, although it was inferior to doxorubicin against two cell lines [GI_{50} (MCF-7) = 4.17 μM; GI_{50} (HeLa) = 5.57 μM].[168]

Zhao *et al.*[169] described a series of 3-cyanopyrazolo[1,5-*a*]-pyrimidines **163** containing a nitrogen mustard analogue [$R^1 = N((CH_2)_2Cl)_2$] (Fig. 85). The authors found that

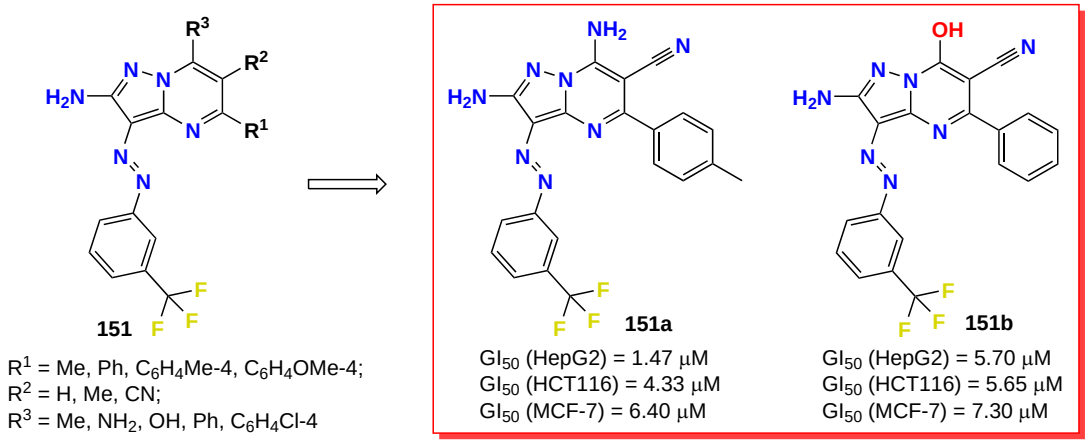


Figure 78. Structures of pyrazolopyrimidines **151** and activity data for the most promising derivatives **151a**,**b**.

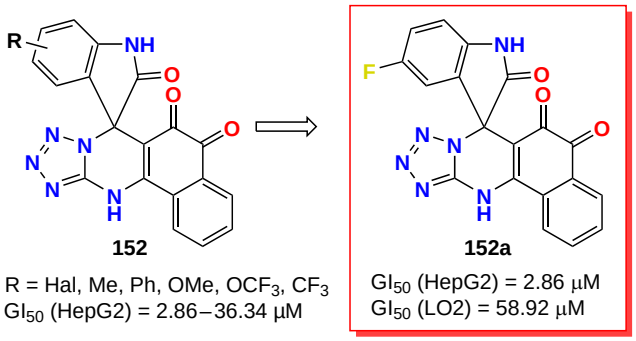


Figure 79. Structures and activity data for compounds **152**, including the most promising derivative **152a**.

compounds **163**, in which the bis(chloroethyl)amino group is located at the methylene atom at C(5) [$R^2 = R^3 = (CH_2)_2Cl$], have virtually no effect on tumour cells. Conversely, the introduction of this moiety into the benzene ring of the aniline substituent gives compounds with a pronounced cytotoxicity. It is noteworthy that *para*-substituted compounds are more effective (*e.g.*, compound **163a**) than *meta*-isomers.

Among polycyclic fused heterocycles based on azole[1,5-*a*]-pyrimidines, there are also compounds with antiproliferative activity. Huang *et al.*[170] synthesized a series of derivatives **164**, in which a steroid moiety was annulated to a [1,2,4]triazolo-[1,5-*a*]pyrimidine system (Fig. 86). Variation of the (hetero)aryl moiety at the C(7) atom demonstrated that most of compounds **164** had no cytotoxic activity against three cancer cell lines:

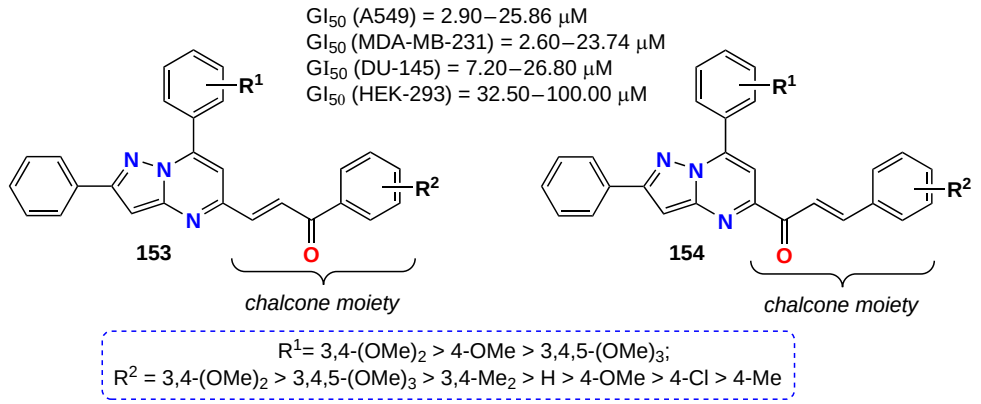


Figure 80. Structures, SARs, and activity data for compounds **153** and **154**.

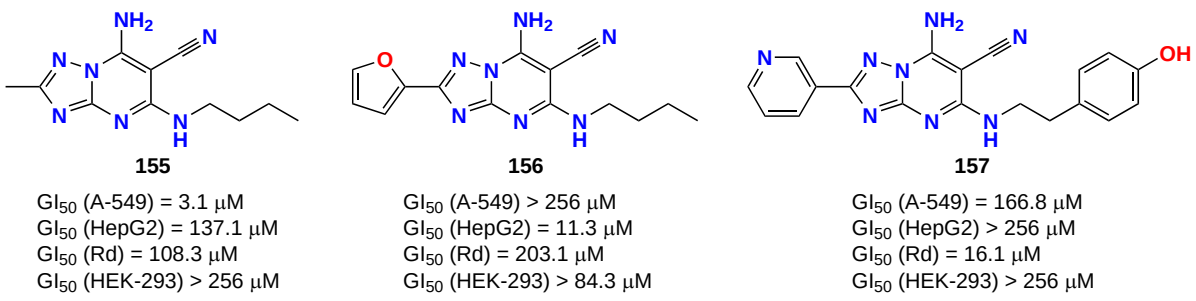


Figure 81. Structures and activity data for compounds **155**–**157**.

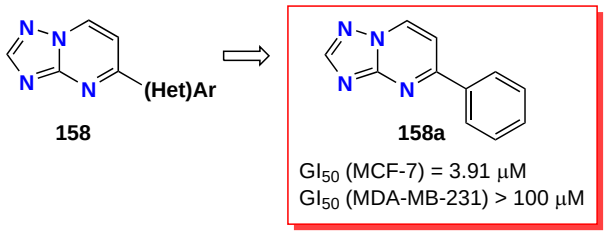


Figure 82. Structures of compounds **158** and activity data for the most promising derivative **158a**.

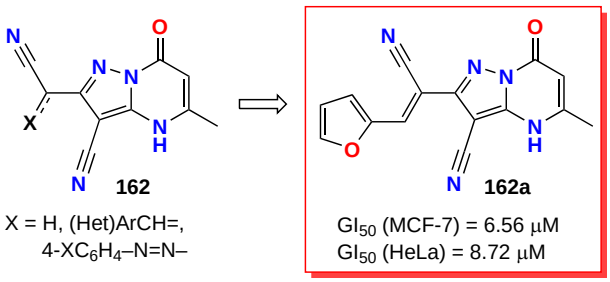


Figure 84. Structures of compounds **162** and data on the activity of the most promising derivative **162a**.

MCF-7, PC-2 (human pancreatic carcinoma), and EC9706 (human esophageal squamous cell carcinoma). However, several exceptions were found: for example, derivatives **164a** and **164b** reduced cell proliferation in the low- and mid-micromolar ranges.

Two structurally similar heterocycles were reported by Bondock *et al.*[171] Despite their similar structures, compounds **165** and **166** markedly differed in the cytotoxic activity (Fig. 87).

The cytotoxicity of compounds **167** (see Fig. 87) against HeLa cervical adenocarcinoma cells depended on the number of halogen atoms on the phenyl moieties linked to the pyrazolo[1,5-*a*]pyrimidine skeleton either directly or *via* an amide linker.[172] The highest activity was observed for compounds containing at least three halogen atoms, with chlorine being more beneficial than fluorine.

The antiproliferative activity of 5-substituted 7-(1-methylindol-3-yl)-[1,2,4]triazolo[1,5-*a*]pyrimidines **168** against the MGC-803 (human gastric cancer), HCT116 (human colorectal carcinoma), and MCF-7 (breast ductal adenocarcinoma) cell lines was investigated by Yu *et al.*[173] (Fig. 88); however, the authors did not establish any SARs. It was shown that most compounds exhibited moderate antiproliferative activity against the above cell lines, while compound **168a** had a substantial cytotoxicity.

3.2. Compounds with cytotoxic activity in the mid-micromolar range

Some ester derivatives of pyrazolo[1,5-*a*]pyrimidines **169** and **170** were considered by Naik *et al.*[174] (Fig. 89); however, no targeted SAR studies were carried out. The available data indicate that the most active compounds, in particular heterocycle **170a**, are slightly less cytotoxic than paclitaxel (GI_{50} = 3.23–6.31 μM).

A search for pyrazolo[1,5-*a*]pyrimidines exhibiting cytotoxicity against U-251MG glioblastoma cells among fifteen structures **171** was described by He *et al.* (Fig. 90).[175] It was found that for a compound to be active, a benzene ring must be present at the C(5) position of the molecule (the molecule with a *tert*-butyl group was inactive); conversely, an alkyl group is

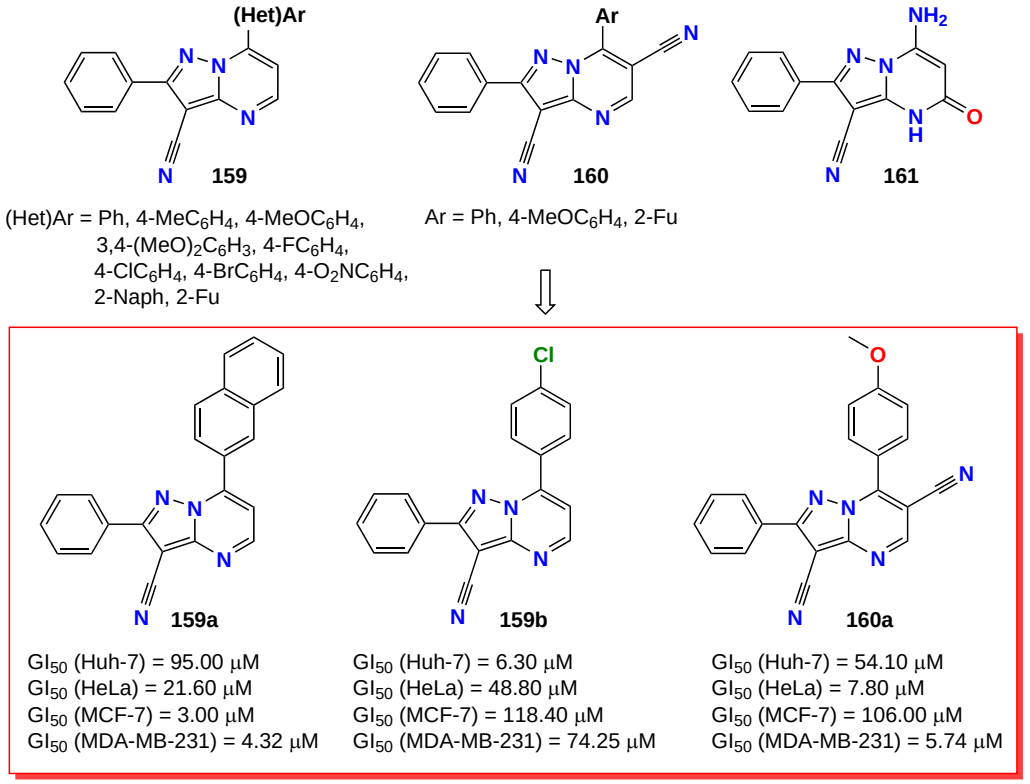


Figure 83. Structures of compounds **159**–**161** and activity data for the most promising derivatives **159a**,**b** and **160a**.

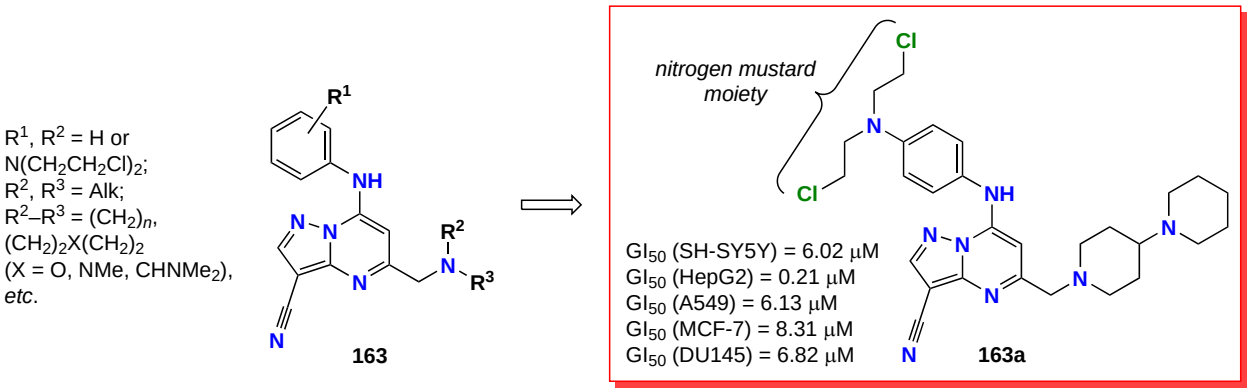


Figure 85. Structures of compounds **163** and activity data for the most promising derivative **163a**. SH-SY5Y is a human neuroblastoma cell line.

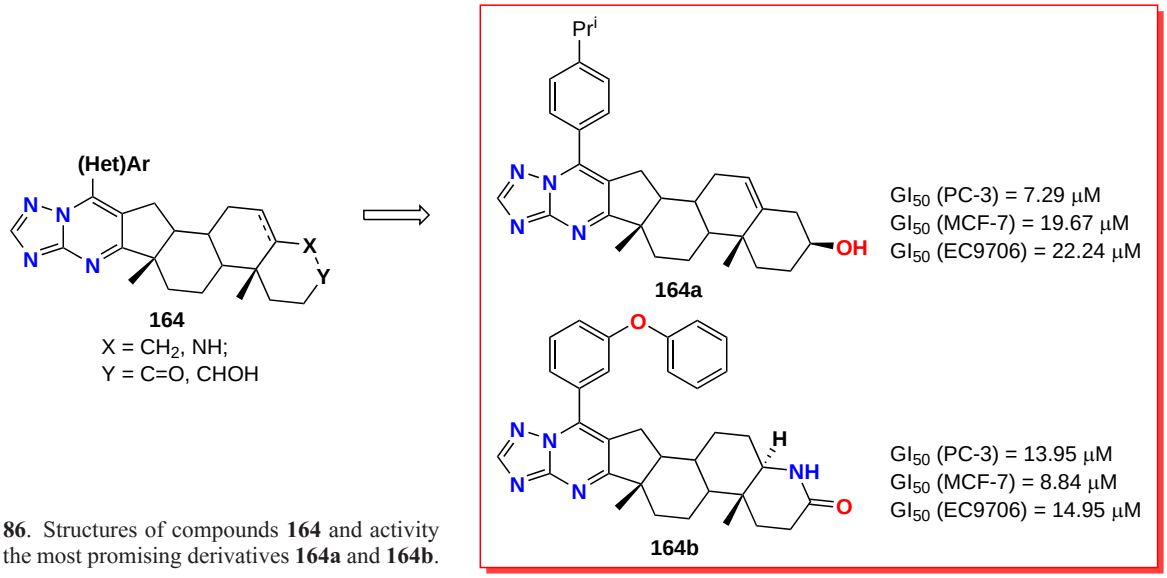


Figure 86. Structures of compounds **164** and activity data for the most promising derivatives **164a** and **164b**.

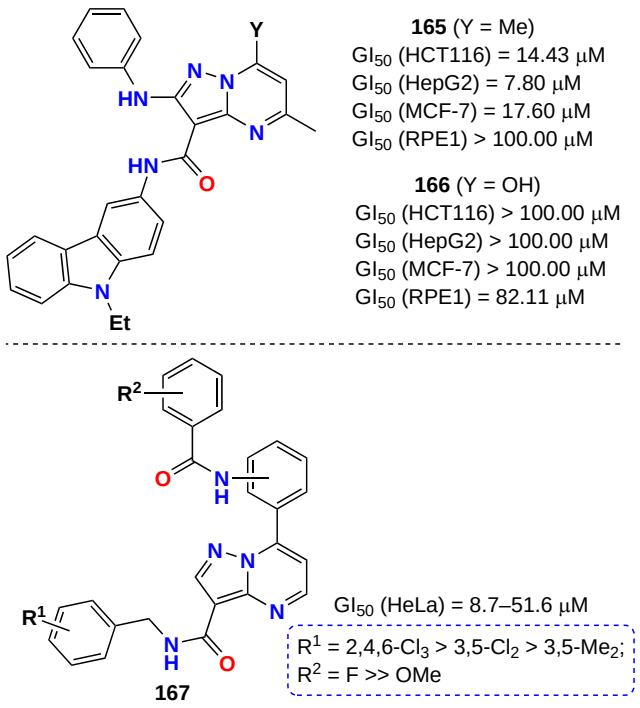


Figure 87. Structures and activity data for compounds **165**–**167** and SARs for derivatives **167**. RPE1 is a telomerase-immortalized human retinal pigment epithelial cell line.

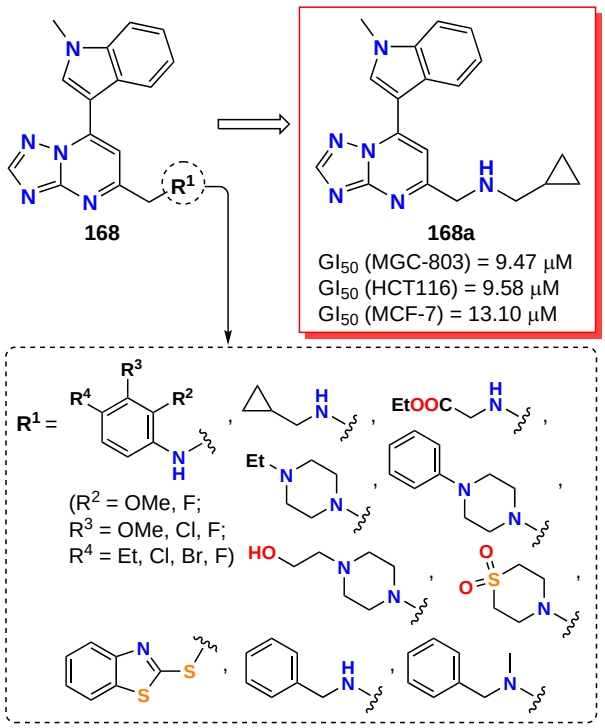


Figure 88. Structures of compounds **168** and activity data for the most promising compound **168a**.

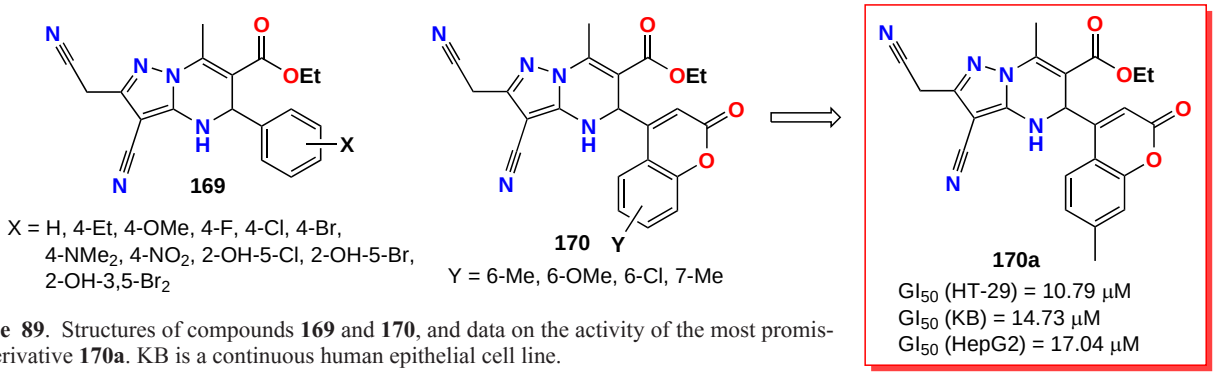


Figure 89. Structures of compounds **169** and **170**, and data on the activity of the most promising derivative **170a**. KB is a continuous human epithelial cell line.

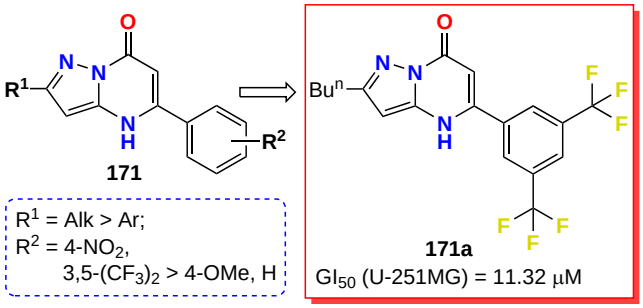


Figure 90. Structures and SARs for compounds **171** and activity data for the most promising derivative **171a**.

required at the C(2) position (aryl-substituted derivatives proved to be less cytotoxic). Most of compounds **171** had a GI_{50} value in the high micromolar range; however, the most promising compound **171a** was an order of magnitude more active.

Fused pyrido[2′,3′:3,4]pyrazolo[1,5-*a*]pyrimidine systems **172** (Fig. 91) were investigated for cytotoxicity against a number of cell lines: stage IV prostate cancer (PC3), cervical adenocarcinoma (HeLa), triple-negative breast cancer (MDA-MB-231), hepatocellular carcinoma (HepG2), and human umbilical vein endothelial cells (HUVEC).[176] It was found that the cytotoxic effect is attenuated in the presence of electron-donating alkyl substituents in the pyrimidine ring. A similar pattern was observed for aryl-substituted derivatives: electron-donating substituents in the aromatic ring decreased the activity,

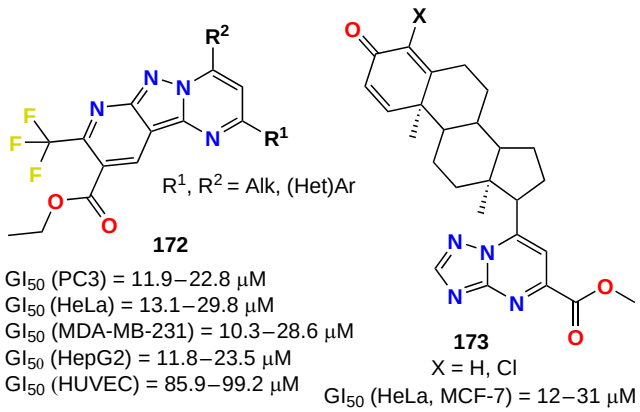


Figure 91. Structures and data on the activity of compounds **172** and **173**.

while electron-withdrawing substituents, conversely, ensured a higher activity. Nevertheless, all compounds **172** were inferior to 5-fluorouracil (GI_{50} = 1.6–1.9 μM, SI = 41.89–49.75) in terms of cytotoxicity and selectivity index (SI).

Two derivatives **173** (see Fig. 91), belonging to the class of [1,2,4]triazolo[1,5-*a*]pyrimidines and containing a steroid moiety, were inferior to etoposide [GI_{50} (HeLa) = 0.8 μM; GI_{50} (MCF-7) = 3.1 μM] in decreasing the viability of HeLa cells and MCF-7 breast ductal adenocarcinoma cells. For these heterocycles taken at a concentration of 50 μM, the inhibition ranged from 24 to 62%, while for etoposide it was 86–90%.[177]

Zhai *et al.*[178,179] and Zhao *et al.*[180] investigated the dependence of cytotoxic activity against Bel-7402 hepatocellular carcinoma cells and HT-1080 human fibrosarcoma cells on the nature of the side chain at the C(2) position and on substituents at the C(7) atom of azolo[1,5-*a*]pyrimidines **174**. It was shown that substituents R^1 in the aniline moiety have a more pronounced effect (Fig. 92): fluorine-containing groups on the benzene ring are preferred (compounds **174a**,**b**). Thus, derivative **174a**, which had the highest cytotoxicity, was four times more active than cisplatin, which has GI_{50} (Bel-7402) = 35.5 μM and GI_{50} (HT-1080) = 22.7 μM.

A few compounds with cytotoxicity in the mid-micromolar range were found among 7-amino-azolo[1,5-*a*]pyrimidines **175** (Fig. 93), *e.g.*, compounds **175a**,**b**. However, almost all of derivatives **175** also reduced the proliferative capacity of human embryonic kidney cells (HEK-293), with the best selectivity index being 4.82.[21]

Among pyrazolo[1,5-*a*]pyrimidines **176**, many compounds exhibited cytotoxic activity against cancer cells in the mid-micromolar range; however, these molecules often inhibit the viability of normal diploid cells (WI-38) to a greater extent (Fig. 94).[181]

Tetrazolo[1,5-*a*]pyrimidine-6-carbonitriles **177**, containing an indol-3-yl substituent at the C(5) position, were investigated for cytotoxic activity against the HCT116 colorectal cancer cells, MCF-7 breast ductal adenocarcinoma cells, MDA-MB-231 triple-negative breast cancer cells, A549 lung adenocarcinoma cells, and telomerase-immortalized human retinal pigment epithelial cells (RPE1). HCT-116 cells proved to be most sensitive to the action of compounds **177**, whereas the proliferative capacity of immortalized normal RPE1 cells was affected to the least extent (see Fig. 94).[182]

The T-24 bladder carcinoma cells were found to be most sensitive to the action of azole[1,5-*a*]pyrimidin-7-ones **178**; however, the cytotoxic effect was often accompanied by a decrease in proliferation of normal HEK-293 cells (Fig. 95).

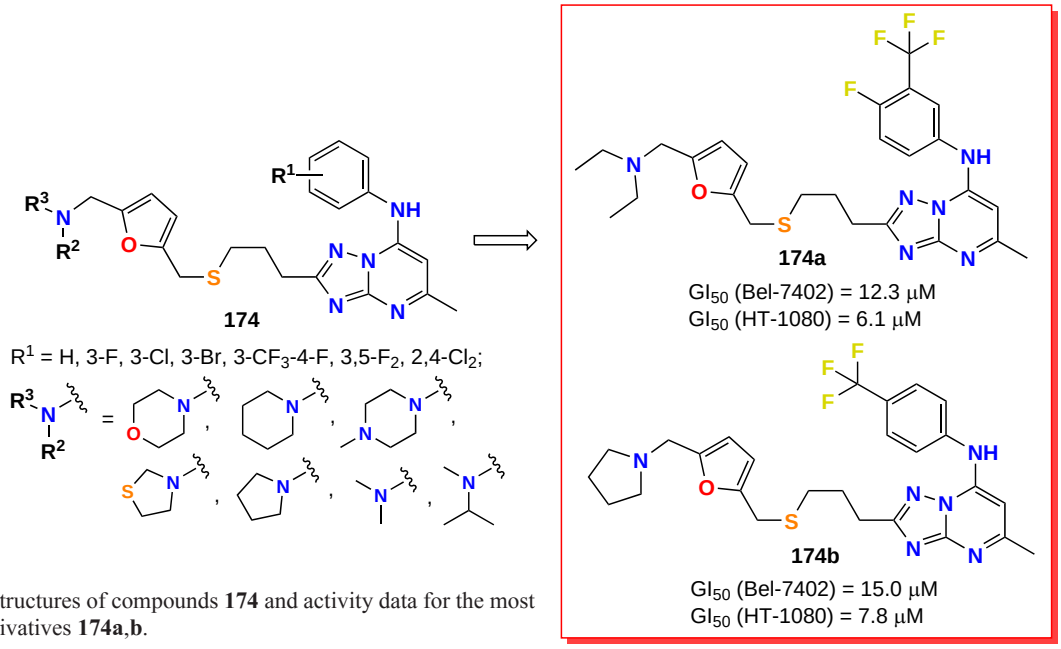


Figure 92. Structures of compounds **174** and activity data for the most promising derivatives **174a**,**b**.

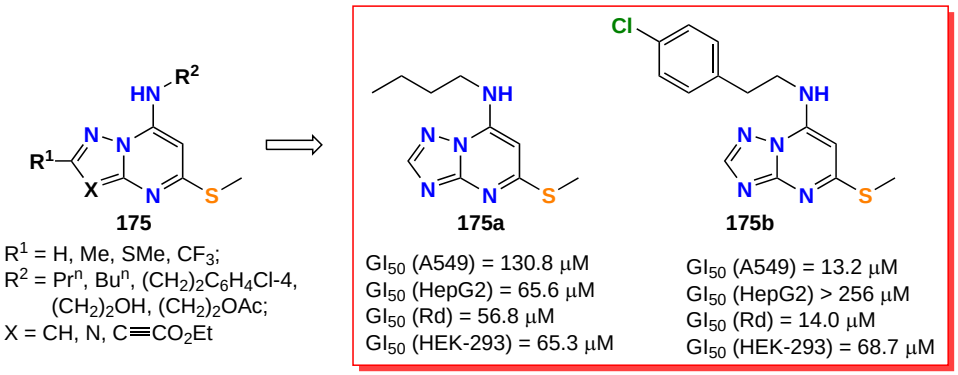


Figure 93. Structures of compounds **175** and activity data for the most promising derivatives **175a**,**b**.

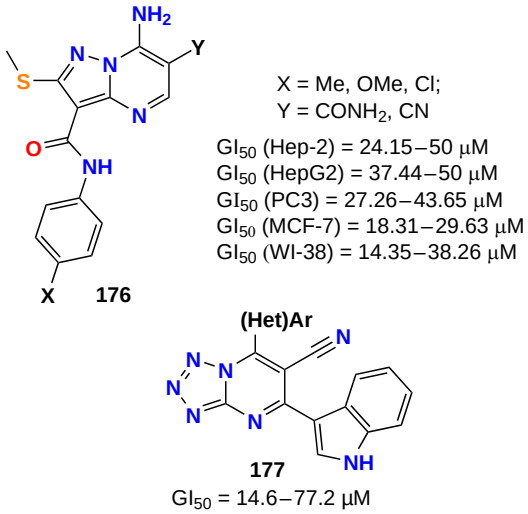


Figure 94. Structures and activity data for compounds **176** and **177**.

Screening identified two derivatives, **178a** and **178b**, which had selective cytotoxicity in the mid-micromolar range.[16]

Ushakova *et al.*[18] evaluated the cytotoxicity of the regioisomeric alkylation products of 7-amino[1,2,4]triazolo[1,5-*a*]pyrimidines **179** and **180** against embryonic rhabdomyosarcoma cells (Rd), colorectal adenocarcinoma cells (Caco-2), bladder carcinoma cells (T-24), and human lung fibroblasts (WI-38) (Fig. 96). Among 3-substituted [1,2,4]triazolo[1,5-*a*]pyrimidines **179**, compound **179a** demonstrated the greatest cytotoxic effect against tumour cells, while exhibiting some selectivity relative to normal cells. The authors did not present the cytotoxicity data for C(6)-non-halogenated analogue of compound **179a**; hence, it is impossible to evaluate the effect of the halogen atom present in the molecule on the anticancer activity. Meanwhile, 4-alkyl derivatives **180** had a less pronounced effect on the division of both tumour and normal cells, with derivative **180a** being the most active.

Testing of 2,7-diarylpyrazolo[1,5-*a*]pyrimidines **181** for their ability to decrease the viability of HCT116 colorectal carcinoma cells and normal HEK-293 human embryonic kidney cells revealed that the most active compounds contain a methoxy group in the benzene ring linked to the pyrazole ring (Table 1).[183]

Bersneva *et al.*[17] considered the cytotoxic activity of thirteen compounds belonging to a new family of pyrimido[5,4-*e*]-azolo[1,5-*a*]pyrimidines and pyrimido[4,5-*e*][1,2,4]triazolo-

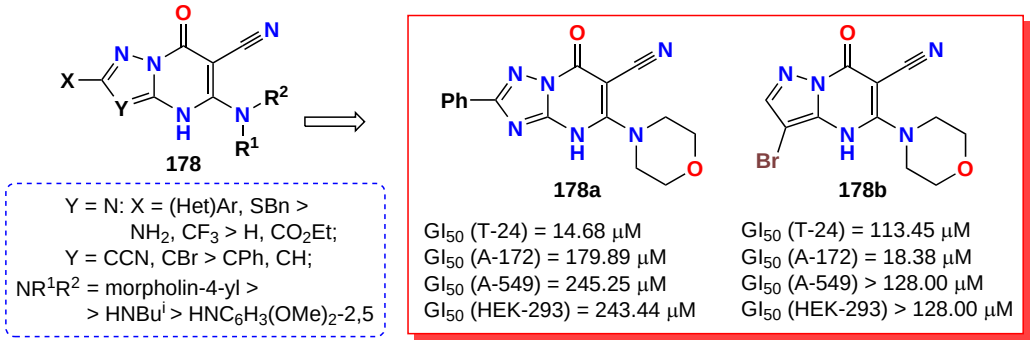


Figure 95. Structures and SARs for compounds **178** and activity data for the most promising derivatives **178a**,**b**. A-172 is a glioblastoma cell line.

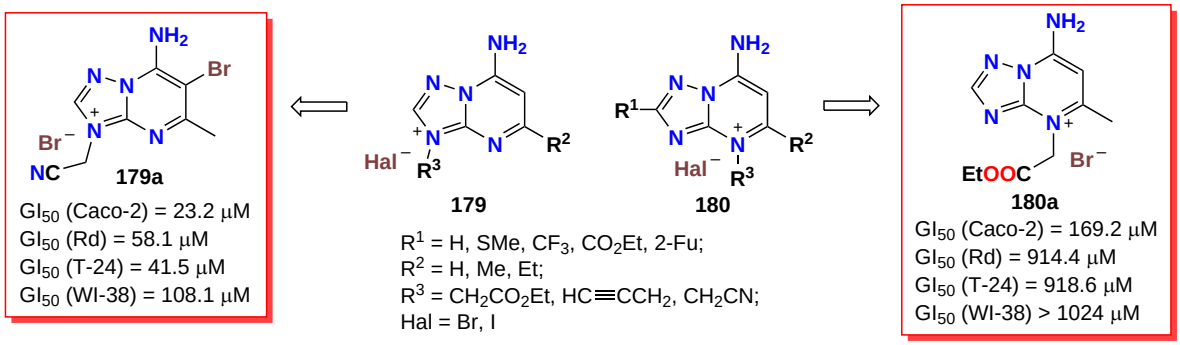


Figure 96. Structures of compounds **179** and **180** and activity data for the most promising derivatives **179a** and **180a**.

Structure 181

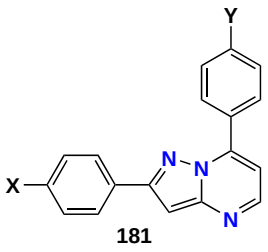


Table 1. Cytotoxicity of compounds **181** at a concentration of 10 μM.[183]

X	Y	Cell viability (%)	
		HCT116	HEK-293
H	OMe	26.0±2.3	67.3±0.1
OMe	Cl	37.0±2.3	92.7±0.4
OMe	OMe	39.4±2.6	80.1±0.2
Cl	OMe	40.8±4.4	81.3±0.0
Cl	Cl	49.7±1.8	44.2±0.4
H	Cl	53.3±3.9	88.0±0.6
H	H	54.1±3.9	92.9±0.4
OMe	H	58.0±3.5	48.0±0.1
Cl	H	70.1±3.1	93.2±0.2

[5,1-*c*][1,2,4]triazines against the following cell lines: HepG2 human hepatocellular carcinoma, A-172 glioblastoma, A-549 lung adenocarcinoma, and HEK-293 human embryonic kidney cells (Fig. 97). Pyrimidoazoloazines **182** and **183** did not exhibit significant cytotoxicity against either cancer or normal cells. The introduction of a 5-methylsulfanyl group into the

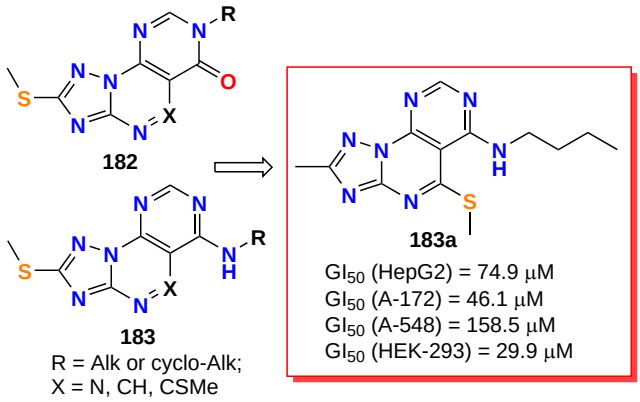


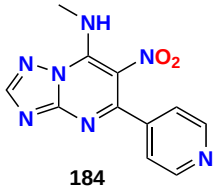
Figure 97. Structures of compounds **182**, **183** and activity data for the most promising derivative **183a**.

heterocyclic skeleton furnished compound **183a**, which was found to be cytotoxic against the HepG2 and A-172 cells in the micromolar range and also to inhibit proliferation of HEK-293 cells.

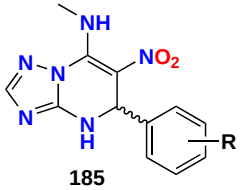
It was found that none of the triazolopyrimidine nitro derivatives **184** and **185** described by Safari *et al.*[184] were cytotoxic against human dermal fibroblasts (HDF). At the same time heterocycle **184**, containing a pyridin-4-yl ring, and 4,5-dihydro derivative **185** with a *para*-nitrophenyl moiety reduced the viability of LNCaP human prostate adenocarcinoma cells to the same extent as the reference drug etoposide (Table 2).[184]

Study of the cytotoxicity of a small series of azolopyrimidines **186** on the MCF-7 breast ductal adenocarcinoma cells indicated that only heterocycle **186a** effectively reduced cell viability at a

Structures 184, 185



184



185

Table 2. Cytotoxic action of compounds **184** and **185** against selected cell lines.184

Compound	R	GI_{50}, μM			
		PC3	A375	LNCaP	HDF
184	–	>100	>100	31.67±0.01	>100
185a	3-F	55.61±0.008	61.33±0.07	>100	>100
185b	4-NO_2	65.03±0.012	31.73±0.015	28.57±0.07	>100
185c	4-Cl	>100	>100	>100	>100
185d	4-Br	>100	>100	>100	>100
185e	2-Cl	63.33±0.069	>100	>100	>100
185f	H	45.02±0.063	>100	>100	>100
185g	4-CF_3	>100	63.41±0.036	>100	>100
Etoposide	–	30±0.037	24.46±0.019	31.21±0.005	>100

concentration of 25 μM (Fig. 98).[185] *In silico* docking revealed a relatively high affinity for dihydroorotate dehydrogenase (DHODH), the effect on which is likely to be responsible for the observed cytotoxicity.

The unusual phosphonate derivatives of pyrazolopyrimidines **187** and **188** (see Fig. 98) slightly reduced the proliferative capacity of the MCF-7 breast ductal adenocarcinoma cells, and showed no activity against the HepG2 hepatocellular carcinoma, HCT116 colorectal carcinoma, or PC-3 prostate adenocarcinoma cell lines.[186]

A low cytotoxic effect was observed in HepG2 cells for derivatives **189** and **190**, in which an aliphatic ring was fused to the triazolopyrimidine system (see Fig. 98).[187]

3.3. Compounds showing cytotoxicity in the high micromolar range or showing no cytotoxicity

Hassan *et al.*[188] performed a comparison of the cytotoxic activitis of a series of pyrazolopyrimidines **191** and doxorubicin (Fig. 99). Only a few compounds of this series were comparable in activity with this anthracycline antibiotic; however, their cytotoxicity indices GI_{50} were in a high micromolar range.

In a later study,[189] a similar cytotoxicity level was noted for a related series of pyrazolopyrimidines **192** (see Fig. 99): their cytotoxicity slightly exceeded that of doxorubicin (GI_{50} = 148.85 and 120.70 μM for the HepG2 and MCF-7 cell lines, respectively), but fell within the high micromolar range.

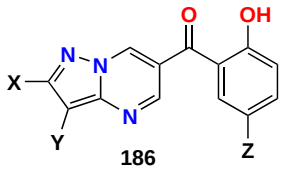
Further modification of this scaffold afforded compounds **193** (see Fig. 99), which exhibited a somewhat more pronounced cytotoxic effect, again slightly exceeding that of doxorubicin.[190]

Almehizia *et al.*[191] investigated the biological effects of heterocycles **194** and **195**, including their cytotoxicity against lung adenocarcinoma (A549) and colorectal adenocarcinoma (Caco-2) cells and diploid lung fibroblasts (WI-38). The GI_{50} cytotoxicity indices found for these compounds were in the mid- and high micromolar ranges, with a certain degree of selectivity in relation to the normal WI-38 cell line (Fig. 100).

5-(Methylsulfanyl)azolo[1,5-*a*]pyrimidin-7-one series **196** (see Fig. 100) did not exhibit pronounced cytotoxic properties against the A549 lung adenocarcinoma cells, Rd embryonic rhabdomyosarcoma cells, HepG2 hepatocellular carcinoma cells, or HEK-293 human embryonic kidney cells.[20]

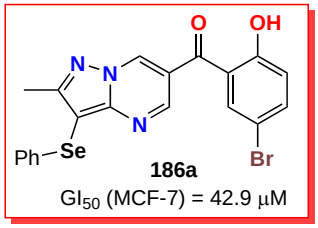
Some preliminary data on the cytotoxicity of derivatives **197** were obtained by Kaping *et al.*[192] (Fig. 101). A study of the effect of these heterocycles on the ability of Chinese hamster ovary cells (CHO-K1) to metabolize MTT indicated that they may possess this effect; however, quantitative values for the activity were not provided in the publication.

Evaluation of seven pyrazolo[1,5-*a*]pyrimidine derivatives **198**, **199** (see Fig. 101) on an extensive panel of cell lines (approximately 50 types) revealed that these heterocycles do not possess pronounced cytotoxic activity. The proliferative capacity of the most sensitive SR lymphoma and UO-31 renal carcinoma cells was inhibited by 41.3% in the presence of these compounds at a concentration of 10 mM.[193]



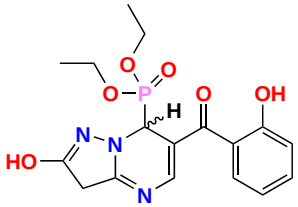
186

X = Me, Ph;
Y = H, SePh;
Z = F, Br



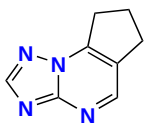
186a

GI_{50} (MCF-7) = 42.9 μM



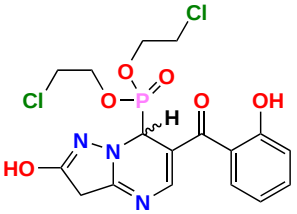
187

GI_{50} (MCF-7) = 55.7 μM



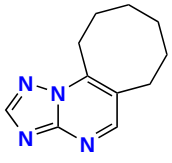
189

GI_{50} (HepG2) = 92.2 μM



188

GI_{50} (MCF-7) = 85.9 μM



190

GI_{50} (HepG2) = 60.0 μM

Figure 98. Structures and activity data for compounds **186**–**190**, including the most promising compound **186a**.

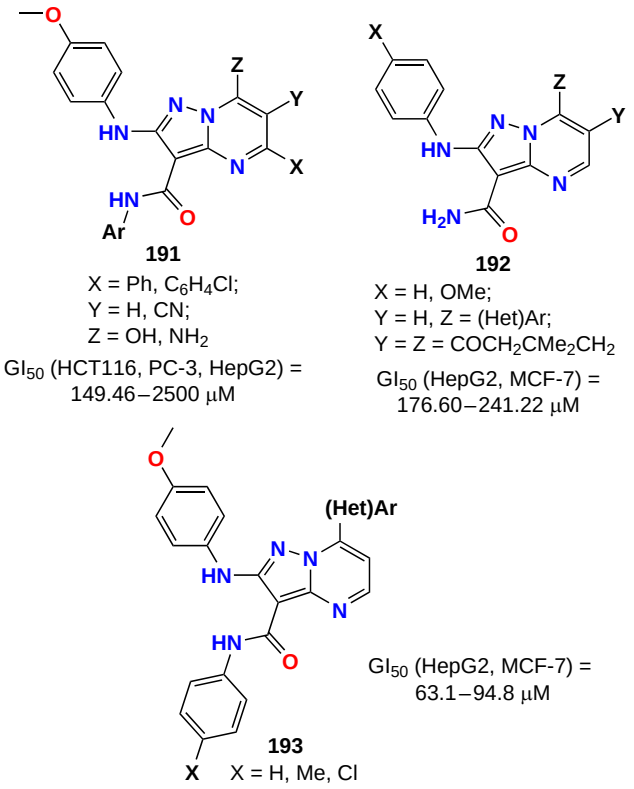


Figure 99. Structures and data on the activity of compounds **191**–**193**.

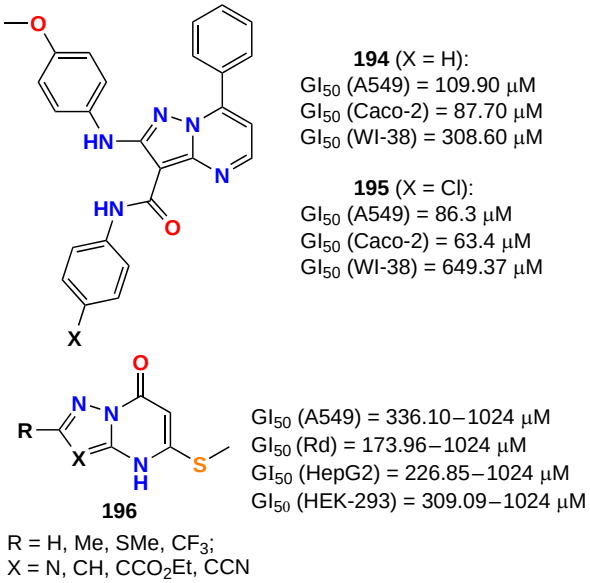


Figure 100. Structures and data on the activity of compounds **194**–**196**.

Metwally *et al.*[194] discussed the effect of the 3-azo derivatives of pyrazolo[1,5-*a*]pyrimidines **200** and **201** (Fig. 102) on the proliferative capacity of Ehrlich ascites carcinoma cells. The authors postulated that these compounds possess marked anticancer properties; however, the format in which they presented the results precluded an objective assessment of this type of activity.

Ajeesh *et al.*[195] varied the substituents in the amide moiety linked to the pyrazole ring in compounds **202**, while maintaining

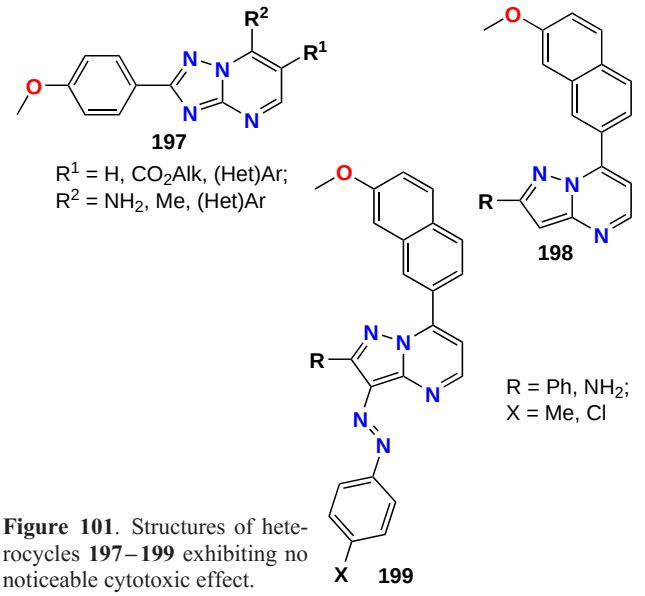


Figure 101. Structures of heterocycles **197**–**199** exhibiting no noticeable cytotoxic effect.

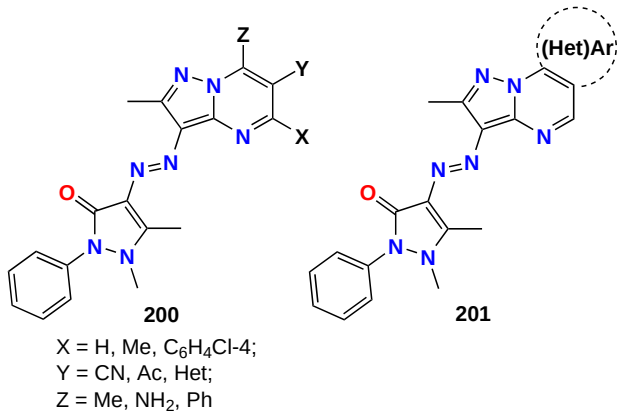


Figure 102. Structures of compounds **200** and **201**.

the substitution pattern on the pyrimidine ring (Fig. 103). According to cytotoxicity assays for these compounds against a number of cell lines, the presence of a trifluoromethyl group increases the cytotoxicity, while compounds with a 4-methoxy group in the Ar[1] substituent, conversely, slightly reduced the proliferative capacity of tumour cells.

The cytotoxicity of pyrazolo[1,5-*a*]pyrimidines **203** (see Fig. 103) was investigated using the CHO-K1 Chinese hamster ovary cell line. Although some of the compounds **203** reduced the viability of these cells, the half-maximal concentrations were around 27 mM, which means that these derivatives cannot be considered to be promising for the development of anticancer drugs.[196]

3.4. Summary of Section 3

Analysis of publications dealing with the cytotoxic properties of azolo[1,5-*a*]pyrimidines indicates that the most frequently mentioned (>10 studies) cell lines are MCF-7 breast ductal adenocarcinoma cells, HCT116 colorectal carcinoma cells, HepG2 hepatocellular carcinoma cells, HeLa cervical carcinoma cells, and A549 lung adenocarcinoma cells. The studies that address the effect of azolo[*a*]pyrimidines on these tumour cells give cytotoxicity indices falling within the low

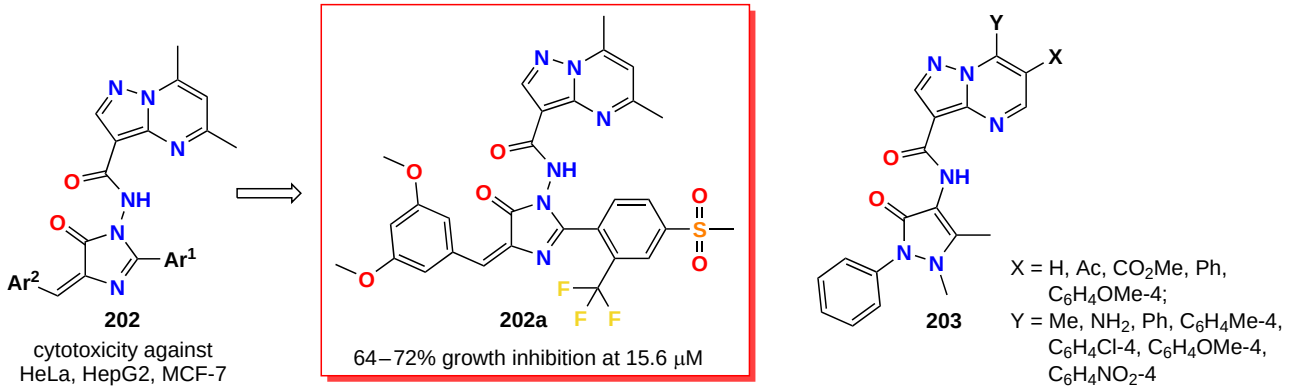


Figure 103. Structures of compounds **202**, **203**, and data on the activity of the most promising derivative **202a**.

micromolar range (GI_{50} < 10 μM) in approximately 50% of cases, indicating the sensitivity of these cells to the action of the heterocycles in question. The Rd embryonic rhabdomyosarcoma cells, MDA-MB-231 triple-negative breast cancer cells, and DU-145 and PC-3 prostate cancer cells are less frequently (5–7 times) encountered in the literature. Furthermore, regarding the three last-mentioned types of cells, almost half of the publications consider azolo[1,5-*a*]-pyrimidines exhibiting cytotoxicity at concentrations <10 μM, whereas for Rd cells, the most effective compound has a GI_{50} value of 14 μM. Pyrazolo[1,5-*a*]pyrimidines and [1,2,4]tri-azolo[1,5-*a*]pyrimidines are addressed in cytotoxicity studies in approximately equal proportions.

As regards identification of particular moieties that provide most pronounced cytotoxicity against tumour cells, it can be noted that the introduction of a 3,4,5-trimethoxyphenyl group (a fragment of the natural antitumour compound combretastatin) resulted in the synthesis of compounds **204**, **205** with GI_{50} values in the mid-nanomolar range. A similar activity was also observed for some 3-cyanopyrazolopyrimidines **206**. Furthermore, structures exhibiting pronounced cytotoxicity were characterized by relatively high lipophilicity; therefore, the introduction of fluorine-containing moieties or annulation of a steroid scaffold furnished derivatives with cytotoxic activity in the low micromolar range (Fig. 104).

It is noteworthy that among C(3)-substituted pyrazolo-[1,5-*a*]pyrimidines **207**–**209**, the highest activity was inherent in the derivatives containing a benzophenone moiety or its heterocyclic analogue at this position (compound **207**). Meanwhile, structurally similar amides **208** or azo compounds **209** exhibited a less pronounced ability to influence tumour cell proliferation (Fig. 105).

It was noted that [1,2,4]triazolo[1,5-*a*]pyrimidines rarely have a substituent other than a hydrogen atom at the C(6) position, and even in such cases, the effect of this substituent on the antitumour activity has not been elucidated. The results of studies into the effect of [1,2,4]triazolo[1,5-*a*]pyrimidines on α-tubulin polymerization indicate that a pronounced effect is caused by a substituted benzene ring at the C(6) position of the molecule (*e.g.*, compounds **210**) (Fig. 106). However, compounds that inhibit β-tubulin polymerization to the highest extent lack a substituent at this position, as indicated by the *in silico* and *in vitro* studies presented by Kim *et al.*[144] On the other hand, particularly for derivative **131a** investigated as an α-tubulin polymerization inhibitor, an antitumour effect against U87-MG glioblastoma was found *in vivo*.

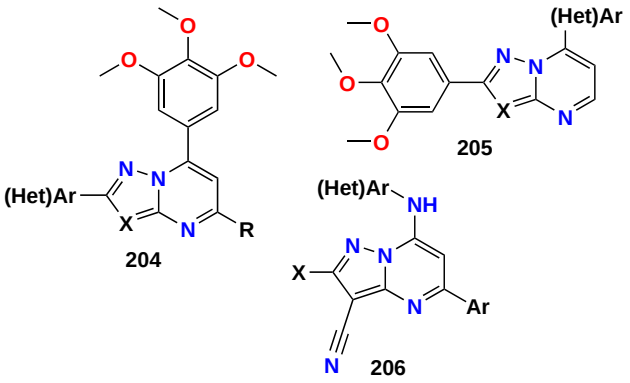


Figure 104. Structures of compounds **204**–**206** exhibiting cytotoxic activity in the mid-nanomolar range.

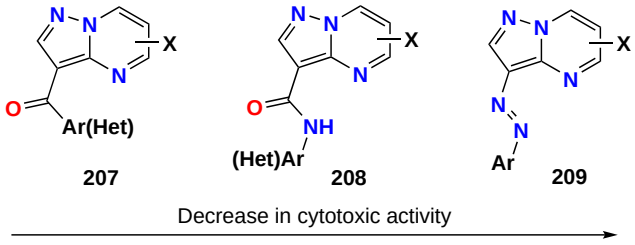


Figure 105. Structures and variation of the cytotoxicity in the series of 3-substituted azole[1,5-*a*]pyrimidines **207**–**209**.

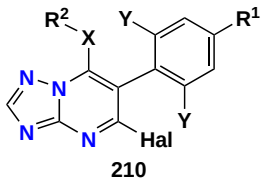


Figure 106. Structure of triazolopyrimidines **210**.

4. Conclusion

The information presented above provides the conclusion that azole[1,5-*a*]pyrimidines represent an important and promising platform for the development of anticancer agents. A key benefit of these compounds is their ability to interact with a variety of macromolecular targets, which opens up opportunities to

overcome the chemoresistance acquired by tumour cells. However, the transition to clinically significant results requires not only in-depth studies of metabolism, but also standardization of initial screening protocols as well as the implementation of computer-aided design methods for the targeted construction of active molecules. In this context, the development of highly selective and bioavailable anticancer drugs, free from undesirable toxic effects, represents a central challenge facing medicinal chemistry in the foreseeable future.

The performed literature review covering both information on the direct cytotoxic activity of azolo[1,5-*a*]pyrimidines against a wide range of tumour cell lines and data on their interaction with particular molecular targets makes it possible to systematize the accumulated data and identify key features that determine the antitumour potential of compounds in this class. Such heterocycles are capable of inhibiting a variety of macromolecular targets ranging from classic kinases to apoptosis regulators and transcription factors. Determination of the cytotoxic action systems provides clear structure–activity relationships: an increase in the π-deficiency of the system through the introduction of electron-withdrawing groups correlates with enhancement of the cytotoxic effect of these heterocycles.

However, along with the obvious achievements in identification of hits among compounds of this class, the review highlights a systemic problem in these studies: the lack of integrated data on the solubility, bioavailability and metabolic stability *in vivo* for these compounds. The currently available body of information represents rather a set of structural ideas than a pool of candidates for preclinical trials. This dictates the need to combine efforts in the field of pharmacokinetic screening and experimental *in vivo* validation of the most active members of this class.

This work was carried out with the financial support of the Ministry of Science and Higher Education of the Russian Federation (theme № FEUZ-2026-0008).

5. List of abbreviations and symbols

The following abbreviations and symbols are used in this review:

K_i — inhibition constant,
ALK — anaplastic lymphoma kinase,
ATR — ataxia telangiectasia mutated Rad3-related protein,
Boc — *tert*-butoxycarbonyl,
BTK — Bruton's tyrosine kinase,
CDK — cyclin-dependent kinase,
cGAMP — cyclic guanosine monophosphate-adenosine monophosphate,
Chk1 — serine/threonine kinase,
CK2 — casein kinase 2,
DHODH — dihydroorotate dehydrogenase,
EC_{50} — half-maximal effective concentration,
EDG — electron-donating group,
EGFR — epidermal growth factor receptor,
ENPP — ectonucleotide pyrophosphatase/phosphodiesterase,
EWG — electron-withdrawing group,
FDA — US Food and Drug Administration,
2-Fu — furan-2-yl,
FUBP1 — FUSE-binding protein 1,
hCA — carbonic anhydrases,
HBA — hydrogen bond acceptor,
HBD — hydrogen-bond donor,
HDAC — histone deacetylases,
GI_{50} — half-maximal growth inhibitory concentration,
IC_{50} — half-maximal inhibitory concentration,
ITP — inhibition of tubulin polymerization,
JAK2 — Janus kinase 2,
LD_{50} — median lethal dose,
LSD — lysine-specific histone demethylase,
MAT — methionine adenosyltransferase,
MetAP — methionine aminopeptidase,
MGC-803 — hybrid gastric cancer cells,
MTAP — methylthioadenosine phosphorylase,
MTT — 3-(4,5-dimethylthiazol-2-yl)-2,5-diphenyltetrazolium bromide,
1(2)-Naph — naphthalen-1(2)-yl,
PI3K — phosphatidylinositol 3-kinase,
2(3)-Py — pyridin-2(3)-yl,
ROCK — Rho-associated kinase linked to a coiled-coil protein,
SAR — structure–activity relationship,
SI — selectivity index,
Skp2 — S-phase kinase-associated protein 2,
SMOX — spermine oxidase,
STING — interferon gene stimulator,
TDP — tyrosyl-DNA phosphodiesterase,
2-Th — thiophen-2-yl,
Topo — topoisomerases,
TRK — tropomyosin-receptor kinase,
TRPC6 — transient receptor potential channel 6,
TSPO — translocation protein,
TTK — threonine tyrosine kinase,
VEGFR — vascular endothelial growth factor receptors,
WRN — Werner syndrome helicase.

Cell line designations:
A2780 — endometrioid ovarian carcinoma,
A549 — lung adenocarcinoma,
A375 and A875 — melanoma,
A-172 — glioblastoma,
ACHN — renal adenocarcinoma,
B16-F10 — mouse melanoma,
Bel-7402 — hepatocellular carcinoma,
BHK — normal cells from the kidneys of baby Syrian hamsters,
Caco-2 — human colorectal adenocarcinoma,
CHO-K1 — Chinese hamster ovary cells,
COLO 205 — human colorectal adenocarcinoma cells,
CT26 — murine colorectal carcinoma cells,
DLD-1 — colorectal cancer,
DU-145 and PC3 — prostate adenocarcinoma cells,
EC109 and EC9706 — human esophageal squamous cell carcinoma,
EKVX — human non-small cell lung cancer,
FHC — normal human colon epithelial cells,
HCT-116 — colorectal carcinoma cells,
HDF — human dermal fibroblasts,
HEK-293 — human embryonic kidney cells,
HeLa — cervical adenocarcinoma,
HELF — human embryonic lung fibroblasts,
HepG2 — hepatocellular carcinoma,
HK-2 — human renal proximal tubular epithelial cell line derived from normal human kidney cortex,
HL-60 — promyelocytic leukaemia,
HT-29 — colorectal adenocarcinoma,
HT-1080 — human fibrosarcoma,
Huh-7 — hepatocellular carcinoma,

HUVEC — human umbilical vein endothelial cells,
KB — continuous human epithelial cell line,
LNCaP — human prostate adenocarcinoma,
LO2 — hepatocytes,
MCF-10A — non-tumorigenic breast epithelial cell line,
MC38 — mouse colon adenocarcinoma,
MC-80 — breast cancer,
MCF-7 — breast ductal adenocarcinoma,
MDA-MB-231 — triple-negative breast cancer,
MGC-803 — human gastric cancer,
MKN-45 — gastric adenocarcinoma,
MOLM-13 — acute monocytic leukaemia,
MOLT-4T — lymphoblastic leukaemia,
MV4-11 — acute myeloid leukaemia,
NCI-H1703 — squamous cell lung cancer,
PBMC — normal peripheral blood mononuclear cells,
PC-2 — human pancreatic carcinoma,
PC-3 — stage IV prostate cancer,
PC-9 — non-small cell lung cancer,
QSG-7701 — normal human liver cells,
Rd — embryonic rhabdomyosarcoma,
RPE1 — telomerase-immortalized human retinal pigment epithelial cells,
SH-SY5Y — human neuroblastoma,
SiHa — squamous cell cervical carcinoma,
SK-N-MC — Ewing's sarcoma,
SR — lymphoma,
SW48 and SW620 — metastatic colorectal adenocarcinoma,
T47D — breast ductal carcinoma,
T98G — human glioblastoma,
T-24 — bladder carcinoma,
4T1 — triple-negative breast cancer,
U87-MG and U-251MG — glioblastoma,
UO-31 — renal carcinoma,
WI-38 — human lung fibroblasts,
WM266-4 — malignant melanoma.

6. References

1. M.C.S.Wong, W.B.Goggins, H.H.X.Wang, F.D.H.Fung, C.Leung, S.Y.S.Wong, C.F.Ng, J.J.Y.Sung. *Eur. Urol.*, **70**, 862 (2016); https://doi.org/10.1016/j.eururo.2016.05.043
2. C.M.Croce. *New Engl. J. Med.*, **358**, 502 (2008); https://doi.org/10.1056/NEJMra072367
3. S.Srivastava, D.Singh, S.K.Verma, M.Pandey, A.Sharma, H.Pandey, A.Mishra. *Vacunas*, **25**, 97 (2024); https://doi.org/10.1016/j.vacune.2024.02.011
4. R.Alemany. *Clin. Transl. Oncol.*, **15**, 182 (2013); https://doi.org/10.1007/s12094-012-0951-7
5. S.Paul, M.F.Konig, D.M.Pardoll, C.Bettegowda, N.Papadopoulos, K.M.Wright, S.B.Gabelli, M.Ho, A.Van Elsas, S.Zhou. *Nat. Rev. Cancer*, **24**, 399 (2024); https://doi.org/10.1038/s41568-024-00690-x
6. A.Mullard. *Nat. Rev. Drug Discov.*, **25**, 81 (2026); https://doi.org/10.1038/d41573-026-00001-z
7. N.Kerru, L.Gummidi, S.Maddila, K.K.Gangu, S.B.Jonnalagadda. *Molecules*, **25**, 1909 (2020); https://doi.org/10.3390/molecules25081909
8. G.V.Urakov, K.V.Savateev, P.A.Slepukhin, V.L.Rusinov, U.M.Ibragimova, R.D.Danilov, X.I.Zhukova, S.A.Sorokina, V.R.Raiberg, R.A.Litvinov, A.A.Spasov, D.A.Babkov. *Bioorg. Med. Chem. Lett.*, **128**, 130333 (2025); https://doi.org/10.1016/j.bmcl.2025.130333
9. M.V.Korokin, S.K.Kotovskaya, T.V.Avtina, I.S.Koklin, I.I.Butorin, K.V.Savateev, G.V.Urakov, E.I.Taran, S.V.Androv, A.A.Kochkarov, L.V.Korokina, V.V.Fedotov, T.D.Moseev, O.S.Gudyrev, N.V.Koroleva, V.V.Vasyutkin, P.I.Pykhtina. *Res. Results Pharmacol.*, **11**, 90 (2025); https://doi.org/10.18413/rrpharmacology.11.862
10. O.N.Chupakhin, V.L.Rusinov, M.V.Varaksin, E.N.Ulomskiy, K.V.Savateev, I.I.Butorin, W.Du, Z.Sun, V.N.Charushin. *Int. J. Mol. Sci.*, **23**, 14537 (2022); https://doi.org/10.3390/ijms232314537
11. K.V.Savateev, V.L.Rusinov, S.K.Kotovskaya, A.A.Spasov, L.V.Naumenko, A.S.Taran, A.A.Brigadirova, D.S.Yakovlev, K.T.Sultanova, N.M.Shcherbakova. *Russ. J. Bioorg. Chem.*, **48**, 777 (2022); https://doi.org/10.1134/S1068162022040185
12. K.V.Savateev, A.A.Spasov, V.L.Rusinov. *Russ. Chem. Rev.*, **91** (6), RCR5041 (2022); https://doi.org/10.1070/RCR5041
13. A.Spasov, V.Kosolapov, D.Babkov, V.Klochkov, E.Sokolova, M.Miroshnikov, A.Borisov, Y.Velikorodnaya, A.Smirnov, K.Savateev, V.Fedotov, S.Kotovskaya, V.Rusinov. *Pharmaceuticals*, **15**, 537 (2022); https://doi.org/10.3390/ph15050537
14. E.K.Voinkov, R.A.Drokin, V.V.Fedotov, I.I.Butorin, K.V.Savateev, D.N.Lyapustin, D.A.Gazizov, E.B.Gorbunov, P.A.Slepukhin, N.A.Gerasimova, N.P.Evstigneeva, N.V.Zilberberg, N.V.Kungurov, E.N.Ulomsky, V.L.Rusinov. *ChemistrySelect*, **7**, e202104253 (2022); https://doi.org/10.1002/slct.202104253
15. K.V.Savateev, V.V.Fedotov, V.L.Rusinov, S.K.Kotovskaya, A.A.Spasov, A.F.Kucheryavenko, P.M.Vasiliev, V.A.Kosolapov, V.S.Sirotenko, K.A.Gaidukova, G.M.Uskov. *Molecules*, **27**, 274 (2022); https://doi.org/10.3390/molecules27010274
16. V.V.Dolgova, K.V.Savateev, G.V.Urakov, E.T.Shabunina, T.E.Sbrodova, E.A.Lvova, I.I.Butorin, E.A.Fesenko, V.V.Melekhin, M.D.Tokhtueva, A.V.Paramonova, A.A.Zonov, S.K.Kotovskaya, V.L.Rusinov. *ChemMedChem*, **20**, e202500535 (2025); https://doi.org/10.1002/cmdc.202500535
17. E.V.Bersneva, K.V.Savateev, P.A.Slepukhin, V.V.Melekhin, M.D.Tokhtueva, V.L.Rusinov. *Org. Biomol. Chem.*, **23**, 1945 (2025); https://doi.org/10.1039/D4OB01853B
18. A.A.Ushakova, V.V.Fedotov, V.V.Melekhin, M.D.Tokhtueva, A.V.Paramonova, S.K.Kotovskaya, E.N.Ulomsky, V.L.Rusinov. *Russ. Chem. Bull.*, **74**, 461 (2025); https://doi.org/10.1007/s11172-025-4538-1
19. I.I.Butorin, V.V.Melekhin, D.D.Chirkov, M.D.Tokhtueva, A.A.Zonov, O.A.Konovalova, E.A.Fesenko, A.E.Chernysheva, P.A.Slepukhin, S.K.Kotovskaya, V.L.Rusinov. *Chim. Tech. Acta*, **12**, 12202 (2025); https://doi.org/10.15826/chimtech.2025.12.2.02
20. D.N.Lyapustin, D.F.Fayzullina, I.V.Marusich, S.K.Kotovskaya, V.V.Melekhin, M.D.Tokhtueva, E.N.Ulomsky, V.L.Rusinov. *Chem. Heterocycl. Compd.*, **60**, 52 (2024); https://doi.org/10.1007/s10593-024-03293-4
21. D.N.Lyapustin, D.F.Fayzullina, I.V.Marusich, S.K.Kotovskaya, I.I.Butorin, V.V.Melekhin, M.D.Tokhtueva, I.N.Ganebnykh, E.N.Ulomsky, V.L.Rusinov. *Tetrahedron Lett.*, **151**, 155324 (2024); https://doi.org/10.1016/j.tetlet.2024.155324
22. G.V.Urakov, K.V.Savateev, V.V.Melekhin, S.K.Kotovskaya, V.L.Rusinov. *Russ. Chem. Bull.*, **72**, 3022 (2023); https://doi.org/10.1007/s11172-023-4114-5
23. F.Safari, M.Bayat, S.Nasri, S.Karami. *Bioorg. Med. Chem. Lett.*, **30**, 127111 (2020); https://doi.org/10.1016/j.bmcl.2020.127111
24. Y.Y.Syed. *Drugs*, **80**, 91 (2020); https://doi.org/10.1007/s40265-019-01252-4
25. L.J.Scott. *Drugs*, **79**, 201 (2019); https://doi.org/10.1007/s40265-018-1044-x
26. A.Drilon, S.-H.I.Ou, B.C.Cho, D.-W.Kim, J.Lee, J.J.Lin, V.W.Zhu, M.-J.Ahn, D.R.Camidge, J.Nguyen, D.Zhai, W.Deng, Z.Huang, E.Rogers, J.Liu, J.Whitten, J.K.Lim, S.Stopatschinskaja, D.M.Hyman, R.C.Doebele, J.J.Cui, A.T.Shaw. *Cancer Discov.*, **8**, 1227 (2018); https://doi.org/10.1158/2159-8290.CD-18-0484

27. D.Parry, T.Guzi, F.Shanahan, N.Davis, D.Prabhavalkar, D.Wiswell, W.Seghezzi, K.Paruch, M.P.Dwyer, R.Doll, A.Nomeir, W.Windsor, T.Fischmann, Y.Wang, M.Oft, T.Chen, P.Kirschmeier, E.M.Lees. *Mol. Cancer Ther*., **9**, 2344 (2010); https://doi.org/10.1158/1535-7163.MCT-10-0324
28. R.C.Coombes, S.Howell, S.R.Lord, L.Kenny, J.Mansi, Z.Mitri, C.Palmieri, L.I.Chap, P.Richards, W.Gradishar, S.Sardesai, J.Melear, J.O'Shaughnessy, P.Ward, P.Chalasani, T.Arkenau, R.D.Baird, R.Jeselsohn, S.Ali, G.Clack, A.Bahl, S.McIntosh, M.G.Krebs. *Nat. Commun*., **14**, 4444 (2023); https://doi.org/10.1038/s41467-023-40061-y
29. K.Oukoloff, B.Lucero, K.R.Francisco, K.R.Brunden, C.Ballatore. *Eur. J. Med. Chem.*, **165**, 332 (2019); https://doi.org/10.1016/j.ejmech.2019.01.027
30. S.Cherukupalli, R.Karpoormath, B.Chandrasekaran, G.A.Hampannavar, N.Thapliyal, V.N.Palakollu. *Eur. J. Med. Chem.*, **126**, 298 (2017); https://doi.org/10.1016/j.ejmech.2016.11.019
31. M.M.Hammouda, H.E.Gaffer, K.M.Elattar. *RSC Med. Chem.*, **13**, 1150 (2022); https://doi.org/10.1039/D2MD00192F
32. P.K.Singh, S.Choudhary, A.Kashyap, H.Verma, S.Kapil, M.Kumar, M.Arora, O.Silakari. *Bioorg. Chem*., **88**, 102919 (2019); https://doi.org/10.1016/j.bioorg.2019.102919
33. S.R.Merugu, S.Cherukupalli, R.Karpoormath. *Chem. Biodivers*., **19**, e202200291 (2022); https://doi.org/10.1002/cbdv.202200291
34. X.-J.Dai, L.-P.Xue, S.-K.Ji, Y.Zhou, Y.Gao, Y.-C.Zheng, H.-M.Liu, H.-M.Liu. *Eur. J. Med. Chem.*, **249**, 115101 (2023); https://doi.org/10.1016/j.ejmech.2023.115101
35. V.Asati, A.Anant, P.Patel, K.Kaur, G.D.Gupta. *Eur. J. Med. Chem.*, **225**, 113781 (2021); https://doi.org/10.1016/j.ejmech.2021.113781
36. C.C.Eze, A.M.Ezeokonkwo, I.D.Ugwu, U.F.Eze, E.L.Onyeyilim, I.S.Attah, I.V.Okonkwo. *Anti-Cancer Agents Med. Chem*., **22**, 2822 (2022); https://doi.org/10.2174/1871520622666220318090147
37. K.Kandhasamy, R.R.Surajambika, P.K.Velayudham. *Med. Chem*., **20**, 293 (2024); https://doi.org/10.2174/0115734064251256231018104623
38. T.H.Iorkula, O.J.-K.Osayawe, D.A.Odogwu, L.O.Ganiyu, E.Faderin, R.F.Awoyemi, B.O.Akodu, I.H.Ifijen, O.R.Aworinde, P.Agyemang, O.L.Onyinyechi. *RSC Adv.*, **15**, 3756 (2025); https://doi.org/10.1039/D4RA07556K
39. A.W.Murray. *Cell*, **116**, 221 (2004); https://doi.org/10.1016/S0092-8674(03)01080-8
40. T.Chohan, H.Qian, Y.Pan, J.-Z.Chen. *Curr. Med. Chem*., **22**, 237 (2014); https://doi.org/10.2174/0929867321666141106113633
41. A.A.E.-H.El-Rahmany, N.A.Khalil, M.S.Nafie, W.M.Eldehna, H.A.Abdel-Aziz, M.S.A.Hassan. *Bioorg. Med. Chem.*, **134**, 118535 (2026); https://doi.org/10.1016/j.bmc.2025.118535
42. S.J.Almehmadi, A.M.R.Alsaedi, M.F.Harras, T.A.Farghaly. *Bioorg. Chem.*, **117**, 105431 (2021); https://doi.org/10.1016/j.bioorg.2021.105431
43. G.M.E.Ali, D.A.Ibrahim, A.M.Elmetwali, N.S.M.Ismail. *Bioorg. Chem.*, **86**, 1 (2019); https://doi.org/10.1016/j.bioorg.2019.01.008
44. L.J.Phillipson, D.H.Segal, T.L.Nero, M.W.Parker, S.S.Wan, M.De Silva, M.A.Guthridge, A.H.Wei, C.J.Burns. *Bioorg. Med. Chem.*, **23**, 6280 (2015); https://doi.org/10.1016/j.bmc.2015.08.035
45. E.M.Husseiny. *Bioorg. Chem*., **102**, 104053 (2020); https://doi.org/10.1016/j.bioorg.2020.104053
46. H.R.Elgiushy, M.E.Soliman, M.E.El-Khouly, K.A.M.Abouzid, S.F.Hammad. *Bioorg. Chem.*, **164**, 108792 (2025); https://doi.org/10.1016/j.bioorg.2025.108792
47. Yu.L.Volodina, A.A.Shtil. *Mol. Biol*., **46**, 381 (2012); https://doi.org/10.1134/S0026893312020203
48. A.Krämer, C.G.Kurz, B.-T.Berger, I.E.Celik, A.Tjaden, F.A.Greco, S.Knapp, T.Hanke. *Eur. J. Med. Chem.*, **208**, 112770 (2020); https://doi.org/10.1016/j.ejmech.2020.112770
49. W.McCoull, R.D.Abrams, E.Anderson, K.Blades, P.Barton, M.Box, J.Burgess, K.Byth, Q.Cao, C.Chuaqui, R.J.Carbajo, T.Cheung, E.Code, A.D.Ferguson, S.Fillery, N.O.Fuller, E.Gangl, N.Gao, M.Grist, D.Hargreaves, M.R.Howard, J.Hu, P.D.Kemmitt, J.E.Nelson, N.O'Connell, D.B.Prince, P.Raubo, P.B.Rawlins, G.R.Robb, J.Shi, M.J.Waring, D.Whittaker, M.Wylot, X.Zhu. *J. Med. Chem.*, **60**, 4386 (2017); https://doi.org/10.1021/acs.jmedchem.7b00359
50. J.E.Dowling, C.Chuaqui, T.W.Pontz, P.D.Lyne, N.A.Larsen, M.H.Block, H.Chen, N.Su, A.Wu, D.Russell, H.Pollard, J.W.Lee, B.Peng, K.Thakur, Q.Ye, T.Zhang, P.Brassil, V.Racicot, L.Bao, C.R.Denz, E.Cooke. *ACS Med. Chem. Lett.*, **3**, 278 (2012); https://doi.org/10.1021/ml200257n
51. J.E.Dowling, M.Alimzhanov, L.Bao, M.H.Block, C.Chuaqui, E.L.Cooke, C.R.Denz, A.Hird, S.Huang, N.A.Larsen, B.Peng, T.W.Pontz, C.Rivard-Costa, J.C.Saeh, K.Thakur, Q.Ye, T.Zhang, P.D.Lyne. *ACS Med. Chem. Lett.*, **4**, 800 (2013); https://doi.org/10.1021/ml400197u
52. G.V.Urakov, K.V.Savateev, S.K.Kotovskaya, V.L.Rusinov, A.A.Spasov, D.A.Babkov, E.V.Sokolova. *Molecules*, **27**, 8697 (2022); https://doi.org/10.3390/molecules27248697
53. X.Wang, S.Magnuson, R.Pastor, E.Fan, H.Hu, V.Tsui, W.Deng, J.Murray, M.Steffek, H.Wallweber, J.Moffat, J.Drummond, G.Chan, E.Harstad, A.J.Ebens. *Bioorg. Med. Chem. Lett*., **23**, 3149 (2013); https://doi.org/10.1016/j.bmcl.2013.04.020
54. V.Munugalavadla, L.Berry, Y.-H.Chen, G.Deshmukh, J.Drummond, C.Du, M.Eby, K.Fitzgerald, L.S.Friedman, S.E.Gould, J.R.Kenny, H.Maecker, J.Moffat, M.Moskalenko, P.Pacheco, A.Saadat, D.Slaga, L.Sun, G.Wang, Y.Yang, A.J.Ebens. *Blood*, **116**, 4084 (2010); https://doi.org/10.1182/blood.V116.21.4084.4084
55. M.P.Dwyer, K.Keertikar, K.Paruch, C.Alvarez, M.Labroli, C.Poker, T.O.Fischmann, R.Mayer-Ezell, R.Bond, Y.Wang, R.Azevedo, T.J.Guzi. *Bioorg. Med. Chem.*, **23**, 6178 (2013); https://doi.org/10.1016/j.bmcl.2013.08.110
56. A.M.Cohen, B.Grinblat, H.Bessler, D.A.Kristt, A.Kremer, S.Shalom, A.Schwartz, M.Halperin, D.Merkel, J.Don. *Leuk. Lymphoma*, **45**, 951 (2004); https://doi.org/10.1080/10428190310001641251
57. Y.Xu, B.G.Brenning, S.G.Kultgen, J.M.Foulks, A.Clifford, S.Lai, A.Chan, S.Merx, M.V.McCullar, S.B.Kanner, K.-K.Ho. *ACS Med. Chem. Lett.*, **6**, 63 (2015); https://doi.org/10.1021/ml500300c
58. F.G.Abdulrahman, R.Sabour, S.M.A.El-Gilil, A.B.M.Mehany, E.A.Taha. *J. Mol. Struct.*, **1295**, 136811 (2024); https://doi.org/10.1016/j.molstruc.2023.136811
59. T.A.Farghaly, Z.A.Muhammad, A.M.R.Alsaedi, S.A.Al-Hussain, M.E.A.Zaki, A.M.A.Alnjaa, A.S.Younes. *J. Mol. Struct*., **1339**, 142412 (2025); https://doi.org/10.1016/j.molstruc.2025.142412
60. J.N.Philoppes, M.A.Khedr, M.H.A.Hassan, G.Kamel, P.F.Lamie. *Bioorg. Chem*., **100**, 103944 (2020); https://doi.org/10.1016/j.bioorg.2020.103944
61. H.Davies, G.R.Bignell, C.Cox, P.Stephens, S.Edkins, S.Clegg, J.Teague, H.Woffendin, M.J.Garnett, W.Bottomley, N.Davis, E.Dicks, R.Ewing, Y.Floyd, K.Gray, S.Hall, R.Hawes, J.Hughes, V.Kosmidou, A.Menzies, C.Mould, A.Parker, C.Stevens, S.Watt, S.Hooper, R.Wilson, H.Jayatilake, B.A.Gusterson, C.Cooper, J.Shipley, D.Hargrave, K.Pritchard-Jones, N.Maitland, G.Chenevix-Trench, G.J.Riggins, D.D.Bigner, G.Palmieri, A.Cossu, A.Flanagan, A.Nicholson, J.W.C.Ho, S.Y.Leung, S.T.Yuen, B.L.Weber, H.F.Seigler, T.L.Darrow, H.Paterson, R.Marais, C.J.Marshall, R.Wooster, M.R.Stratton, P.A.Futreal. *Nature*, **417**, 949 (2002); https://doi.org/10.1038/nature00766
62. X.Wang, D.M.Berger, E.J.Salaski, N.Torres, Y.Hu, J.I.Levin, D.Powell, D.Wojciechowicz, K.Collins, E.Frommer. *Bioorg. Med. Chem. Lett*., **19**, 6571 (2009); https://doi.org/10.1016/j.bmcl.2009.10.030

63. M.J.Di Grandi, D.M.Berger, D.W.Hopper, C.Zhang, M.Dutia, A.L.Dunnick, N.Torres, J.I.Levin, G.Diamantidis, C.W.Zapf, J.D.Bloom, Y.Hu, D.Powell, D.Wojciechowicz, K.Collins, E.Frommer. *Bioorg. Med. Chem.*, **19**, 6957 (2009); https://doi.org/10.1016/j.bmcl.2009.10.058
64. D.M.Berger, N.Torres, M.Dutia, D.Powell, G.Ciszewski, A.Gopalsamy, J.I.Levin, K.-H.Kim, W.Xu, J.Wilhelm, Y.Hu, K.Collins, L.Feldberg, S.Kim, E.Frommer, D.Wojciechowicz, R.Mallon. *Bioorg. Med. Chem.*, **19**, 6519 (2009); https://doi.org/10.1016/j.bmcl.2009.10.049
65. A.Gopalsamy, G.Ciszewski, Y.Hu, F.Lee, L.Feldberg, E.Frommer, S.Kim, K.Collins, D.Wojciechowicz, R.Mallon. *Bioorg. Med. Chem.*, **19**, 2735 (2009); https://doi.org/10.1016/j.bmcl.2009.03.129
66. M.B.Kastan, J.Bartek. *Nature*, **432**, 316 (2004); https://doi.org/10.1038/nature03097
67. M.P.Dwyer, K.Paruch, M.Labroli, C.Alvarez, K.M.Keertikar, C.Poker, R.Rossman, T.O.Fischmann, J.S.Duca, V.Madison, D.Parry, N.Davis, W.Seghezzi, D.Wiswell, T.J.Guzi. *Bioorg. Med. Chem.*, **21**, 467 (2011); https://doi.org/10.1016/j.bmcl.2010.10.113
68. M.Labroli, K.Paruch, M.P.Dwyer, C.Alvarez, K.Keertikar, C.Poker, R.Rossman, J.S.Duca, T.O.Fischmann, V.Madison, D.Parry, N.Davis, W.Seghezzi, D.Wiswell, T.J.Guzi. *Bioorg. Med. Chem. Lett*., **21**, 471 (2011); https://doi.org/10.1016/j.bmcl.2010.10.114
69. M.E.Conley, A.K.Dobbs, D.M.Farmer, S.Kilic, K.Paris, S.Grigoriadou, E.Coustan-Smith, V.Howard, D.Campana. *Annu. Rev. Immunol.*, **27**, 199 (2009); https://doi.org/10.1146/annurev.immunol.021908.132649
70. Z.Pan, H.Scheerens, S.Li, B.E.Schultz, P.A.Sprengeler, L.C.Burrill, R.V.Mendonca, M.D.Sweeney, K.C.K.Scott, P.G.Grothaus, D.A.Jeffery, J.M.Spoerke, L.A.Honigberg, P.R.Young, S.A.Dalrymple, J.T.Palmer. *ChemMedChem*, **2**, 58 (2007); https://doi.org/10.1002/cmdc.200600221
71. Y.Guo, Y.Liu, N.Hu, D.Yu, C.Zhou, G.Shi, B.Zhang, M.Wei, J.Liu, L.Luo, Z.Tang, H.Song, Y.Guo, X.Liu, D.Su, S.Zhang, X.Song, X.Zhou, Y.Hong, S.Chen, Z.Cheng, S.Young, Q.Wei, H.Wang, Q.Wang, L.Lv, F.Wang, H.Xu, H.Sun, H.Xing, N.Li, W.Zhang, Z.Wang, G.Liu, Z.Sun, D.Zhou, W.Li, L.Liu, L.Wang, Z.Wang. *J. Med. Chem.*, **62**, 7923 (2019); https://doi.org/10.1021/acs.jmedchem.9b00687
72. R.L.Levine, A.Pardanani, A.Tefferi, D.G.Gilliland. *Nat. Rev. Cancer*, **7**, 673 (2007); https://doi.org/10.1038/nrc2210
73. E.J.Hanan, A.Van Abbema, K.Barrett, W.S.Blair, J.Blaney, C.Chang, C.Eigenbrot, S.Flynn, P.Gibbons, C.A.Hurley, J.R.Kenny, J.Kulagowski, L.Lee, S.R.Magnuson, C.Morris, J.Murray, R.M.Pastor, T.Rawson, M.Siu, M.Ultsch, A.Zhou, D.Sampath, J.P.Lyssikatos. *J. Med. Chem.*, **55**, 10090 (2012); https://doi.org/10.1021/jm3012239
74. T.Jiang, G.Wang, Y.Liu, L.Feng, M.Wang, J.Liu, Y.Chen, L.Ouyang. *Acta Pharm. Sin., B*, **12**, 2963 (2022); https://doi.org/10.1016/j.apsb.2022.02.028
75. Y.Gong, F.-X.Wu, M.-S.Wang, H.-C.Xu, L.-S.Zhuo, G.-F.Yang, W.Huang. *Eur. J. Med. Chem.*, **241**, 114654 (2022); https://doi.org/10.1016/j.ejmech.2022.114654
76. Y.Zhang, Y.Liu, Y.Zhou, Q.Zhang, T.Han, C.Tang, W.Fan. *Bioorg. Med. Chem. Lett*., **31**, 127712 (2021); https://doi.org/10.1016/j.bmcl.2020.127712
77. C.Jiang, K.Chen, D.Li, S.Hu, Q.Jin. *Eur. J. Med. Chem.*, **302**, 118271 (2026); https://doi.org/10.1016/j.ejmech.2025.118271
78. A.Barreca, E.Lasorsa, L.Riera, R.Machiorlatti, R.Piva, M.Ponzoni, I.Kwee, F.Bertoni, P.P.Piccaluga, S.A.Pileri, G.Inghirami. *J. Mol. Endocrinol*., **47**, R11 (2011); https://doi.org/10.1530/JME-11-0004
79. F.Liu, S.Wen, M.Liu, Y.Min, Z.Zhang, L.Shi, K.Wang, Y.Deng, Z.Yang, F.Yang, S.Ke. *Bioorg. Chem*., **153**, 107847 (2024); https://doi.org/10.1016/j.bioorg.2024.107847
80. W.M.Rashed. *Crit. Oncol. Hematol*., **131**, 7 (2018); https://doi.org/10.1016/j.critrevonc.2018.08.007
81. G.Luo, Y.Ma, X.Liang, G.Xie, Y.Luo, D.Zha, S.Wang, L.Yu, X.Zheng, W.Wu, C.Zhang. *Bioorg. Chem*., **104**, 104356 (2020); https://doi.org/10.1016/j.bioorg.2020.104356
82. H.Jia, G.Dai, W.Su, K.Xiao, J.Weng, Z.Zhang, Q.Wang, T.Yuan, F.Shi, Z.Zhang, W.Chen, Y.Sai, J.Wang, X.Li, Y.Cai, J.Yu, P.Ren, J.Venable, T.Rao, J.P.Edwards, S.D.Bembenek. *J. Med. Chem.*, **62**, 4936 (2019); https://doi.org/10.1021/acs.jmedchem.8b02014
83. L.Benetatos, E.Voulgaris, G.Vartholomatos. *Med. Oncol*., **34**, 39 (2017); https://doi.org/10.1007/s12032-017-0897-2
84. X.Liang, M.Deng, F.Zou, Z.Qi, C.Wang, J.Liu, Q.Liu, B.Wang, S.Qi, J.Ge, H.Yu, A.Wang, Q.Liu, J.Liu. *Eur. J. Med. Chem.*, **260**, 115768 (2023); https://doi.org/10.1016/j.ejmech.2023.115768
85. C.Wang, F.Zou, Z.Qi, Q.Liu, L.Shen, X.Yuan, M.Deng, A.Wang, B.Wang, L.Wang, X.Liang, Q.Liu, J.Liu. *J. Med. Chem.*, **67**, 15199 (2024); https://doi.org/10.1021/acs.jmedchem.4c00817
86. K.E.Anwer, B.Y.Beshay, M.M.Shamaa, N.E.A.Abd El-Sattar, A. Senbel. *Biomed. Pharmacother*., **192**, 118679 (2025); https://doi.org/10.1016/j.biopha.2025.118679
87. L.Grisetti, C.J.C.Garcia, A.A.Saponaro, C.Tiribelli, D.Pascut. *Cell Prolif*., **57**, e13641 (2024); https://doi.org/10.1111/cpr.13641
88. M.Alsulaimany, M.F.Athary Abdulhaleem, R.Alghamdi, N.E.A.Abd El-Sattar, S.A.Almadani, W.A.Samman, H.Y.Alharbi, M.S.Aljohani, S.M.Tayeb, T.Nasr, K.El-Adl, K.E.Anwer. *Bioorg. Chem.*, **163**, 108746 (2025); https://doi.org/10.1016/j.bioorg.2025.108746
89. M.Juchum, M.Günther, S.A.Laufer. *Drug Resist. Updates*, **20**, 12 (2015); https://doi.org/10.1016/j.drup.2015.05.002
90. G.Sivaiah, R.Raveesha, S.B.B.Prasad, K.Y.Kumar, M.S.Raghu, F.Alharethy, Mk.Prashanth, B.-H.Jeon. *J. Mol. Struct*., **1289**, 135877 (2023); https://doi.org/10.1016/j.molstruc.2023.135877
91. M.A.Al-Qadhi, H.A.Allam, S.H.Fahim, T.A.A.Yahya, F.A.F.Ragab. *Eur. J. Med. Chem.*, **262**, 115918 (2023); https://doi.org/10.1016/j.ejmech.2023.115918
92. A.H.Eldeeb, M.I.Shahin, M.Y.Jaballah, A.R.Elaraby, T.M.Ibrahim, M.M.Elaasser, H.A.Abdel-Aziz, D.S.Lasheen, D.A.Abou El Ella. *Bioorg. Chem.*, **165**, 108899 (2025); https://doi.org/10.1016/j.bioorg.2025.108899
93. C.T.Supuran, V.Alterio, A.Di Fiore, K. D'Ambrosio, F.Carta, S.M.Monti, G.De Simone. *Med. Res. Rev*., **38**, 1799 (2018); https://doi.org/10.1002/med.21497
94. M.A.Said, W.M.Eldehna, A.Nocentini, A.Bonardi, S.H.Fahim, S.Bua, D.H.Soliman, H.A.Abdel-Aziz, P.Gratteri, S.M.Abou-Seri, C.T.Supuran. *Eur. J. Med. Chem.*, **185**, 111843 (2020); https://doi.org/10.1016/j.ejmech.2019.111843
95. M.S.Elkotamy, M.A.Abdelrahman, S.Giovannuzzi, M.A.Alkabbani, A.Nocentini, C.T.Supuran, W.M.Eldehna, H.A.Abdel-Aziz, S.M.Abou-Seri. *Int. J. Biol. Macromol*., **303**, 140462 (2025); https://doi.org/10.1016/j.ijbiomac.2025.140462
96. M.S.Elkotamy, M.A.Abdelrahman, S.Giovannuzzi, M.A.Alkabbani, A.Nocentini, C.T.Supuran, W.M.Eldehna, H.A.Abdel-Aziz, S.M.Abou-Seri. *Eur. J. Med. Chem.*, **310**, 118789 (2026); https://doi.org/10.1016/j.ejmech.2026.118789
97. M.S.Elkotamy, I.A.Elkelesh, S.Giovannuzzi, R.S.M.Ismail, W.M.El-Refaie, A.A.Almehizia, A.M.Naglah, A.Nocentini, C.T.Supuran, M.Fares, H.A.Ghabbour, R.Salem, W.M.Eldehna, H.A.Abdel-Aziz. *Eur. J. Med. Chem.*, **293**, 117752 (2025); https://doi.org/10.1016/j.ejmech.2025.117752
98. J.-R.J.Yeh, R.Ju, C.M.Brdlik, W.Zhang, Y.Zhang, M.E.Matyskiela, J.D.Shotwell, C.M.Crews. *Proc. Natl. Acad. Sci. USA*, **103**, 10379 (2006); https://doi.org/10.1073/pnas.0511313103
99. K.Becker, J.D.Mueller, C.Schulmacher, K.Ott, U.Fink, R.Busch, K.Böttcher, J.R.Siewert, H.Höfler. *Cancer*, **98**, 1521 (2003); https://doi.org/10.1002/cncr.11660
100. T.Heinrich, H.-P.Buchstaller, B.Cezanne, F.Rohdich, J.Bomke, M.Friese-Hamim, M.Krier, T.Knöchel, D.Musil, B.Leuthner,

F.Zenke. *Bioorg. Med. Chem.*, **27**, 551 (2017); https://doi.org/10.1016/j.bmcl.2016.12.019
101. K.M.McNamara, J.C.Sierra, Y.L.Latour, C.V.Hawkins, M.Asim, K.J.Williams, D.P.Barry, M.M.Allaman, I.Zagol-Ikapitte, P.B.Luis, C.Schneider, A.G.Delgado, M.B.Piazuelo, R.N.Tyree, K.S.Carson, Y.A.Choksi, L.A.Coburn, A.P.Gobert, K.T.Wilson. *Oncogene*, **44**, 296 (2025); https://doi.org/10.1038/s41388-024-03218-7
102. J.Llaveria, S.Adhikary, C.Buyck, S.Cañellas, J.M.Cid, B.Danna, F.Delgado, E.Diaz, A.Diéguez-Vázquez, L.Fang, F.O.Fernandez Candelaria, G.Gibbons, V.N.A.Klaren, D.J.Krosky, A.Impagliazzo, M.L.Linares, C.M.Lamenca, A.Misale, M.Pryor, J.Shang, J.Suarez. *J. Med. Chem.*, **68**, 22507 (2025); https://doi.org/10.1021/acs.jmedchem.5c01449
103. K.Marjon, M.J.Cameron, P.Quang, M.F.Clasquin, E.Mandley, K.Kunii, M.McVay, S.Choe, A.Kernytsky, S.Gross, Z.Konteatis, J.Murtie, M.L.Blake, J.Travins, M.Dorsch, S.A.Biller, K.M.Marks. *Cell Rep.*, **15**, 574 (2016); https://doi.org/10.1016/j.celrep.2016.03.043
104. Z.Konteatis, J.Travins, S.Gross, K.Marjon, A.Barnett, E.Mandley, B.Nicolay, R.Nagaraja, Y.Chen, Y.Sun, Z.Liu, J.Yu, Z.Ye, F.Jiang, W.Wei, C.Fang, Y.Gao, P.Kalev, M.L.Hyer, B.DeLaBarre, L.Jin, A.K.Padyana, L.Dang, J.Murtie, S.A.Biller, Z.Sui, K.M.Marks. *J. Med. Chem.*, **64**, 4430 (2021); https://doi.org/10.1021/acs.jmedchem.0c01895
105. P.M.Do, L.Varanasi, S.Fan, C.Li, I.Kubacka, V.Newman, K.Chauhan, S.R.Daniels, M.Boccetta, M.R.Garrett, R.Li, L.A.Martinez. *Genes Dev.*, **26**, 830 (2012); https://doi.org/10.1101/gad.181685.111
106. C.J.A.Ribeiro, J.Kankanala, J.Xie, J.Williams, H.Aihara, Z.Wang. *Bioorg. Med. Chem. Lett*., **29**, 257 (2019); https://doi.org/10.1016/j.bmcl.2018.11.044
107. J.Qu, H.Yan, Y.Hou, W.Cao, Y.Liu, E.Zhang, J.He, Z.Cai. *J. Hematol. Oncol.*, **15**, 8 (2022); https://doi.org/10.1186/s13045-022-01224-4
108. Y.-Z.Wang, H.-Y.Li, Y.Zhang, R.-X.Jiang, J.Xu, J.Gu, Z.Jiang, Z.-Y.Jiang, Q.-D.You, X.-K.Guo. *J. Med. Chem.*, **66**, 15944 (2023); https://doi.org/10.1021/acs.jmedchem.3c01374
109. S.Hayami, J.D.Kelly, H.Cho, M.Yoshimatsu, M.Unoki, T.Tsunoda, H.I.Field, D.E.Neal, H.Yamaue, B.A.J.Ponder, Y.Nakamura, R.Hamamoto. *Int. J. Cancer*, **128**, 574 (2011); https://doi.org/10.1002/ijc.25349
110. S.Wang, Z.-R.Li, F.-Z.Suo, X.-H.Yuan, B.Yu, H.-M.Liu. *Eur. J. Med. Chem.*, **167**, 388 (2019); https://doi.org/10.1016/j.ejmech.2019.02.039
111. W.Yan, M.Feng, K.Yang, C.Yu, W.Zhang, J.Liu, C.Xie, J.Cheng. *J. Med. Chem.*, **69**, 6038 (2026); https://doi.org/10.1021/acs.jmedchem.5c03481
112. J.Barcelo, R.Samain, V.Sanz-Moreno. *Trends Cancer*, **9**, 250 (2023); https://doi.org/10.1016/j.trecan.2022.12.001
113. Z.Cao, X.Wei, S.Xing, Jiacao Zhang, S.Wang, L.Yue, Jiahe Zhang, N.Jiang, X.Zhai. *Bioorg. Chem.*, **151**, 107675 (2024); https://doi.org/10.1016/j.bioorg.2024.107675
114. J.L.Nitiss. *Nat. Rev. Cancer*, **9**, 338 (2009); https://doi.org/10.1038/nrc2607
115. T.A.Farghaly, H.Gaber Abdulwahab, H.Y.Medrasi, M.A.Al-sheikh, D.F.Katowah, A.M.R.Alsaedi. *Bioorg. Chem*., **128**, 106043 (2022); https://doi.org/10.1016/j.bioorg.2022.106043
116. E.M.Chan, T.Shibue, J.M.McFarland, B.Gaeta, M.Ghandi, N.Dumont, A.Gonzalez, J.S.McPartlan, T.Li, Y.Zhang, J.Bin Liu, J.-B.Lazaro, P.Gu, C.G.Piett, A.Apffel, S.O.Ali, R.Deasy, P.Keskula, R.W.S.Ng, E.A.Roberts, E.Reznichenko, L.Leung, M.Alimova, M.Schenone, M.Islam, Y.E.Maruvka, Y.Liu, J.Roper, S.Raghavan, M.Giannakis, Y.-Y.Tseng, Z.D.Nagel, A.D'Andrea, D.E.Root, J.S.Boehm, G.Getz, S.Chang, T.R.Golub, A.Tsherniak, F.Vazquez, A.J.Bass. *Nature*, **568**, 551 (2019); https://doi.org/10.1038/s41586-019-1102-x
117. S.Ferretti, J.Hamon, R.De Kanter, C.Scheufler, R.Andraos-Rey, S.Barbe, E.Bechter, J.Blank, V.Bordas, E.Dammassa, A.Decker, N.Di Nanni, M.Dourdoigne, E.Gavioli, M.Hattenberger, A.Heuser, C.Hemmerlin, J.Hinrichs, G.Kerr, L.Laborde, I.Jaco, E.J.Núñez, H.-J.Martus, C.Quadt, M.Reschke, V.Romanet, F.Schaeffer, J.Schoepfer, M.Schrapp, R.Strang, H.Voshol, M.Wartmann, S.Welly, F.Zécri, F. Hofmann, H.Möbitz, M.Cortés-Cros. *Nature*, **629**, 443 (2024); https://doi.org/10.1038/s41586-024-07350-y
118. Q.Sui, Y.Zhou, M.Li, D.Wang, R.Cui, X.Cai, J.Liu, X.Wang, D.Teng, J.Zhou, H.Hou, S.Zhang, M.Zheng. *Eur. J. Med. Chem.*, **282**, 117039 (2025); https://doi.org/10.1016/j.ejmech.2024.117039
119. N.Y.L.Ngoi, P.G.Pilié, D.J.McGrail, M.Zimmermann, K.Schlacher, T.A.Yap. *Nat. Rev. Clin. Oncol*., **21**, 278 (2024); https://doi.org/10.1038/s41571-024-00863-5
120. M.Wu, X.Chen, H.Wang, C.Li, W.Liu, X.Zheng, J.Yang, X.Ye, Y.Weng, T.Fan, H.Hou. *J. Med. Chem.*, **68**, 5292 (2025); https://doi.org/10.1021/acs.jmedchem.4c02380
121. J.I.Fletcher, R.T.Williams, M.J.Henderson, M.D.Norris, M.Haber. *Drug Resist. Updates*, **26**, 1 (2016); https://doi.org/10.1016/j.drup.2016.03.001
122. S.Wang, S.-Q.Wang, Q.-X.Teng, L.Yang, Z.-N.Lei, X.-H.Yuan, J.-F.Huo, X.-B.Chen, M.Wang, B.Yu, Z.-S.Chen, H.-M.Liu. *J. Med. Chem.*, **63**, 15979 (2020); https://doi.org/10.1021/acs.jmedchem.0c01741
123. L.Chang, M.Xiao, L.Yang, S.Wang, S.-Q.Wang, A.Bender, A.Hu, Z.-S.Chen, B.Yu, H.-M.Liu. *Bioorg. Med. Chem.*, **26**, 5006 (2018); https://doi.org/10.1016/j.bmc.2018.08.021
124. X.-J.Fu, N.Li, J.Wu, Z.-Y.Wang, R.-R.Liu, J.-B.Niu, M.Taleb, S.Yuan, H.-M.Liu, J.Song, S.-Y.Zhang. *Eur. J. Med. Chem.*, **277**, 116761 (2024); https://doi.org/10.1016/j.ejmech.2024.116761
125. A.Batarseh, V.Papadopoulos. *Mol. Cell. Endocrinol*., **327**, 1 (2010); https://doi.org/10.1016/j.mce.2010.06.013
126. J.Li, M.L.Schulte, M.L.Nickels, H.C.Manning. *Bioorg. Med. Chem. Lett*., **26**, 3472 (2016); https://doi.org/10.1016/j.bmcl.2016.06.041
127. E.L.Werry, V.A.King, M.L.Barron, S.D.Banister, R.Sokias, M.Kassiou. *Eur. J. Pharm. Sci.*, **96**, 186 (2017); https://doi.org/10.1016/j.ejps.2016.09.026
128. T.Rodrigues, F.Sieglitz, G.J.L.Bernardes. *Chem. Soc. Rev*., **45**, 6130 (2016); https://doi.org/10.1039/C5CS00916B
129. M.Ding, H.Wang, C.Qu, F.Xu, Y.Zhu, G.Lv, Y.Lu, Q.Zhou, H.Zhou, X.Zeng, J.Zhang, C.Yan, J.Lin, H.-R.Luo, Z.Deng, Y.Xiao, J.Tian, M.X.Zhu, X.Hong. *Cancer Lett.*, **432**, 47 (2018); https://doi.org/10.1016/j.canlet.2018.05.041
130. I.Sarkaria, P.O-charoenrat, S.G.Talbot, P.G.Reddy, I.Ngai, E.Maghami, K.N.Patel, B.Lee, Y.Yonekawa, M.Dudas, A.Kaufman, R.Ryan, R.Ghossein, P.H.Rao, A.Stoffel, Y.Ramanathan, B.Singh. *Cancer Res.*, **66**, 9437 (2006); https://doi.org/10.1158/0008-5472.CAN-06-2074
131. S.Wang, L.Zhao, X.-J.Shi, L.Ding, L.Yang, Z.-Z.Wang, D.Shen, K.Tang, X.-J.Li, M.Mamun, H.Li, B.Yu, Y.-C.Zheng, S.Wang, H.-M.Liu. *J. Med. Chem.*, **62**, 2772 (2019); https://doi.org/10.1021/acs.jmedchem.9b00113
132. J.Wu, L.Sun, X.Chen, F.Du, H.Shi, C.Chen, Z.J.Chen. *Science*, **339**, 826 (2013); https://doi.org/10.1126/science.1229963
133. L.Li, Q.Yin, P.Kuss, Z.Maliga, J.L.Millán, H.Wu, T.J.Mitchison. *Nat. Chem. Biol*., **10**, 1043 (2014); https://doi.org/10.1038/nchembio.1661
134. M.Kawaguchi, S.Minami, N.Ieda, H.Nakagawa. *Bioorg. Med. Chem.*, **110**, 129820 (2024); https://doi.org/10.1016/j.bmcl.2024.129820
135. U.Rabenhorst, R.Beinoraviciute-Kellner, M.-L.Brezniceanu, S.Joos, F.Devens, P.Lichter, R.J.Rieker, J.Trojan, H.-J.Chung, D.L.Levens, M.Zörnig. *Hepatology*, **50**, 1121 (2009); https://doi.org/10.1002/hep.23098
136. S.Hauck, K.Hiesinger, S.Khageh Hosseini, J.Achenbach, R.M.Biondi, E.Proschak, M.Zörnig, D.Odadzic. *Bioorg. Med. Chem.*, **24**, 5717 (2016); https://doi.org/10.1016/j.bmc.2016.09.015
137. C.-H.Chan, J.K.Morrow, C.-F.Li, Y.Gao, G.Jin, A.Moten, L.J.Stagg, J.E.Ladbury, Z.Cai, D.Xu, C.J.Logothetis,

M.-C.Hung, S.Zhang, H.-K.Lin. *Cell*., **154**, 556 (2013); https://doi.org/10.1016/j.cell.2013.06.048
138. K.Hu, Y.Luo, P.Miao, L.Zhao, B.Zhao, X.-J.Shi, H.-M.Liu. *J. Med. Chem.*, **67**, 16435 (2024); https://doi.org/10.1021/acs.jmedchem.4c01283
139. S.Zhang, J.Qiu, H.Zhang, B.Chen, X.Zhang, D.Li, G.Li, G.Shan. *J. Med. Chem.*, **68**, 10048 (2025); https://doi.org/10.1021/acs.jmedchem.4c03075
140. M.M.El-Enany, M.M.Kamel, O.M.Khalil, H.B.El-Nassan. *Eur. J. Chem.*, **2**, 331 (2011); https://doi.org/10.5155/eurjchem.2.3.331-336.319
141. G.Li, Y.Wang, L.Li, Y.Ren, X.Deng, J.Liu, W.Wang, M.Luo, S.Liu, J.Chen. *Eur. J. Med. Chem*., **202**, 112519 (2020); https://doi.org/10.1016/j.ejmech.2020.112519
142. D.N.Bhogireddy, S.R.Surapureddi, T.Syed, T.Prashanth, B.R.Tadiboina. *Synth. Commun*., **52**, 861 (2022); https://doi.org/10.1080/00397911.2022.2056846
143. X.-S.Huo, X.-E.Jian, J.Ou-Yang, L.Chen, F.Yang, D.-X.Lv, W.-W.You, J.-J.Rao, P.-L.Zhao. *Eur. J. Med. Chem.*, **220**, 113449 (2021); https://doi.org/10.1016/j.ejmech.2021.113449
144. N.D.Kim, E.-S.Park, Y.H.Kim, S.K.Moon, S.S.Lee, S.K.Ahn, D.-Y.Yu, K.T.No, K.-H.Kim. *Bioorg. Med. Chem.*, **18**, 7092 (2010); https://doi.org/10.1016/j.bmc.2010.07.072
145. N.Zhang, S.Ayral-Kaloustian, T.Nguyen, J.Afragola, R.Hernandez, J.Lucas, J.Gibbons, C.Beyer. *J. Med. Chem.*, **50**, 319 (2007); https://doi.org/10.1021/jm060717i
146. C.F.Beyer, N.Zhang, R.Hernandez, D.Vitale, J.Lucas, T.Nguyen, C.Discafani, S.Ayral-Kaloustian, J.J.Gibbons. *Cancer Res.*, **68**, 2292 (2008); https://doi.org/10.1158/0008-5472.CAN-07-1420
147. C.F.Beyer, N.Zhang, R.Hernandez, D.Vitale, T.Nguyen, S.Ayral-Kaloustian, J.J.Gibbons. *Cancer Chemother. Pharmacol*., **64**, 681 (2009); https://doi.org/10.1007/s00280-008-0916-2
148. S.Ayral-Kaloustian, N.Zhang, C.Beyer. *Methods Find. Exp. Clin. Pharmacol*., **31**, 443 (2009); https://doi.org/10.1358/mf.2009.31.7.1410793
149. A.Wang-Gillam, S.M.Arnold, R.M.Bukowski, M.L.Rothenberg, W.Cooper, K.K.Wang, E.Gauthier, A.C.Lockhart. *Invest. New Drugs*, **30**, 266 (2012); https://doi.org/10.1007/s10637-010-9506-3
150. G.Sáez-Calvo, A.Sharma, F.D.A.Balaguer, I.Barasoain, J.Rodríguez-Salarichs, N.Olieric, H.Muñoz-Hernández, M.Á.Berbís, S.Wendeborn, M.A.Peñalva, R.Matesanz, Á.Canales, A.E.Prota, J.Jímenez-Barbero, J.M.Andreu, C.Lamberth, M.O.Steinmetz, J.F.Díaz. *Cell Chem. Biol*., **24**, 737 (2017); https://doi.org/10.1016/j.chembiol.2017.05.016
151. J.D.Singleton, R.Dass, N.R.Neubert, R.M.Smith, Z.Webber, M.D.H.Hansen, M.A.Peterson. *Bioorg. Med. Chem. Lett*., **30**, 126813 (2020); https://doi.org/10.1016/j.bmcl.2019.126813
152. S.Wang, L.-J.Zhao, Y.-C.Zheng, D.-D.Shen, E.-F.Miao, X.-P.Qiao, L.-J.Zhao, Y.Liu, R.Huang, B.Yu, H.-M.Liu. *Eur. J. Med. Chem.*, **125**, 940 (2017); https://doi.org/10.1016/j.ejmech.2016.10.021
153. A.M.Fouda, H.-A.S.Abbas, E.H.Ahmed, A.A.Shati, M.Y.Alfaifi, S.E.I.Elbehairi. *Molecules*, **24**, 1080 (2019); https://doi.org/10.3390/molecules24061080
154. F.Yang, L.-Z.Yu, P.-C.Diao, X.-E.Jian, M.-F.Zhou, C.-S.Jiang, W.-W.You, W.-F.Ma, P.-L.Zhao. *Bioorg. Chem*., **92**, 103260 (2019); https://doi.org/10.1016/j.bioorg.2019.103260
155. O.M.Ahmed, M.A.Mohamed, R.R.Ahmed, S.A.Ahmed. *Eur. J. Med. Chem.*, **44**, 3519 (2009); https://doi.org/10.1016/j.ejmech.2009.03.042
156. H.A.Abdel-Aziz, T.S.Saleh, H.S.A.El-Zahabi. *Arch. Pharm.*, **343**, 24 (2010); https://doi.org/10.1002/ardp.200900082
157. M.Wachtel, B.W.Schäfer. *Cancer Treat. Rev*., **36**, 318 (2010); https://doi.org/10.1016/j.ctrv.2010.02.007
158. Ž.Zajec, J.Dernovšek, M.Distel, M.Gobec, T.Tomašič. *Bioorg. Chem.*, **131**, 106311 (2023); https://doi.org/10.1016/j.bioorg.2022.106311
159. A.Kamal, J.R.Tamboli, M.J.Ramaiah, S.F.Adil, G.Koteswara Rao, A.Viswanath, A.Mallareddy, S.N.C.V.L.Pushpavalli, M.Pal-Bhadra. *ChemMedChem*, **7**, 1453 (2012); https://doi.org/10.1002/cmdc.201200205
160. L.Allen. *Semin. Oncol.*, **30**, 105 (2003); https://doi.org/10.1053/j.seminoncol.2003.08.012
161. A.Kamal, J.R.Tamboli, V.L.Nayak, S.F.Adil, M.V.P.S.Vishnuvardhan, S.Ramakrishna. *Bioorg. Med. Chem.*, **23**, 3208 (2013); https://doi.org/10.1016/j.bmcl.2013.03.129
162. A.Kamal, S.Faazil, S.M.A.Hussaini, M.J.Ramaiah, M.Balakrishna, N.Patel, S.N.C.V.L.Pushpavalli, M.Pal-Bhadra. *Bioorg. Med. Chem.*, **26**, 2077 (2016); https://doi.org/10.1016/j.bmcl.2016.02.072
163. E.A.Fayed, S.I.Eissa, A.H.Bayoumi, N.A.Gohar, A.B.M.Mehany, Y.A.Ammar. *Mol. Divers*., **23**, 165 (2019); https://doi.org/10.1007/s11030-018-9865-9
164. L.Wu, Y.Liu, Y.Li. *Molecules*, **23**, 2330 (2018); https://doi.org/10.3390/molecules23092330
165. C.Bagul, G.K.Rao, V.K.K.Makani, J.R.Tamboli, M.Pal-Bhadra, A.Kamal. *Med. Chem. Commun.*, **8**, 1810 (2017); https://doi.org/10.1039/C7MD00193B
166. M.Gilandoust, K.B.Harsha, C.D.Mohan, A.R.Raquib, S.Rangappa, V.Pandey, P.E.Lobie, S.Basappa, K.S.Rangappa. *Bioorg. Med. Chem.*, **28**, 2314 (2018); https://doi.org/10.1016/j.bmcl.2018.05.020
167. M.H.Attia, E.Z.Elrazaz, S.Z.El-Emam, A.T.Taher, H.A.Abdel-Aziz, K.A.M.Abouzid. *Bioorg. Chem.*, **94**, 103458 (2020); https://doi.org/10.1016/j.bioorg.2019.103458
168. N.H.Metwally, M.S.Mohamed, E.A.Ragb. *Bioorg. Chem*., **88**, 102929 (2019); https://doi.org/10.1016/j.bioorg.2019.102929
169. M.Zhao, H.Ren, J.Chang, D.Zhang, Y.Yang, Y.He, C.Qi, H.Zhang. *Eur. J. Med. Chem.*, **119**, 183 (2016); https://doi.org/10.1016/j.ejmech.2016.04.068
170. L.-H.Huang, Y.-F.Zheng, Y.-Z.Lu, C.-J.Song, Y.-G.Wang, B.Yu, H.-M.Liu. *Steroids*, **77**, 710 (2012); https://doi.org/10.1016/j.steroids.2012.03.002
171. S.Bondock, S.Alqahtani, A.M.Fouda. *J. Heterocycl. Chem*., **58**, 56 (2021); https://doi.org/10.1002/jhet.4148
172. A.K.Ajeesh Kumar, Y.D.Bodke, P.S.Lakra, G.Sambasivam, K.G.Bhat. *Med. Chem. Res*., **26**, 714 (2017); https://doi.org/10.1007/s00044-016-1770-0
173. G.-X.Yu, Y.Hu, W.-X.Zhang, X.-Y.Tian, S.-Y.Zhang, Y.Zhang, S.Yuan, J.Song. *Molecules*, **27**, 4996 (2022); https://doi.org/10.3390/molecules27154996
174. N.S.Naik, L.A.Shastri, B.M.Chougala, S.Samundeeswari, M.Holiyachi, S.D.Joshi, V.Sunagar. *Chem. Data Collect*., **30**, 100550 (2020); https://doi.org/10.1016/j.cdc.2020.100550
175. Z.He, C.Charleton, R.W.Devine, M.Kelada, J.M.D.Walsh, G.E.Conway, S.Gunes, J.R.M.Mondala, F.Tian, B.Tiwari, G.K.Kinsella, R.Malone, D.O'Shea, M.Devereux, W.Wang, P.J.Cullen, J.C.Stephens, J.F.Curtin. *Eur. J. Med. Chem.*, **224**, 113736 (2021); https://doi.org/10.1016/j.ejmech.2021.113736
176. N.Ravi Kumar, Y.Poornachandra, D.Krishna Swaroop, G.Jitender Dev, C.Ganesh Kumar, B.Narsaiah. *Bioorg. Med. Chem. Lett*., **26**, 5203 (2016); https://doi.org/10.1016/j.bmcl.2016.09.062
177. N.-J.Fan, Y.Li, S.Liang, J.-J.Tang. *J. Chem. Res*., **41**, 413 (2017); https://doi.org/10.3184/174751917X14967701767003
178. X.Zhai, N.Jiang, K.L.Zhang, F.Bao, P.Gong. *Chin. J. Chem*., **20**, 1179 (2009); https://doi.org/10.1016/j.cclet.2009.04.027
179. X.Zhai, Y.-F.Zhao, Y.-J.Liu, Y.Zhang, F.-Q.Xun, J.Liu, P.Gong. *Chem. Pharm. Bull*., **56**, 941 (2008); https://doi.org/10.1248/cpb.56.941
180. X.-L.Zhao, Y.-F.Zhao, S.-C.Guo, H.-S.Song, D.Wang, P.Gong. *Molecules*, **12**, 1136 (2007); https://doi.org/10.3390/12051136
181. A.Hossan, A.F.Alrefaei, H.A.Katouah, A.Bayazeed, B.H.Asghar, F.Shaaban, N.M.El-Metwaly. *J. Saudi Chem. Soc*., **27**, 101599 (2023); https://doi.org/10.1016/j.jscs.2023.101599

182. M.A.A.Radwan, F.M.Alminderej, H.M.Awad. *Molecules*, **25**, 255 (2020); https://doi.org/10.3390/molecules25020255
183. A.Ballesteros-Casallas, M.Paulino, P.Vidossich, C.Melo, E.Jiménez, J.-C.Castillo, J.Portilla, G.P.Miscione. *Eur. J. Med. Chem. Rep.*, **4**, 100028 (2022); https://doi.org/10.1016/j.ejmcr.2021.100028
184. F.Safari, M.Bayat, S.Nasri, S.Karami. *Bioorg. Med. Chem. Lett*., **30**, 127111 (2020); https://doi.org/10.1016/j.bmcl.2020.127111
185. H.A.Hassan, A.Q.Ramle, C.H.Tan, Y.S.Tan, M.Al-Amin, S.M.Salhimi, E.Abdullah, E.R.T.Tiekink, W.J.Basirun. *J. Mol. Struct*., **1338**, 142278 (2025); https://doi.org/10.1016/j.molstruc.2025.142278
186. T.E.Ali, M.M.Ali, S.M.Abdel-Kariem, M.M.Ahmed. *Synth. Commun*., **47**, 1458 (2017); https://doi.org/10.1080/00397911.2017.1332224
187. S.A.Ahmed, O.M.Ahmed, A.O.Abdelhamid. *Eur. J. Chem.*, **5**, 334 (2014); https://doi.org/10.5155/eurjchem.5.2.334-338.910
188. A.S.Hassan, M.F.Mady, H.M.Awad, T.S.Hafez. *Chin. J. Chem*., **28**, 388 (2017); https://doi.org/10.1016/j.cclet.2016.10.022
189. A.S.Hassan, G.O.Moustafa, H.M.Awad. *Synth. Commun*., **47**, 1963 (2017); https://doi.org/10.1080/00397911.2017.1358368
190. M.El-Naggar, A.S.Hassan, H.M.Awad, M.F.Mady. *Molecules*, **23**, 1249 (2018); https://doi.org/10.3390/molecules23061249
191. A.A.Almehizia, W.M.Aboulthana, A.M.Naglah, A.S.Hassan. *RSC Adv.*, **14**, 8397 (2024); https://doi.org/10.1039/D4RA00423J
192. S.Kaping, U.Kalita, M.Sunn, L.I.Singha, J.N.Vishwakarma. *Monatsh. Chem*., **147**, 1257 (2016); https://doi.org/10.1007/s00706-015-1638-x
193. M.T.El Sayed, H.A.R.Hussein, N.M.Elebiary, G.S.Hassan, S.M.Elmessery, A.R.Elsheakh, M.Nayel, H.A.Abdel-Aziz. *Bioorg. Chem.*, **78**, 312 (2018); https://doi.org/10.1016/j.bioorg.2018.03.009
194. M.A.Metwally, M.A.Gouda, A.N.Harmal, A.M.Khalil. *Int. J. Modern Org. Chem*., **2**, 96 (2012)
195. A.K.Ajeesh, Y.D. Bodke, A.N.Gowda, G.Sambasivam, K.G.Bhat. *J. Heterocycl. Chem*., **54**, 1904 (2017); https://doi.org/10.1002/jhet.2786
196. S.Kaping, M.Sunn, L.I.Singha, J.N.Vishwakarma. *Eur. J. Chem.*, **11**, 68 (2020); https://doi.org/10.5155/eurjchem.11.1.68-79.1942